UNIVERSITEIT VAN PRETORIA
UNIVERSITY OF PRETORIA
YUNIBESITHI YA PRETORIA

Pricing of options with Lévy processes associated with orthogonal polynomials

by

Tarutira Chikukwa

(Student no 11327465)

submitted in partial fulfillment of the requirements for the degree

Magister Scientiae

in Financial Engineering

in the Department of Mathematics and Applied Mathematics

in the Faculty of Natural and Agricultural Sciences

University of Pretoria

Pretoria

December 2018

Abstract

A Lévy process is a stochastic process that has stationary and independent increments. Log returns of financial assets tend to portray stochastic behaviours possessing distributions with heavy tails, high peaks and negative skewness which justifies the adoption of Lévy processes on modeling these phenomena. In this dissertation we consider two Lévy processes linked to orthogonal polynomials which are the Meixner process and Brownian motion. We build two option pricing models based on these Lévy processes. Both models make use of the Fourier transform methods and their efficiency is judged by the size of the error measures that calculate the distance between the market and model prices. The two models are compared to each other in terms of efficiency, simplicity in application and completeness. We use data from S&P500 index and JSE indices to determine the performances of the models in both liquid (US) and illiquid (SA) markets.

Declaration

I, the undersigned, declare that the dissertation, which I hereby submit for the degree Magister Scientiae in Financial Engineering at the University of Pretoria, is my own independent work and has not previously been submitted by me for a degree at this or any other tertiary institution.

Signature: T. C.

Name: Tarutira Chikukwa

Date: November 2018

Acknowledgements

My gratitude goes to my supervisors Dr Alta Jooste and Dr Gusti van Zyl for their combined effort, suggestions and corrections throughout the course of the research. They pushed me out of my comfort zones for me to be able to complete my research. I am grateful to Dr Michael Chapwanya for his assistance on Matlab coding. I also owe my appreciation to Mastercard Foundation Scholarship and Dr Aquilina Mawadza for their support, funding and motivation. I will forever be grateful to God and my parents for making me who I am today.

Contents

List of Tables

List of Figures

Chapter 1

Introduction

1.1 Overview

Prices of derivatives are not easily determined with certainty, due to their stochastic nature. The main aim of this research is to introduce the models which are based on Lévy processes related to orthogonal polynomials, in order to find a way to price options efficiently. The prices of derivatives depend on the underlying assets which may be shares, indexes or any other asset.

The main objectives of this research are as follows:

- To price options using Lévy processes linked to orthogonal polynomials.
- To classify the processes as Lévy processes by showing that they are infinitely divisible.
- To determine the effects of parameter changes on a distribution modeling the behaviour of the selected Lévy processes.
- To clearly justify why a selected Lévy process is suited for modeling the behaviour of log returns of the underlying assets by establishing its properties.
- To check the goodness of fit of the processes to the log returns of the underlying asset.
- To ensure that there is no-arbitrage and to determine if the pricing model is complete.
- To apply the Fourier Transform or the Fast Fourier Transform (FFT) method together with the mean-correcting of martingale measures on pricing options.
- To use error measures to determine the pricing model that is close enough to the market prices.
- To apply an optimization procedure to reduce the size of error measures through calibration of the pricing models to the market prices.
- To determine the sensitivity of the pricing models to the changes in the price of an underlying asset.

The inspiration of the research is from the increase in financial crises for example the 2007-2008 global crisis and the European crisis which heavily affected Greece, Spain, Portugal and Ireland from 2009. Many investment banks in the USA were forced into bankruptcy like Lehman brothers and the near fall of the Bear Stearns. The case of the losses for the JP Morgan's Synthetic portfolio (nicknamed "London Whale") in 2012, also adds to the disasters that keep on increasing in the derivative market. A model's efficiency only depends on the underlying assumptions used to create the model. Although the blame cannot entirely be shifted to the models that are being used in finance, model risks can play a big role in causing losses. One of the logical ways to improve the efficiency of the model used, is to find a way in which the real world scenarios are being incorporated in the model. Most financial crises partially emanate from using inefficient models as pointed out by many analysts [29, pp. xv-xvii].

The assumption commonly used in finance is that the distributions of asset returns are modeled by a normal distribution. Many models are established on the foundation of the normality of the returns which may fail to apply in real life situations. The Black-Scholes model is one of the most commonly applied models in the financial industry for option pricing, because of its simplicity and its basis on normality of log returns. The problem with this notion is that log returns of financial asset do not seem to agree on this assumption and this contributes to a lot of challenges. A distribution that governs the log returns of the financial assets is expected to have the following:

- a location parameter which explains how the distribution is centered;
- a kurtosis parameter which measures the thickness of the tails and the peakedness of the distribution;
- a shape parameter which determines if the distribution is symmetric or not;
- a scale parameter that measures how spread the graph of a distribution is.

The Black-Scholes model assumes normality of log returns of underlying assets, hence the shape parameter is zero, which indicates that the distribution of log returns is symmetric and there is no possibility of heavy tails being considered, due to the absence of excess kurtosis. Many scholars argued against this by pointing out that financial assets usually have a positive excess kurtosis, contrary to the normal distribution with an excess kurtosis of zero [32]. The issue of no heavy tails depicted by the normal distribution is less appealing, considering that it is possible to experience many large negative or positive returns which lead to heavy tails of the returns distribution. Some scholars pointed out that the Black-Scholes model fails to detect volatility smile (high volatility in out-of-the-money and in-the-money but low volatility at-the-money) exhibited by derivative prices (see [7, pp. 8-11]). It was also argued that the stock data contains jumps that are not incorporated by the Black-Scholes model [25]. All these justified arguments suggest the need for adoption of other models that are more closely related to the stochastic nature of the derivatives prices which incorporates jumps (see [45]).

In this research the focus is on pricing options under the Brownian motion and the Meixner process and they all belong to a family of Lévy processes. We will show that the two processes are linked to orthogonal polynomials.

1.2 Behaviours of financial assets and models in the market

The most popular debate in finance is whether the assumption of normality should continue to be used in building models. Rachev et al [29, pp. xv-xvii] indicated that the assumption of normality is not accurate by doing an analysis on the trends determined from financial time series of returns of financial assets. The first trend they discovered is that of heavy tails. This means there are time periods which are showing many extreme positive or negative returns. This may be caused by other factors that are not predicted at the outset like the company crisis or in general, the economic crisis. By default, the assumption of normality does not incorporate heavy tails because the tails of a normal distribution approaches zero at an exponential rate. Secondly, financial returns tend to indicate skewness which cannot be represented by a normal distribution since negative returns are mirror images of the positive returns in the normal case. Thirdly, under normal distribution, volatility is constant but Rachev et al [29, p. xvii] have discovered that the returns tend to show signs of volatility clustering. Volatility clustering is when the large changes of financial asset prices are succeeded by large changes while small changes are also succeeded by small asset price changes [24].

Under the pricing of options it has been proved by some scholars (see [7, p. 9]) that volatility is affected by the strike price. There are two scenarios which have been discovered to happen on the volatility of the asset prices, which are volatility skew and volatility smile. Volatility skew is a scenario where the prices of options are decreasing in relation to an increase in strike price of an option. Volatility smile is the trend that shows a "U" shaped relationship with the strike price of an option, the lowest volatility is thus observed when the option is at-the-money, but increases as the option becomes deeply in-the-money or out-of-the-money, hence the shape "U".

However, Cont and Tankov [7, p. ix] pointed out that the models that rely on Brownian motion are more frequently preferred, since the Mathematics behind them are less technical as compared to the modeling techniques of the other classes of Lévy processes. The major source of complexity of the latter processes is due to the fact that they incorporate jumps (for example the Meixner process). Although this is an advantage, this is not always user friendly as some users have limited knowledge of the literature of stochastic processes. When a model is chosen, the parameters of the model are estimated in relation to the data for the underlying asset returns, which will give a room for the model to be compared to the actual data trends. It is argued by Cont and Tankov [7, p. 103] that the process of estimation may be a very challenging task if the model has many parameters, which is mostly the case with most Lévy processes, since it is a major challenge to estimate their parameters, because the maximum likelihood estimation (MLE) is not always applicable. This difficulty in getting the estimators may render the model less useful. The other method of estimation of parameters is the method of moments, but it remains a challenge to estimate parameters from a model with many parameters. In this case the models which are based on the normality assumption are preferred.

One of the most meaningful arguments raised by other scholars [7, p. 3] is that the time

scale of returns calculations influence the distribution of the asset returns. This has an effect of yielding different distributions by considering different time scales. As the time scale becomes large, the shape of the asset returns distribution tends to a normal distribution. This was another justification for the assumption of normality by many pricing models like the Black-Scholes model. Moreover, the issue of volatility clustering which is not addressed under normal distribution, is also left unsolved by other models that belong to the Lévy family, because they have independent increments, as pointed out by Cont and Tankov [7, p. 227, Table 7.2]. To summarise the arguments made by several contributors on the pricing of the derivatives, it can be noticed that no model can be perfect and each model has some advantages attached to it. In this research we do an analysis of the models to reveal the merits and demerits of orthogonal polynomial related models of pricing options. We either justify the claims stipulated by several scholars on this issue, or we give a contradiction to some suggested theories.

1.3 Outline of the research

In Chapter 2 we introduce orthogonal polynomials. We focus on Hermite and Meixner-Pollaczek polynomials because of their relationship with Brownian motion and the Meixner process, respectively. In Chapter 3 we introduce Lévy processes and in Chapter 4 these processes are fit to the data from the S&P500 share index and South African data, by making use of histograms, chi-squared test and quantile-quantile (q-q) plots. Parameter estimation is done by the methods of moments. The pricing of European vanilla options is done in Chapter 5. The Fourier methods are explained in detail in this chapter. In Chapter 6 we focus on the calibration of the pricing models, designed in Chapter 5, to the market prices of options. This calibration allows us to compare the normal and Meixner models on option pricing. In Chapter 7 we discuss our observations.

Chapter 2

Overview of orthogonal polynomials

A set of polynomials $\{P_n\}_{n=0}^{N}$, where N can be finite or infinite and degree$[P_n] = n$, is orthogonal with respect to a positive and continuous weight function $w(x)$ on an interval $[a, b]$ (finite or infinite) if [20, p. 2, Equation 1.1.9]

$$\int_a^b P_m(x)P_n(x)w(x)dx = d_n^2\delta_{mn}, \tag{2.0.1}$$

where:

- $d_n^2 = \int_a^b P_n^2(x)w(x)dx$,
- $\delta_{mn} = \begin{cases} 0 \; for \; m \neq n \\ 1 \; for \; m = n \end{cases} \quad m, n \epsilon \{0, 1, 2, 3, \ldots\}.$

If a positive weight function $w(x)$ is constant at a countable number of jump points in the interval $[a, b]$, then the set of polynomials $\{P_n\}_{n=0}^{N}$ is discrete orthogonal if [20, p. 2, Equation 1.1.10]

$$\sum_{i=1}^{N} P_m(x_i)P_n(x_i)w(x_i) = d_n^2\delta_{mn}, \tag{2.0.2}$$

where $d_n^2 = \sum_{i=1}^{N} P_n^2(x)w(x_i)$.

2.1 Classical orthogonal polynomials

2.1.1 Continuous classical orthogonal polynomials

Continuous classical orthogonal polynomials are solutions of second order differential equations (hypergeometric differential equations) [31, Equation 1.6]

$$g(x)y'' + h(x)y' + \lambda y = 0, \tag{2.1.1}$$

where:

- $g(x)$ is a polynomial of degree at most 2,
- $h(x)$ denotes a polynomial of degree at most 1,
- λ is a non-zero constant.

There are three types of continuous classical orthogonal polynomials namely the Hermite, Laguerre and Jacobi polynomials [11, p. 26].

Using the Pearson differential equation [20, p. 82, Equation 4.2.2]

$$(w(x)g(x))' = w(x)h(x), \tag{2.1.2}$$

we can write (2.1.1) in the self-adjoint form [20, p. 82, Equation 4.2.1]

$$(g(x)w(x)y')' + \lambda w(x)y = 0. \tag{2.1.3}$$

We prove this by multiplying (2.1.1) by $w(x)$ to obtain

$$g(x)w(x)y'' + w(x)h(x)y' + \lambda w(x)y = 0,$$

and by using the Pearson differential equation, we have

$$g(x)w(x)y'' + (w(x)g(x))'y' + \lambda w(x)y = 0,$$

which leads to (2.1.3).

We can use the self-adjoint form to prove the orthogonality relation of classical orthogonal polynomials. Suppose polynomials $y_n(x)$ and $y_m(x)$ are solutions of (2.1.1) for any two non-zero constants λ_n and λ_m respectively, we assume $\lambda_n - \lambda_m \neq 0$ for $m \neq n$ [20, p. 82]. By making use of (2.1.3), we obtain the following equations:

$$(g(x)w(x)y_n'(x))' + \lambda_n w(x)y_n(x) = 0, \tag{2.1.4}$$
$$(g(x)w(x)y_m'(x))' + \lambda_m w(x)y_m(x) = 0. \tag{2.1.5}$$

Multiplying equations (2.1.4) and (2.1.5) by $y_m(x)$ and $y_n(x)$, respectively, and subtracting the resulting equations, we get

$$(g(x)w(x)y_n'(x))'y_m(x) - (g(x)w(x)y_m'(x))'y_n(x) + (\lambda_n - \lambda_m)w(x)y_n(x)y_m(x) = 0. \tag{2.1.6}$$

If we integrate equation (2.1.6) over the interval (a, b) we see that

$$(\lambda_n - \lambda_m)\int_a^b w(x)y_n(x)y_m(x)dx = \int_a^b (g(x)w(x)y_m'(x))'y_n(x)dx - \int_a^b (g(x)w(x)y_n'(x))'y_m(x)dx, \tag{2.1.7}$$

and using integration by parts, we obtain

$$(\lambda_n - \lambda_m)\int_a^b w(x)y_n(x)y_m(x)dx = [g(x)w(x)(y_m'(x)y_n(x) - y_n'(x)y_m(x))]\,|_a^b$$
$$= 0,$$

if we assume that $g(a)w(a) = 0$ and $g(b)w(b) = 0$. Since $\lambda_n \neq \lambda_m$ for $m \neq n$ then

$$\int_a^b w(x)y_n(x)y_m(x)dx \;=\; 0.$$

This shows that two different solutions of (2.1.1) are orthogonal to each other.

Using (2.1.2) we obtain an expression for the weight function $w(x)$ that will be referred to later in this dissertation as follows:

$$\begin{aligned} w'(x)g(x) + g'(x)w(x) &= w(x)h(x) \\ \frac{w'(x)}{w(x)} &= \frac{h(x) - g'(x)}{g(x)} \\ \int \frac{w'(x)}{w(x)}dw(x) &= \int \frac{h(x) - g'(x)}{g(x)}dx \\ \ln|w(x)| &= \int \frac{h(x)}{g(x)}dx - \ln|g(x)| + c \\ w(x) &= \frac{A}{g(x)}\exp\left(\int \frac{h(x)}{g(x)}dx\right),\ A, c \in \mathbb{R}. \end{aligned} \tag{2.1.8}$$

Our preference for the form (2.1.3) is motivated by the fact that the self-adjoint form incorporates the weight function (2.1.8) which plays the role of an integrating factor when solving differential equations.

In Table 2.1 we provide the weight functions and the intervals of orthogonality of the continuous classical orthogonal polynomials.

Table 2.1: Weight functions and support intervals of Hermite, Laguerre and Jacobi polynomials [11, p. 29]

Polynomial	Weight $(w(x))$	Support interval
Hermite	$\exp(-x^2)$	$(-\infty, \infty)$
Laguerre	$x^\alpha \exp(-x)$ for $\alpha > -1$	$[0, \infty)$
Jacobi	$(1-x)^\alpha(1+x)^\beta$ for $\alpha, \beta > -1$	$[-1, 1]$

2.1.2 Discrete classical orthogonal polynomials

The discrete classical orthogonal polynomials are solutions of second-order hypergeometric type difference equations [31, Equation 1.9]

$$g(x)\triangle\nabla y(x) + h(x)\triangle y(x) + \lambda y(x) \;=\; 0, \tag{2.1.9}$$

where:

- $\triangle y(x) = y(x+1) - y(x)$,
- $\nabla y(x) = y(x) - y(x-1)$,
- $g(x)$ is a polynomial with degree of at most 2,
- $h(x)$ is a polynomial with degree of at most 1,
- and λ is a non-zero constant.

The discrete weight function $w(x)$ satisfies the difference equation of Pearson type [31, Equation 1.11]

$$\triangle(g(x)w(x)) \quad = \quad h(x)w(x),$$

which can be simplified to

$$\begin{aligned} g(x+1)w(x+1) - g(x)w(x) &= h(x)w(x) \\ g(x+1)w(x+1) &= h(x)w(x) + g(x)w(x) \\ \frac{w(x+1)}{w(x)} &= \frac{h(x)+g(x)}{g(x+1)}. \end{aligned}$$

Some of the orthogonal polynomials that belong to the discrete classical orthogonal polynomials, that satisfy (2.1.9), are Charlier, Meixner, Krawtchouk and Hahn polynomials.

2.2 Hermite polynomials

The Hermite polynomials, H_n, are solutions of the hypergeometric differential equation (2.1.1), with $g(x) = 1$, $h(x) = -2x$ and $\lambda = 2n$ [20, p. 250, Equation 9.15.5]

$$H_n''(x) - 2xH_n'(x) + 2nH_n(x) \quad = \quad 0.$$

Hermite polynomials are orthogonal on $(-\infty, \infty)$ with respect to the weight function

$$w(x) \quad = \quad \frac{1}{\sqrt{\pi}} \exp(-x^2), \tag{2.2.1}$$

hence satisfying the orthogonality relation [20, p. 250, Equation 9.15.2]

$$\frac{1}{\sqrt{\pi}} \int_{-\infty}^{\infty} \exp(-x^2) H_m(x) H_n(x) dx \quad = \quad 2^n n! \delta_{mn},$$

and the following recurrence relation [20, p. 250, Equation 9.15.3]

$$H_{n+1}(x) - 2xH_n(x) + 2nH_{n-1}(x) \quad = \quad 0.$$

2.3 Meixner-Pollaczek polynomials

The Meixner-Pollaczek polynomials P_n^{λ}, $\lambda > 0$, are solutions of a complex hypergeometric difference equation [20, p. 214, Equation 9.7.5]

$$e^{i\theta}(\lambda - ix)y(x+i) + 2i[x\cos(\theta) - (\lambda+n)\sin(\theta)]y(x) - e^{-i\theta}(\lambda+ix)y(x-i) \quad = \quad 0,$$

where $y(x) = P_n^{\lambda}(x,\theta)$, $i = \sqrt{-1}$ and $0 < \theta < \pi$.
These polynomials are orthogonal on $(-\infty,\infty)$ with respect to the weight function

$$w(x) \quad = \frac{1}{2\pi} \quad e^{(2\theta-\pi)x}|\Gamma(\lambda+ix)|^2, \tag{2.3.1}$$

and satisfy the orthogonality relation [20, p. 213, Equation 9.7.2]

$$\int_{-\infty}^{\infty} w(x)P_m^{\lambda}(x;\theta)P_n^{\lambda}(x;\theta)dx \quad = \quad \frac{\Gamma(n+2\lambda)}{(2\sin(\theta))^{2\lambda}n!}\delta_{mn},$$

and the three-term recurrence equation [20, p. 213, Equation 9.7.3]

$$(n+1)P_{n+1}^{\lambda}(x;\theta) - 2[x\sin(\theta) + (\lambda+n)\cos(\theta)]P_n^{\lambda}(x;\theta) + (n+2\lambda-1)P_{n-1}^{\lambda}(x;\theta) \quad = \quad 0.$$

Chapter 3

Stochastic processes of the Lévy family

In the previous chapter we introduced the theory of orthogonal polynomials and in this chapter we will explain the processes that belong to the Lévy family and are linked to orthogonal polynomials. Stochastic processes are used in this dissertation because their random nature allows us to model randomness of financial asset prices. As a background to this chapter, we have explained the theory of a probability space and random variables in appendix A.

A probability density function (p.d.f.) of a random variable X defined on a probability space$(\Omega, \mathcal{F}, P)$ denoted by $f(x)$ is a function that satisfies [9, pp. 160-161]:

- $\int_a^b f(x)dx = P(a \leq X \leq b)$,
- $\int_{-\infty}^{\infty} f(x)dx = 1$,
- $f(x) \geq 0$,

for any a, $b \in \mathbb{R}$ and $a \leq b$.

We define a distribution function of a random variable X defined on a probability space$(\Omega, \mathcal{F}, P)$ as [1, p. 56]

$$F(x) \quad = \quad P(X \leq x) = \int_{-\infty}^{x} f(t)dt,$$

for any $x \in \mathbb{R}$.

The characteristic function of a random variable X with probability density function $f(x)$ is defined as follows [33, p. 15]:

$$\Phi_X(u) \quad = \quad E[e^{iuX}] = \int_{-\infty}^{\infty} e^{iuX} f(x)dx. \tag{3.0.1}$$

Suppose $\Psi_X(u) = \ln \Phi_X(u)$, then the cumulants of X are defined as [7, p. 31]

$$C_n(X) = \frac{1}{i^n}\left(\frac{\partial^n \Psi(0)}{\partial u^n}\right). \tag{3.0.2}$$

3.0.1 Heaviness of the tails of a distribution

We define the distribution function of the tails of distribution $F(x)$ by

$$\overline{F}(x) = 1 - F(x),$$

where $F(x)$ is a distribution function such that (see appendix)

$$\begin{aligned} F(x) &= P(X \leq x) \\ &= \int_{-\infty}^{x} f(x)dx, \end{aligned}$$

then a distribution has a heavy right tail if the following holds (see [30, p. 49]):

$$\lim_{x\to\infty} e^{\mu x}\overline{F}(x) = \infty, \tag{3.0.3}$$

and a heavy left tail if

$$\lim_{x\to-\infty} e^{-\mu x}F(x) = \infty, \tag{3.0.4}$$

where $\mu > 0$.

The explanation is that if tails of a distribution approach zero slower than the exponential distribution tails, then the distribution has heavy tails. From (3.0.3), as $x \to \infty$, $e^{\mu x}$ approaches ∞ quicker than $\overline{F}$ turns to 0, which forces the whole expression to turn to infinity. The same holds for the left tail. From (3.0.4), as $x \to -\infty$, $F(x) \to 0$ slower than $e^{-\mu x} \to \infty$, which forces the whole expression to turn to infinity. If the distribution has such behaviour, then it has heavy tails.

3.0.2 Moments of a distribution

The first four moments of a distribution are derived from the characteristic function in (3.0.1) by using a cumulant function in (3.0.2) [7, p. 32].

The mean of a distribution is given as

$$\begin{aligned} E(X) &= C_1(X) \\ &= i^{-1}\Psi'(0), \end{aligned} \tag{3.0.5}$$

and the variance of distribution is

$$\begin{aligned} Var(X) &= C_2(X) \\ &= i^{-2}\Psi''(0). \end{aligned} \tag{3.0.6}$$

The third (skewness) and fouth (kurtosis) moments are given respectively as follows:

$$\begin{aligned} Skew(X) &= \frac{C_3(X)}{(C_2(X))^{\frac{3}{2}}} \\ &= \frac{i^{-3}\Psi'''(0)}{[Var(X)]^{\frac{3}{2}}}, \end{aligned} \tag{3.0.7}$$

$$\begin{aligned} Kurtosis(X) &= \frac{C_4(X)}{(C_2(X))^2} + 3 \\ &= \frac{i^{-4}\Psi^{(4)}(0)}{[Var(X)]^2} + 3. \end{aligned} \tag{3.0.8}$$

3.1 Normal distribution

The probability density function of the normal distribution denoted by $Normal(\mu, \sigma^2)$ is given by

$$f(x) \;=\; \frac{1}{\sqrt{2\pi\sigma^2}} \exp\left(-\frac{(x-\mu)^2}{2\sigma^2}\right), \tag{3.1.1}$$

for $\mu \in \mathbb{R}$ and $\sigma^2 > 0$.

The two parameters under the normal distribution are defined as follows:

- μ is the location parameter and
- σ is the scale parameter.

In Figures 3.1 and 3.2 we show the effects of changing the two parameters of a normal distribution. In Figure 3.1 we see that increasing the location parameter μ results in a shift in the graph of the probability density function of the normal distribution to the right. In Figure 3.2 we show that increasing the scale parameter σ causes the graph of the probability density function of a normal distribution to flatten.

Figure 3.1: $Normal(\mu, 1)$ for $\mu = -0.5$ (solid), $\mu = 0$ (dashed) and $\mu = 0.5$ (dotdashed)

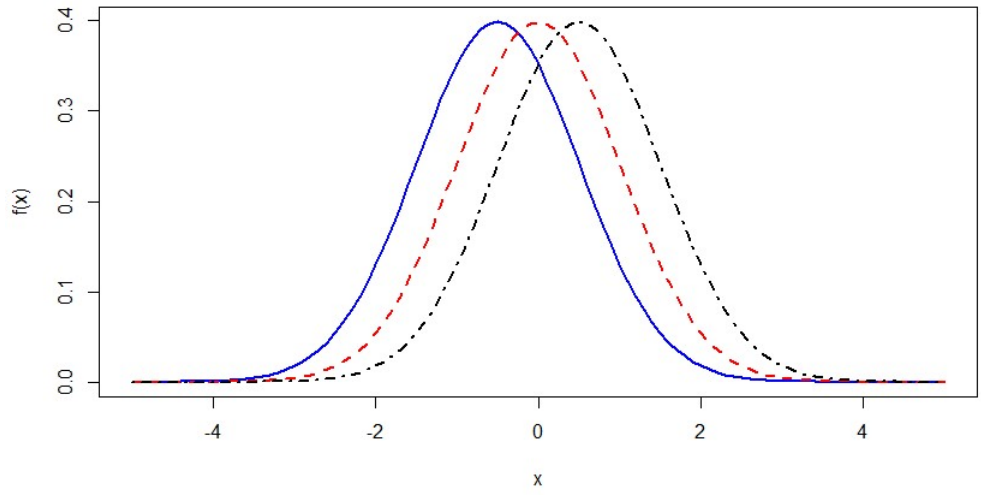

Figure 3.2: $Normal(0, \sigma^2)$ for $\sigma^2 = 1$ (solid), $\sigma^2 = 2$ (dashed) and $\sigma^2 = 3$ (dotdashed)

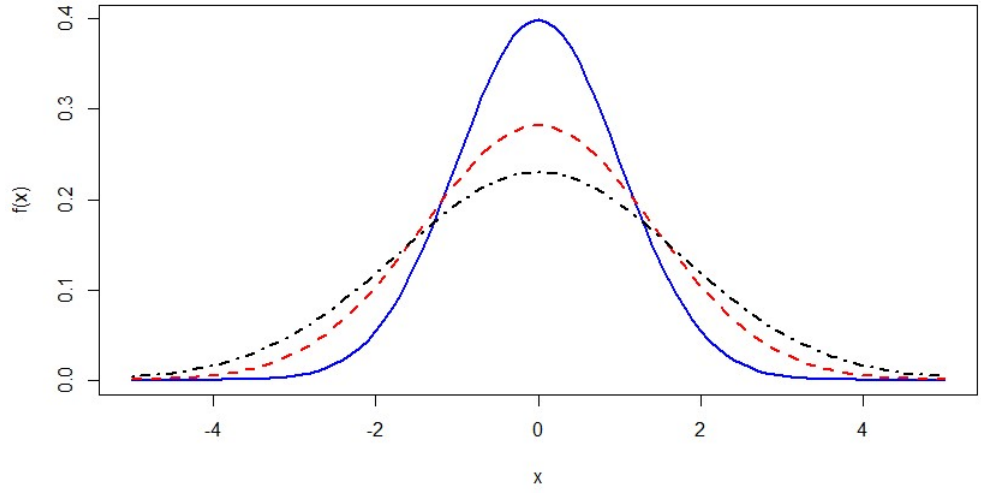

3.1.1 Characteristic function of a normal distribution

Using (3.1.1) and (3.0.1), the characteristic function of the normal distribution is given by

$$\begin{aligned} E[\exp(itX)] &= \int_{-\infty}^{\infty} \exp(itx) \left(\frac{1}{\sqrt{2\pi\sigma^2}} \exp\left(-\frac{(x-\mu)^2}{2\sigma^2} \right) \right) dx \\ &= \int_{-\infty}^{\infty} \frac{1}{\sqrt{2\pi\sigma^2}} \exp\left(itx - \frac{(x-\mu)^2}{2\sigma^2} \right) dx, \end{aligned}$$

and we make a substitution $y = x - \mu$ to get

$$\begin{aligned} E[\exp(itX)] &= \int_{-\infty}^{\infty} \frac{1}{\sqrt{2\pi\sigma^2}} \exp\left(it(y+\mu) - \frac{y^2}{2\sigma^2} \right) dy \\ &= e^{it\mu} \int_{-\infty}^{\infty} \frac{1}{\sqrt{2\pi\sigma^2}} \exp\left(\frac{-y(y - 2it\sigma^2)}{2\sigma^2} \right) dy, \end{aligned}$$

this is simplified by making another substitution $z = y - it\sigma^2$, to get

$$\begin{aligned} E[\exp(itX)] &= e^{it\mu}\int_{-\infty}^{\infty}\frac{1}{\sqrt{2\pi\sigma^2}}\exp\left(\frac{-(z+it\sigma^2)(z-it\sigma^2)}{2\sigma^2}\right)dz \\ &= e^{it\mu}\int_{-\infty}^{\infty}\frac{1}{\sqrt{2\pi\sigma^2}}\exp\left(\frac{-(z^2+t^2\sigma^4)}{2\sigma^2}\right)dz \\ &= e^{it\mu}e^{-\frac{1}{2}t^2\sigma^2}\int_{-\infty}^{\infty}\frac{1}{\sqrt{2\pi\sigma^2}}\exp\left(\frac{-z^2}{2\sigma^2}\right)dz \qquad (3.1.2) \\ &= e^{it\mu-\frac{1}{2}t^2\sigma^2}, \qquad (3.1.3) \end{aligned}$$

since the expression inside the integration in (3.1.2) is the probability density function of a normal distribution with parameters $\mu = 0$ and σ^2, the value of the integral in (3.1.2) is one.

3.1.2 Moments of a normal distribution

We can find the moments of the normal distribution by using (3.1.3) as follows:

$$\begin{aligned} \Psi(t) &= \ln(e^{it\mu-\frac{1}{2}t^2\sigma^2}) \\ &= it\mu - \frac{1}{2}\sigma^2t^2. \qquad (3.1.4) \end{aligned}$$

By differentiating (3.1.4) we have

$$\begin{aligned} \Psi'(t) &= i\mu - \sigma^2t \\ \Psi''(t) &= -\sigma^2 \\ \Psi'''(t) &= 0 \\ \Psi^{(4)}(t) &= 0 \end{aligned}$$

Hence, from (3.0.5), the mean is given by

$$\begin{aligned} E(X) &= i^{-1}(i\mu) \\ &= \mu \qquad (3.1.5) \end{aligned}$$

and from (3.0.6), the variance is

$$\begin{aligned} Var(X) &= i^{-2}(-\sigma^2) \\ &= \sigma^2, \end{aligned}$$

from (3.0.7), the skewness is

$$Skew(X) = 0$$

and finally from (3.0.8), the fourth moment is

$$Kurtosis(X) = 3.$$

3.2 Meixner distribution

The probability density function of a Meixner distribution, denoted by $Meixner(a, b, d, m)$, is as follows [32]:

$$f(x; a, b, d, m) = \frac{\left(2\cos\frac{b}{2}\right)^{2d}}{2a\pi\Gamma(2d)} \exp\left(\frac{b(x-m)}{a}\right) \left|\Gamma\left(d + \frac{i(x-m)}{a}\right)\right|^2 \tag{3.2.1}$$

with $i = \sqrt{-1}$ and Γ is the gamma function.

The four parameters of the Meixner distribution are as follows [14]:

- a is the scale parameter,
- b is the skewness parameter,
- d is the kurtosis parameter and
- m is the location parameter.

The effects of changing the four parameters of the Meixner distribution are shown in Figures 3.3, 3.4, 3.5 and 3.6. In Figure 3.3 we show that changing the parameter a results in changing the spread of the Meixner curve. High values of a result in wider and lower peaked curves as compared to lower values of a. Changing the values of b, as in Figure 3.4, affects the measure of asymmetry and when $b = 0$, the distribution is symmetric around the location parameter m while negative and positive values correspond to negative and positive skewness, respectively. Parameters b and d determine the general shape of the distribution with parameter d having a larger say on the sharpness of the peaks. The lower the values of d, the higher the peaks as shown in Figure 3.5. Figure 3.6 shows that if we increase the values of m, the curves will be shifted to the right, since m is a location parameter. In the later sections of this dissertation we will discuss why these skewness and kurtosis parameters are important in modeling financial data.

Figure 3.3: $Meixner(a, 0.3, 2, 0)$ for $a = 0.5$ (solid), $a = 1$ (dashed) and $a = 2$ (dotdashed)

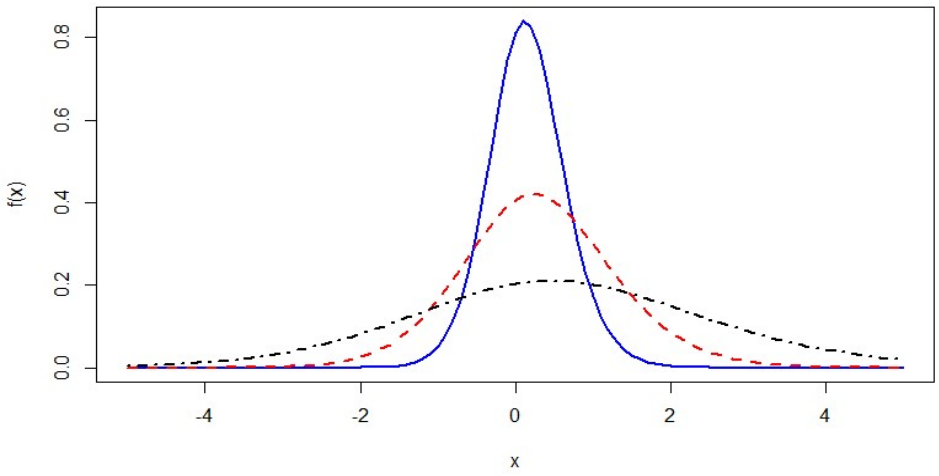

Figure 3.4: $Meixner(1, b, 2, 0)$ for $b = 0.5$ (solid), $b = 0$ (dashed), $b = -0.5$ (dotdashed)

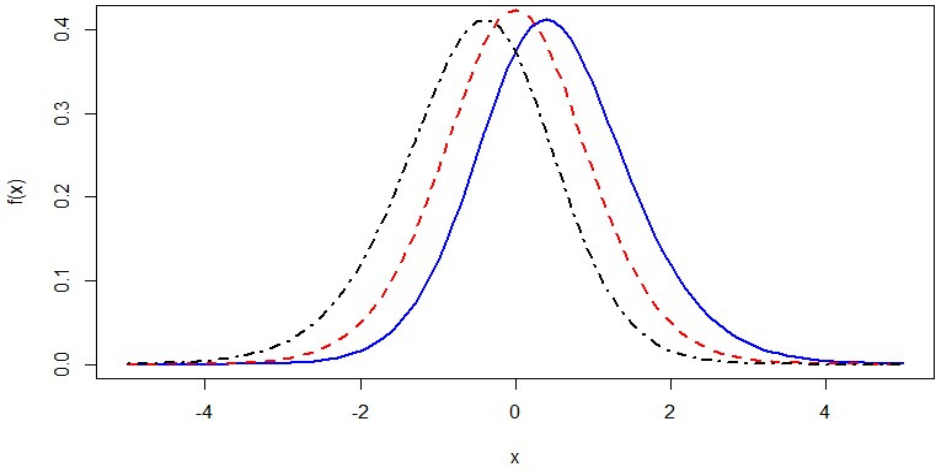

Figure 3.5: $Meixner(1, 0, d, 0)$ for $d = 0.5$ (solid), $d = 1$ (dashed), $d = 2$ (dotdashed)

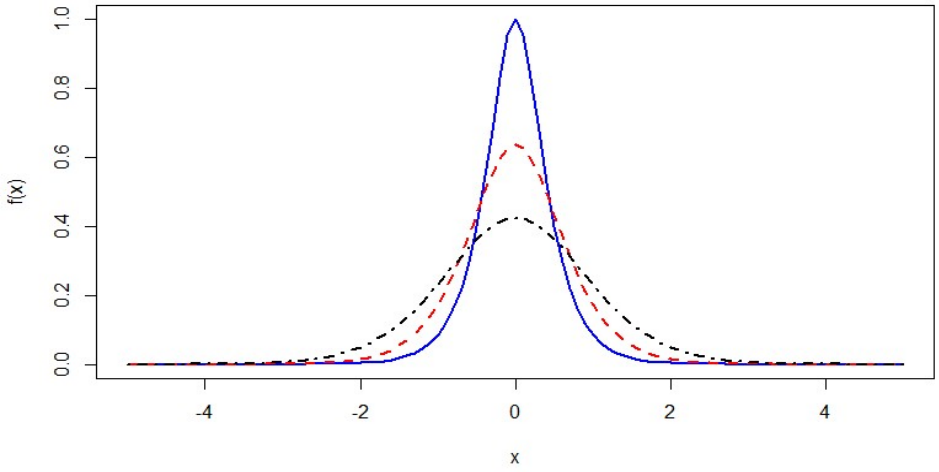

Figure 3.6: $Meixner(1, 0, 1, m)$ for $m = -0.5$ (solid), $m = 0$ (dashed), $m = 0.5$ (dotdashed)

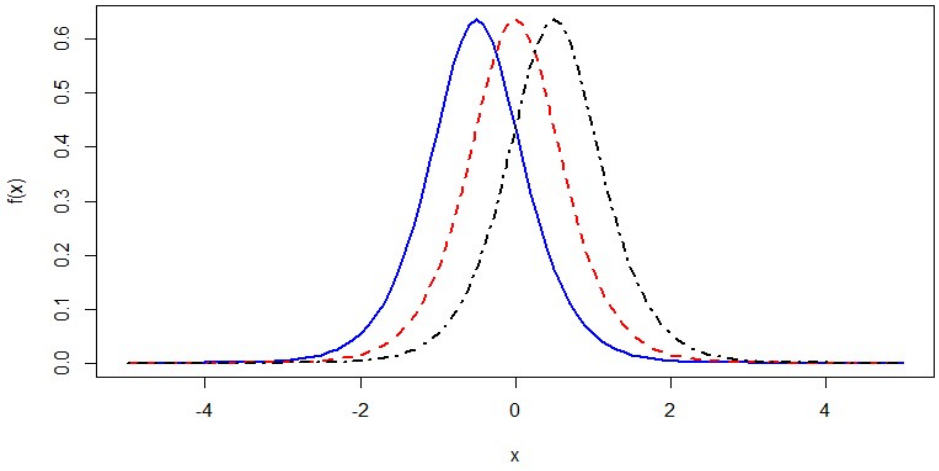

3.2.1 Characteristic function of a Meixner distribution

Using (3.1) and (3.0.1), the Meixner distribution can be expressed in terms of the characteristic function as follows [25]:

$$
\begin{aligned}
&E[\exp(iuX)] \\
&= \int_{-\infty}^{\infty} \exp(iux) f(x; a, b, d, m) dx \\
&= \int_{-\infty}^{\infty} \exp(iux) \frac{\left(2\cos\frac{b}{2}\right)^{2d}}{2a\pi\Gamma(2d)} \exp\left(\frac{b(x-m)}{a}\right) \left|\Gamma\left(d + \frac{i(x-m)}{a}\right)\right|^2 dx \\
&= \int_{-\infty}^{\infty} \exp\left(\frac{iuxa + b(x-m)}{a}\right) \frac{2^{2d}\left(\cos\frac{b}{2}\right)^{2d}}{2a\pi\Gamma(2d)} \left|\Gamma\left(d + \frac{i(x-m)}{a}\right)\right|^2 dx \\
&= \exp(imu) \left(\cos\frac{b}{2}\right)^{2d} \int_{-\infty}^{\infty} \exp\left(\frac{aiu(x-m) + b(x-m)}{a}\right) \frac{2^{2d}}{2a\pi\Gamma(2d)} \left|\Gamma\left(d + \frac{i(x-m)}{a}\right)\right|^2 dx \\
&= \exp(imu) \left(\cos\frac{b}{2}\right)^{2d} \int_{-\infty}^{\infty} \exp\left(\frac{(aiu + b)(x-m)}{a}\right) \frac{2^{2d}}{2a\pi\Gamma(2d)} \left|\Gamma\left(d + \frac{i(x-m)}{a}\right)\right|^2 dx \\
&= \frac{\exp(imu)\left(\cos\frac{b}{2}\right)^{2d}}{\left(\cos(\frac{aiu+b}{2})\right)^{2d}} \int_{-\infty}^{\infty} \exp\left(\frac{(aiu + b)(x-m)}{a}\right) \frac{\left(2\cos\left(\frac{aiu+b}{2}\right)\right)^{2d}}{2a\pi\Gamma(2d)} \left|\Gamma\left(d + \frac{i(x-m)}{a}\right)\right|^2 dx \qquad (3.2.2) \\
&= \left(\frac{\cos\frac{b}{2}}{\cos(\frac{aiu+b}{2})}\right)^{2d} \exp(imu), \qquad (3.2.3)
\end{aligned}
$$

since the expression inside the integral in (3.2.2) is a probability density function of a Meixner distribution, denoted by $Meixner(a, b^*, d, m)$ (where $b^* = aiu+b$), we deduce that the integral in (3.2.2) is equal to 1.

3.2.2 The moments of the Meixner distribution

By using the characteristic function in (3.2.3), the moments of the Meixner distribution can be derived. Under the Meixner distribution we have

$$
\begin{aligned}
\Psi(u) &= \ln\left(\left(\frac{\cos\frac{b}{2}}{\cos(\frac{aiu+b}{2})}\right)^{2d} \exp(imu)\right) \\
&= 2d \ln\cos\left(\frac{b}{2}\right) - 2d \ln\cos\left(\frac{aui + b}{2}\right) + imu \qquad (3.2.4)
\end{aligned}
$$

3.2.2.1 Mean of the Meixner distribution

From (3.2.4) we have

$$
\Psi'(u) \;=\; (adi)\tan\left(\frac{aui + b}{2}\right) + im
$$

and from (3.0.5), the mean is as follows:

$$E(X) = (ad)\tan\left(\frac{b}{2}\right) + m. \tag{3.2.5}$$

3.2.2.2 Variance of the Meixner distribution

Differentiating (3.2.4) twice we get

$$\Psi''(u) = \frac{-a^2 d}{2}\sec^2\left(\frac{aui+b}{2}\right),$$

and from (3.0.6) it follows that

$$Var(X) = \tfrac{a^2 d}{2}\sec^2\left(\tfrac{b}{2}\right) = \frac{a^2 d}{1+\cos(b)}. \tag{3.2.6}$$

3.2.2.3 Skewness of the Meixner distribution

We differentiate (3.2.4) three times to get

$$\Psi'''(u) = \frac{-ia^3 d}{2}\sec^2\left(\frac{aui+b}{2}\right)\tan\left(\frac{aui+b}{2}\right),$$

and from (3.0.7) and (3.2.6) it follows that (see also [14]):

$$\begin{aligned} Skew(X) &= \frac{\frac{a^3 d}{2}\sec^2\left(\frac{b}{2}\right)\tan\left(\frac{b}{2}\right)}{\left[\frac{a^2 d}{2}\sec^2\left(\frac{b}{2}\right)\right]^{\frac{3}{2}}} \\ &= \frac{\sin b}{1+\cos b}\left(\frac{1}{\sqrt{d\left(\frac{1}{1+\cos b}\right)}}\right) \\ &= \frac{\sin b}{\sqrt{d(1+\cos b)}} \\ &= \frac{2\sin\left(\frac{b}{2}\right)\cos\left(\frac{b}{2}\right)}{\sqrt{d\left(2\cos^2\left(\frac{b}{2}\right)\right)}} \\ &= \sqrt{\frac{2}{d}}\sin\left(\frac{b}{2}\right). \end{aligned} \tag{3.2.7}$$

3.2.2.4 Kurtosis of the Meixner distribution

Kurtosis is the fourth moment of the distribution. The fourth derivative of (3.2.4) yields

$$\Psi^{(4)}(u) = \frac{a^4 d}{4}\sec^2\left(\frac{aui+b}{2}\right)\left[\sec^2\left(\frac{aui+b}{2}\right) + 2\tan^2\left(\frac{aui+b}{2}\right)\right],$$

and from (3.0.8) and (3.2.6) it follows that

$$\begin{aligned} Kurtosis(X) &= \frac{\frac{a^4 d}{4}\sec^2\left(\frac{b}{2}\right)\left[\sec^2\left(\frac{b}{2}\right)+2\tan^2\left(\frac{b}{2}\right)\right]}{\left(\frac{a^2 d}{2}\sec^2\left(\frac{b}{2}\right)\right)^2}+3 \\ &= \frac{\sec^2\left(\frac{b}{2}\right)+2\tan^2\left(\frac{b}{2}\right)}{d\sec^2\left(\frac{b}{2}\right)}+3 \\ &= \frac{2-\cos b}{d}+3. \end{aligned} \tag{3.2.8}$$

3.3 Stochastic process

We define a stochastic process as a collection of random variables $X = \{X_t : t \geq 0\}$ on a probability space $(\Omega, \mathcal{F}, P)$ [4, p. 62]. A stochastic process can be explained as a random process due to the fact that the process models how the random events occur. The behaviour of a stochastic process is defined by a probability distribution. We will show that there is a distribution associated with every stochastic process in the later sections of this chapter.

3.3.1 Independent increments

Suppose we have a stochastic process $X = \{X_t : t \geq 0\}$ and for all t_k where $k = 0, 1, 2, \ldots, n$ and $n \in \mathbb{N}$, such that $0 < t_1 < t_2 < \cdots < t_n$, we say the stochastic process has independent increments if the random variables $X_{t_1} - X_0$, $X_{t_2} - X_{t_1}$, $X_{t_3} - X_{t_2}$, $\ldots$, $X_{t_n} - X_{t_{n-1}}$ are independent [29, p. 88].

3.3.2 Stationary increments

A stochastic process is said to have stationary increments if the distribution of $X_t - X_{t-h}$ does not depend on t for t, $h \geq 0$ [29, p. 88].

3.3.3 Infinitely divisible distribution

According to Cont et al [7, p. 69, Definition 3.2], a distribution F is infinitely divisible on $\mathbb{R}$ if, for any integer $n > 1$, there are n identical and independent random variables X_1, X_2, $X_3, \ldots, X_n$ such that $X_1 + X_2 + \cdots + X_n$ has the distribution F. From this definition we determine whether a distribution F is infinitely divisible by considering its characteristic function. If we define the characteristic function of an infinitely divisible distribution F to be $\Phi(u)$ and the characteristic function of each independent and identically distributed random variables X_1, X_2, $X_3, \ldots, X_n$ to be $\Phi_n(u)$ then we have (see [33, p. 44])

$$\Phi(u) \;=\; [\Phi_n(u)]^n.$$

3.4 Lévy process

A stochastic process $X = \{X_t : t \geq 0\}$ is said to be a Lévy process if [29, p. 104]:

- the initial point of the process is $X_0 = 0$ almost surely,
- the increments are independent and stationary,
- it is stochastic continuous that is, $\lim_{s \to t} P(|X_t - X_s| > \varepsilon) = 0$ for all $\varepsilon > 0$,
- it has paths that are right continuous with left limits (this is referred to as a càdlàg stochastic process).

A Lévy process has a property that its paths have left limits and are right continuous. This is a very important property that allows the process to have countable number of jumps. We consider the paths of a stochastic process $X = \{X_t : t \geq 0\}$ to explain that a Lévy process is a càdlàg stochastic process [32, p. 14]. The left limit of the stochastic path for any $t > s$ (that is the limit of X_s as s approaches t from the left [38, p. 93]) is denoted by

$$X_{t^-} = \lim_{s \to t^-} X_s,$$

and the path is said to have a left limit if X_{t^-}exists. The path is right continuous for any $s > t$ (that is the limit of X_s as s approaches t from the right) if there exists a right limit denoted by

$$X_{t^+} = \lim_{s \to t^+} X_s,$$

such that [38, 121]

$$X_{t^+} = X_t$$

For the paths of the stochastic process to be continuous at any point t, the following holds:

$$X_{t^+} = X_{t^-} = X_t.$$

Since the paths are right continuous with left limits, this allows the existence of jumps at any point t given by $X_t - X_{t^-}$[33, p. 14].

If a process is a Lévy process then it has a distribution that is infinitely divisible and the converse is also true [7, p. 68, Proposition 3.1]. We will use this to determine whether a process is a Lévy process, and we will show that both the Brownian motion and the Meixner process are particular cases of Lévy processes.

We can find the distribution of a Lévy process by using its characteristic function represented by a Lévy-Khintchine formula. For a Lévy process $X = \{X_t : t \geq 0\}$ with a characteristic function given by $\Phi_X(u)$ and $\Psi_X(u) = \ln \Phi_X(u)$ then the Lévy-Khintchine formula is as follows[33, p. 44, Definition 5.1.1]:

$$\Psi_X(u) = i\alpha u - \frac{1}{2}\sigma^2 u^2 + \int_{-\infty}^{\infty} (\exp(iux) - 1 - iux1_{\{|x|<1\}})\nu(dx), \tag{3.4.1}$$

where $\alpha \in \mathbb{R}$, $\sigma^2 \geq 0$ and ν is a Lévy measure that determines the occurrence of the jumps and it satisfies $\nu(\{0\}) = 0$ and

$$\int_{-\infty}^{\infty} (1 \wedge x^2)v(dx) < \infty.$$

This results in a Lévy triplet given by $[\alpha, \sigma^2, \nu]$. From the Lévy-Khintchine formula in (3.4.1), we deduce that, a Lévy process consists of three parts that are independent of each other as follows [33, p.45]:

- a drift part (α),
- a Brownian part (σ^2) and
- a pure jump part (ν) .

3.5 Brownian motion

Brownian motion is associated with Hermite polynomials. This process is most applied in finance, since the most commonly used Black-Scholes model is derived from this process. We discuss the definition, the properties and the moments of the Brownian motion, as well as its connection with orthogonal polynomials.

A stochastic process $X = \{X_t : t \geq 0\}$ is a Brownian motion if [33, p. 25, Definition 3.2.1]

- $X_0 = 0$,
- The increments $X_{t+s} - X_t$ are independent and stationary for $s > 0$,
- $X_{t+s} - X_t \sim Normal(0, s)$,
- The paths of the process are continuous [29, p. 96].

3.5.1 Properties of the Brownian motion

The behaviour of Brownian motion is determined by the normal distribution which is infinitely divisible. We show this by proving that for all $n \in \mathbb{Z}^+$, there are independent and identically distributed random variables $X_1, X_2, \ldots, X_n$ such that the distribution of X is identical to the distribution of $\sum_{k=1}^{n} X_k$ [29, p. 76]. To prove that the distributions between two variables are identical, we show that the characteristic functions of the two random variables are identical. Suppose that $X \sim Normal(\mu, \sigma^2)$ and $X_k \sim Normal(\frac{\mu}{n}, \frac{\sigma^2}{n})$ then

$$\begin{aligned} E\left[it\left(\sum_{k=1}^{n} X_k\right)\right] &= E[\exp(it(X_1 + X_2 + \cdots + X_n))] \\ &= E[\exp(itX_1)\exp(itX_2)\cdots\exp(itX_n)] \end{aligned}$$

and since the random variables $X_1, X_2, \ldots, X_n$ are independent, we have

$$E\left[it\left(\sum_{k=1}^{n} X_k\right)\right] = \prod_{k=1}^{n} E[\exp(itX_k)]$$

and since the random variables are identically distributed, we use (3.1.3) to find

$$\begin{aligned} E\left[it\left(\sum_{k=1}^{n} X_k\right)\right] &= \prod_{k=1}^{n} \exp\left(it\frac{\mu}{n} - \frac{\sigma^2}{2n}t^2\right) \\ &= \exp\left(\sum_{k=1}^{n}\left(it\frac{\mu}{n} - \frac{\sigma^2}{2n}t^2\right)\right) \\ &= \exp\left(it\mu - \frac{1}{2}t^2\sigma^2\right) \\ &= E\left[itX\right]. \end{aligned}$$

We thus proved that a normal distribution is infinitely divisible. As a result, Brownian motion is a Lévy process [7, p. 69, Proposition 3.1].

3.6 The Meixner process

A stochastic process $X = \{X_t : t \geq 0\}$ on a probability space $(\Omega, \mathcal{F}, P)$ is said to be a Meixner process of parameters a, b, d, m (with $a > 0$, $-\pi < b < \pi$, $d > 0$ and $m \in \mathbb{R}$) if [32]:

- $X_0 = 0$,
- X has stationary and independent increments,
- and for each $t > 0$, the random variable X_t has the Meixner distribution $Meixner(a, b, dt, mt)$.
- it has paths that are right continuous with left limits allows the presence of jumps [15].

3.6.1 Lévy triplet of a Meixner process

A Meixner process with a distribution $Meixner(a, b, d, m)$ satisfies a Lévy triplet $(\alpha, 0, v)$ [13, Theorem 1], with

$$\alpha = ad \tan\left(\frac{b}{2}\right) - 2d \int_1^\infty \frac{\cosh\left(\frac{bx}{a}\right)}{\sinh\left(\frac{\pi x}{a}\right)} dx + m \tag{3.6.1}$$

and

$$v(dx) = \frac{d \exp\left(\frac{bx}{a}\right)}{x \sinh\left(\frac{\pi x}{a}\right)} dx. \tag{3.6.2}$$

It can thus be concluded that the Meixner process possesses a drift part indicated by α in (3.6.1) and zero Brownian part, but it has a pure jump part that is driven by the Lévy measure given above as $v(dx)$. The Lévy measure (3.6.2) determines how the jumps happen and on a finite interval we can observe finitely many jumps. For a given interval A, the frequencies of the jumps can be monitored by a Poisson process with a parameter given by $\int_A v(dx)$ [32, p. 7].

3.6.2 The properties of the Meixner process

The behaviour of the Meixner process is determined by the Meixner distribution, hence we derive the properties of the process from its distribution.

3.6.2.1 Semi-heavy tails

The tails of the distribution determine the occurrence of extreme events. If a distribution has semi-heavy tails, its tails turn to zero slowly as compared to the tails of the exponential distribution, that is their tails are heavier than normal distribution tails, but lighter than other non-Gaussian distributions. The positive excess kurtosis of the distribution shows that the distribution has heavy tails.

A Meixner distribution, $Meixner(a, b, d, m)$, has semi-heavy tails [33, p. 63] and the behaviour of the tails is modeled by the probability density function $f(x)$ such that [32]:

$$f(x) = K_- |x|^\rho \exp(-\sigma_- |x|) \text{ as } x \to -\infty, \tag{3.6.3}$$

$$f(x) = K_+ |x|^\rho \exp(-\sigma_+ |x|) \text{ as } x \to +\infty, \tag{3.6.4}$$

for $\rho = 2d - 1$, $\sigma_+ = \frac{\pi - b}{a}$, $\sigma_- = \frac{\pi + b}{a}$ and $K_\pm > 0$.

This is one of the most important properties of the Meixner distribution which is needed in finance applications because most financial asset returns tend to have heavy tails. The Meixner distribution is therefore one of the best candidates to model returns of such assets.

3.6.2.2 Infinitely divisible distribution

If $X_i \sim Meixner(a, b, d_i, m_i)$ for $i = 1, \ldots, n$, with the process being mutually independent, $X_1 + X_2 + \cdots + X_n$ follows a $Meixner(a, b, \sum_{i=1}^{n} d_i, \sum_{i=1}^{n} m_i)$ (for the proof, see [13, Corrolary 1]). This shows that the distribution of a Meixner process is infinitely divisible and it is therefore a Lévy process [7, p. 69, Proposition 3.1].

3.6.2.3 Self-decomposable

A random variable X is self-decomposable if, for all $c \in (0, 1)$, there exists an independent random variable Z_c which satisfies $X = cX + Z_c$ [39, 37].

By using the Lévy measure of the Meixner process (3.6.2) and [13, Corollary 3], we observe that the Meixner process is self-decomposable, since

$$\begin{aligned} & -v(x) - xv'(x) \\ =& \frac{d}{2a}\left(\sinh^{-2}\left(\frac{\pi x}{a}\right)\right)\left[(\pi - b)\exp\left(\left(\frac{b+\pi}{a}\right)x\right) + (b+\pi)\exp\left(\left(\frac{b-\pi}{a}\right)x\right)\right] \\ \geq& 0 \end{aligned}$$

for a, $d > 0$, $x, m \in \mathbb{R}$ and $-\pi < b < \pi$.

Barndorff-Nielsen [2] pointed out that if a process is self-decomposable, then its distribution is infinitely divisible confirming the fact that a Meixner process is a Lévy process.

3.7 The link between Lévy processes and orthogonal polynomials

A σ-field sequence given by $\{\mathcal{F}_t : t \geq 0\}$ is called a filtration if, for all $0 \leq s \leq t$, $\mathcal{F}_s \subseteq \mathcal{F}_t$ [29, p. 108]. A filtration can be interpreted as the information that is available for the process at time t.

A stochastic process defined by $X = \{X_t : t \geq 0\}$ is called a $\{\mathcal{F}_t : t \geq 0\}$-adapted process if, for all $t \geq 0$, X_t is $\mathcal{F}_t$-measurable [29, p. 108].

If a process $X = \{X_t : t \geq 0\}$ is a $\{\mathcal{F}_t : t \geq 0\}$-adapted process that satisfies $E[|X_t|] < \infty$ and $X_s = E[X_t|\mathcal{F}_s]$ for all $0 \leq s \leq t$, then it is a martingale [3, p.504, definition C.1].

Now we can link orthogonal polynomials and Lévy processes by considering the following martingale equality [34]:

$$E(P_n(X_t, t)|X_s) \quad = \quad P_n(X_s, s), \tag{3.7.1}$$

where $0 \leq s \leq t$ and $\{X_t : t \geq 0\}$ is a Lévy process.

3.7.1 Link between Brownian motion and Hermite polynomials

Comparing the weight function of Hermite polynomials in (2.2.1) and the probability density function of a normal distribution in (3.1.1), we conclude that the weight function of Hermite polynomials is equivalent to a normal distribution denoted by $Normal(0, \frac{1}{2})$.

The monic Hermite polynomials $\{H_n : n = 0, 1, 2, \ldots\}$ are martingales for a Brownian motion $\{X_t : t \geq 0\}$ [32]:

$$E[H_n(X_t; t)|X_s] = H_n(X_s; s), \tag{3.7.2}$$

where $0 \leq s \leq t$.

3.7.2 Link between the Meixner process and Meixner-Pollaczek polynomials

The probability density function of a Meixner distribution in (3.2.1) is equivalent to the weight function of the Meixner-Pollaczek polynomials in (2.3.1). This shows that the weight function of the Meixner-Pollaczek polynomials is a probability density function of the Meixner distribution $Meixner(1, 2\theta - \pi, \lambda, 0)$.

Monic Meixner-Pollaczek polynomials $\{P_n^\lambda : \lambda > 0,\ n = 0, 1, 2...\}$
are martingales for the Meixner process $\{X_t : t \geq t\}$ for $0 \leq s \leq t$ [32]: :

$$P_n^\lambda(X_s, s) = E[P_n^\lambda(X_t, t)|X_s]. \tag{3.7.3}$$

Chapter 4

Fitting the processes to the log returns

Derivatives derive their prices from the price of the underlying asset which may be anything tradable or non-tradable, but in this dissertation we choose the underlying asset to be share indices or shares with no dividend payments. In this chapter we focus on fitting the distributions to the log returns data. We fit the Meixner and normal distribution to the log returns of stock indices (see [32] and [14]). The results in this chapter makes reference to appendix B.

4.1 Fitting the distributions to the returns of the shares

Since both the Meixner process and Brownian motion belong to the family of Lévy processes, the returns can be calculated using exponential Lévy processes as follows [32]:

$$S_t = S_0 \exp(X_t),\ t > 0 \tag{4.1.1}$$

where X_t is a Lévy process and therefore

$$X_t = \ln\left(\frac{S_t}{S_0}\right). \tag{4.1.2}$$

For time $0 < t < t + h$, where $h > 0$ is a time change, we have

$$\begin{aligned} X_{t+h} - X_t &= \ln\left(\frac{S_{t+h}}{S_0}\right) - \ln\left(\frac{S_t}{S_0}\right) \\ &= \ln\left(\frac{S_{t+h}}{S_t}\right). \end{aligned}$$

By using the expression in (4.1.2), we find the log returns of investing in shares by using a Lévy process. This will be illustrated in the following sections of this chapter.

4.1.1 General features of share prices and log returns data

We need to analyse the features of the data in order to determine the distribution that gives a good fit. The key areas are the measurements of the central tendency (the average), the skewness (whether the data is symmetric or not), the kurtosis (whether there are heavy tails in the data or not) and the spread of the data (variance). We will consider the graphs for the share index and the log returns and further check the goodness of fit of the Meixner and normal distributions. This will assist in defining the process that governs the prices of the options further on in the dissertation.

By using the S&P 500 share index data from 29 April 2013 to 27 April 2018, we determine the fit of the distributions [42]. The data consists of 1259 daily returns obtained by using the log of the daily share prices. We will use the terminology "log returns" and "returns" interchangeably to represent the returns from investing in the shares, calculated using (4.1.2).

Figure 4.1: S&P500 share index determined by closing prices

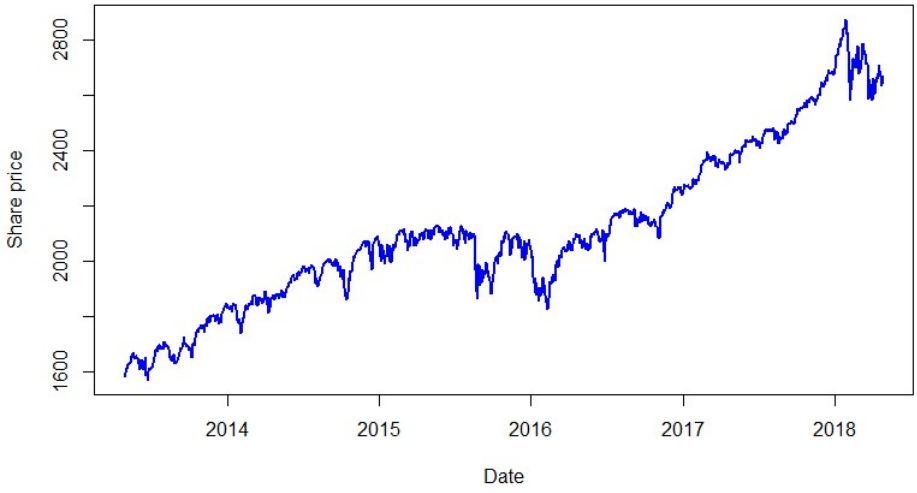

Figure 4.2: Log returns of the S&P500 share index

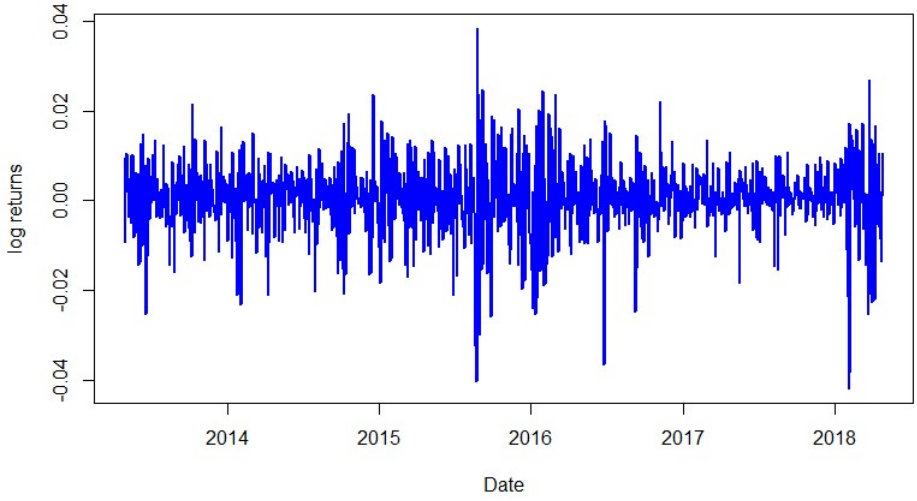

In Figure 4.1 we show the closing prices of the S&P500 share index and in Figure 4.2 we show the log returns of the S&P500 share index. From Figure 4.1 we deduce that the returns are fluctuating continuously with 2015 and 2018 experiencing significant fluctuations (high volatility). Evidently there is a positive drift in the growth of the share index prices. By considering the log of the daily share index prices we can fit a distribution that models the behaviour of the process driving the returns.

In Table 4.1 we give the values of the sample moments and we observe that the data has an excess kurtosis higher than that of a normal distribution (which is zero) and this shows the presence of outliers in the log returns data. Contrary to the expectation that the data is symmetric around the mean, the table shows that returns are negatively skewed and this is also justified by a sample mean (0.0004099) which is less than the median (0.0004925), which makes normal distribution more unlikely to fit the data.

Table 4.1: Moments of the returns data

Sample moments	Values
Sample mean	0.0004099
Sample variance	0.00006232
Simple skewness	-0.5726
Sample kurtosis	6.269

In Figure 4.3 we illustrate the distribution of the log returns by using a box plot and we observe that there are many outliers on the negative side of the tail as compared to the positive side. Checking the box itself, it does not justify a large skewness. A distribution that may be a best fit for this data is thus slightly negatively skewed and must portray tendencies of heavy tails as depicted by the large number of outliers indicated in the box plot.

Figure 4.3: Box plot for the log returns

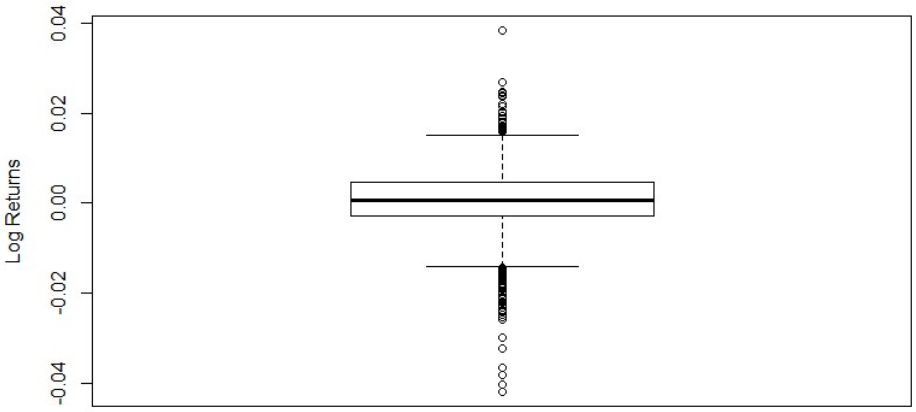

4.1.2 Estimation of parameters

We use the moments from Table 4.1 to fit data using the normal and Meixner distributions. We apply the method of moments method which equates the sample moments to the theoretical formula of the moments for the distribution [9, p. 350]. Fitting the normal distribution is the easiest since it has only two parameters (mean and variance). We will use the following notation:

- $\bar{x}$ - sample mean
- s^2- sample variance
- b_1- sample skewness
- b_2- sample kurtosis.

By using this notation we update Table 4.1 to get Table 4.2 and these values are used for parameter estimation. To estimate the parameters of the normal distribution by method of moments, we equate $\hat{\mu} = \bar{x}$ and $\hat{\sigma}^2 = s^2$.

Table 4.2: Sample estimates of moments

Sample moments	Values
$\bar{x}$	0.0004099
s^2	0.00006232
b_1	-0.5726
b_2	6.269

We also apply method of moments to the Meixner distribution to obtain [14]

$$\bar{x} = \hat{a}\hat{d}\tan\left(\frac{\hat{b}}{2}\right) + \hat{m}, \text{ that is, } \hat{m} = \bar{x} - \hat{a}\hat{d}\tan\left(\frac{\hat{b}}{2}\right)$$

$$s^2 = \frac{\hat{a}^2\hat{d}}{1+\cos\hat{b}}, \text{ that is, } \hat{a} = \sqrt{s^2\left(\frac{\cos\hat{b}+1}{\hat{d}}\right)}$$

$$b_1 = \frac{\sin\hat{b}}{\sqrt{\hat{d}(1+\cos\hat{b})}}$$

$$b_2 = 3 + \frac{2-\cos\hat{b}}{\hat{d}}$$

Solving the last two equations requires some algebra, but they can be simplified to obtain the following [14]:

$$\hat{d} = \frac{1}{b_2 - b_1^2 - 3}$$

$$\hat{b} \quad = \quad \text{sign}(b_1)\arccos(2 - \hat{d}(b_2 - 3))$$

Using the above equations and the values of the sample moments in Table 4.2, the parameters of the Meixner distribution are estimated as shown in Table 4.3. The value of the estimate of b is negative which shows that the distribution is negatively skewed and the estimate of d is also small, which shows a higher kurtosis. This indicates that the Meixner distribution may give a better fit to the log returns data than the normal distribution.

Table 4.3: Estimated parameters of the Meixner distribution

Estimated parameters	Values
$\hat{a}$	0.01860
$\hat{b}$	-0.4767
$\hat{d}$	0.3400
$\hat{m}$	0.001947

Since we succeeded in estimating the parameters of both the Meixner and the normal distribution, we now compare the curves of the two distributions using the estimated parameters. This will illustrate the concepts stated before about kurtosis and heavy tails. Figure 4.4 compares the Meixner and normal distribution of log returns while Figure 4.5 compares the tails of the two distributions.

Figure 4.4: Meixner (bold) and normal (dashed) probability density functions

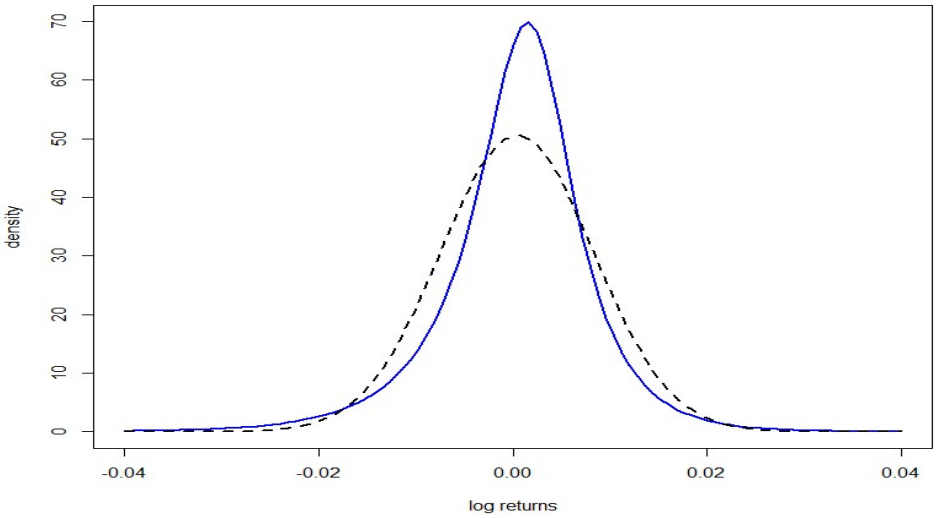

According to Figure 4.4, more returns are expected to be around the central point under the Meixner distribution and this is more than depicted by the normal distribution. This shows that there is a higher peak (a higher kurtosis) under the Meixner distribution than under the normal distribution. From Table 4.1 there is an excess kurtosis which justifies preferring the

Meixner distribution to the normal distribution. In Figure 4.5a as we move from log returns values of -0.01 to -0.05, the dashed line which represents the normal distribution, is initially above the solid line for the Meixner distribution, but it falls quicker than the solid line. This slow movement of the Meixner distribution towards zero is indicating the presence of a heavy left tail. In Figure 4.5b we observe that the normal distribution is initially higher than the Meixner distribution, but decreases to zero faster than the Meixner distribution and this is an indication that the right tail of the Meixner distribution is heavier than that of the normal distribution. This supports the property of semi-heavy tails for a Meixner distribution.

Figure 4.5: Tails for normal (dashed) and Meixner (bold) probability density functions

(a) Left tails

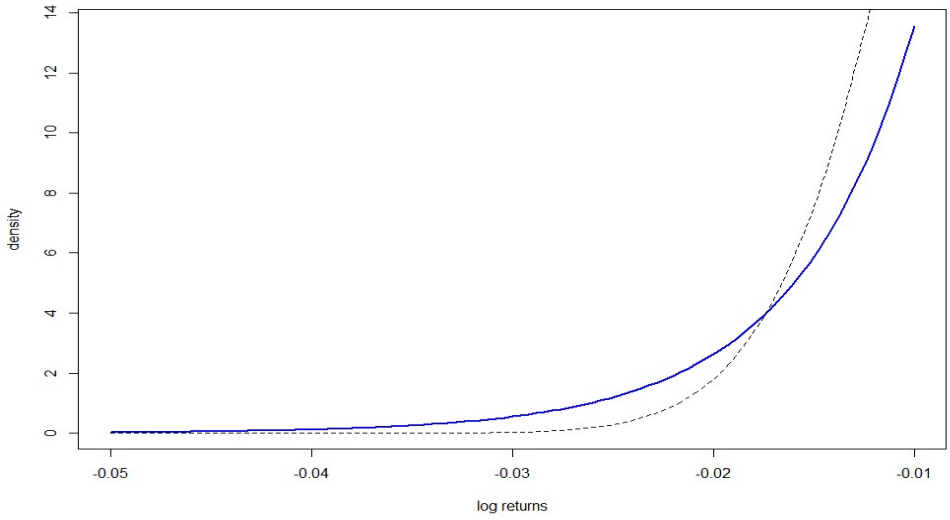

(b) Right tails

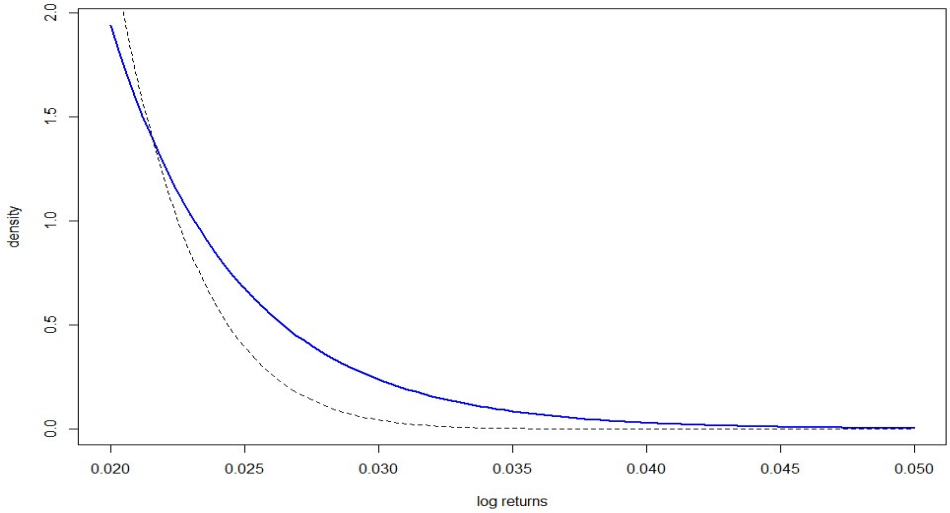

4.2 Measurement of goodness of fit

Generally several methods can be used to investigate if the chosen distributions are showing goodness of fit. In this section we restrict our focus to few basic methods:

- plotting histograms and distribution curves,
- quantile-quantile (q-q) plots and
- chi-squared test.

4.2.1 Goodness of fit by histograms

In Figure 4.6 we show the curves for the normal and Meixner distribution together with the histogram for the log returns of the S&P500 share index data. We observe that there is an improvement when fitting a Meixner distribution curve over the normal distribution curve. It is clear that there is more data around the center which exceeds the normal distribution curve. Furthermore, the tails of the data are thicker than in the normal distribution curve, which indicates leptokurtosis of the data (higher peak and heavy tails). Between log returns intervals $(-0.02, -0.01)$ and $(0.01, 0.02)$, many bars in the histogram are lower than the curve of the normal distribution and this shows a poor fit to the data. We observe that most of the log returns data can be fit by a Meixner curve. It is worth noting that even though the Meixner curve is showing an improved fit, there are still some returns data that are lying outside the curve.

Figure 4.6: Histogram overlayed with Meixner (solid) and normal (dashed) probability density functions

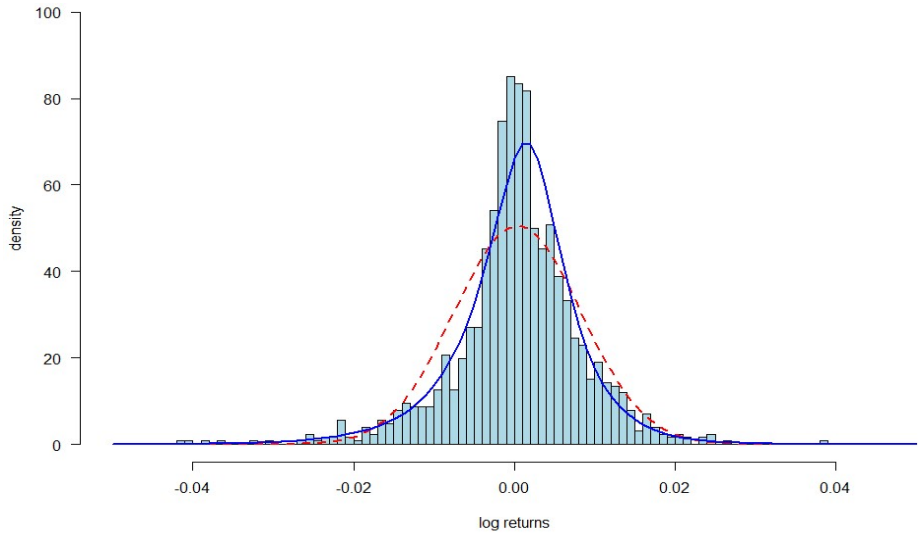

4.2.2 Quantile-Quantile plots

A quantile-quantile plot (q-q plot) is a graphical presentation that shows the plots of the empirical quantiles (also known as percentiles) against the theoretical quantiles of the distribution. We will show the q-q plots under the normal and Meixner distribution. If the data

represents a good fit, the theoretical and the empirical quantiles will lie along the straight line and deviations from the line imply that the distribution is not a proper fit [26].

In Figure 4.7a we plot the q-q plots for the normal distribution using the log returns data for the S&P500 share index. From the graph it is evident that both tails of the distribution are deviating from the straight line showing the presence of heavy tails on the data which can not be detected by the normal distribution. The plot also shows that the other points are close to the line, even though they still deviates from the line and this makes it difficult to conclude any associations of the normal distribution with the data. Taking a closer look at the left tail (the negative tail), the points are heavily pulled away from the straight line as compared to the right tail and it is clear that the data from the log returns is negatively skewed. Under a normal distribution, the data is supposed to be symmetric, which is far from being the case here, therefore it can be concluded that the normal distribution gives a poor fit to the data.

In Figure 4.7b we plot the q-q plots for the Meixner distribution for the log returns of S&P500 share index. We observe that most empirical quantiles are very close the theoretical quantiles (most points are lying along the straight line), which shows a better fit under the Meixner distribution as compared to the normal distribution. It is crucial to note that it is highly unlikely to find a distribution that fits the data completely but we can choose a distribution that gives a better fit.

Figure 4.7: Q-Q plots for the S&P500 log returns

(a) normal distribution

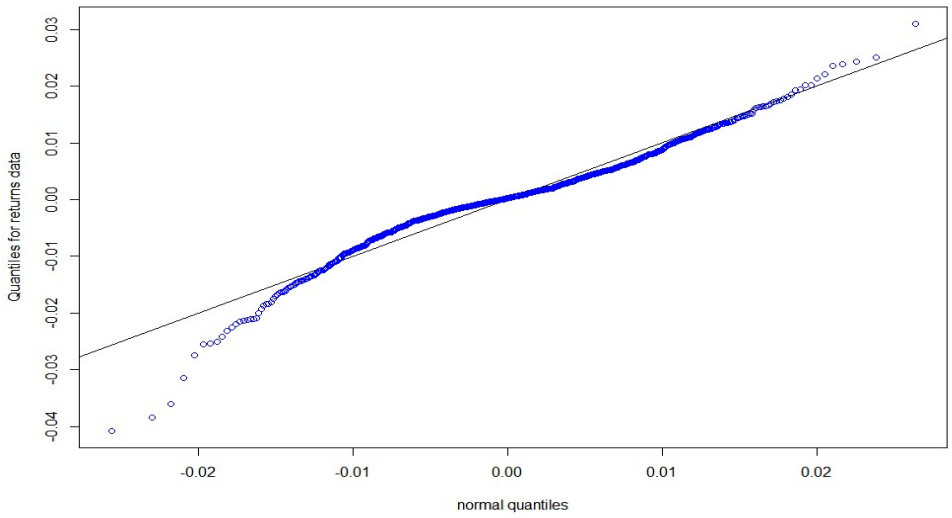

(b) Meixner distribution

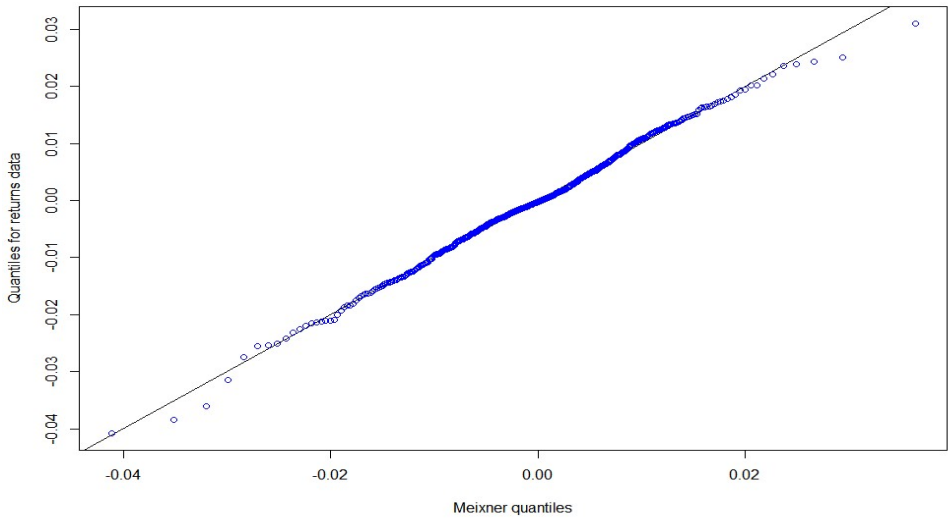

4.2.3 Chi-squared test

A chi-squared test differs from the two previous tests as it uses a hypothesis test to determine the goodness of fit. We classify the log returns data into categories and we calculate the measure of the differences between the observed frequencies of falling in a category and expected frequencies from a specified distribution under a given null hypothesis. A chi-squared test is a very important goodness of fit test but it has several limitations as compared to other goodness of fit tests like q-q plots. A chi-squared test on continuous data depends on the intervals chosen which compromises the results of the test. The test will not work properly if the expected frequency of observations is less than 5 [9, p. 729].

We divide the log returns data for the S&P500 share index into 50 intervals and we define

the following:

- O_i denotes the observed frequencies of being in interval i.
- E_i denotes the expected frequencies of being in interval i.

The null and alternative hypothesis are defined as follows:

H_0 : The log returns data follows a given distribution (normal or Meixner distribution)
H_a : The log returns data does not follow a given distribution (normal or Meixner distribution).

We define the test statistic as follows [9, p. 726]:

$$\chi^2 \;=\; \sum_{i=1}^{50} \frac{(O_i - E_i)^2}{E_i}.$$

We reject the null hypothesis if [9, p. 726]

$$\chi^2 \;\geq\; \chi^2_{0.05;50-k-1},$$

where $\chi^2_{0.05;50-k-1}$ is a critical value at a 5% significance level with degrees of freedom (d.f.) being given by $50-k-1$ (k denotes the number of estimated parameters). Under the normal distribution case we estimate two parameters hence we have 47 degrees of freedom, while under the Meixner distribution case we estimate four parameters hence we have 45 degrees of freedom. The null hypothesis is also rejected when the probability value under a null hypothesis (p-value) is less than the 5% significance level.

Table 4.4 shows the chi-squared test using data from S&P500 share index. We observe that under a 5% level of significance there is no sufficient evidence to reject the null hypothesis which says the log returns data of the S&P500 share index follows a Meixner distribution but we reject the null hypothesis that says log returns data is normally distributed.

Table 4.4: Chi-squared test for the S&P500 log returns

Fitted distribution	Test static (χ^2)	d.f.	Critical value	p-value	Decision
Normal	276.4790	47	64.0011	<0.0001	Reject
Meixner	61.4800	45	61.6562	0.0516	Do not reject

4.2.4 Hypothesis testing for normality

Through the use of histograms and quantile-quantile plots we have observed that a Meixner distribution gives a better fit to the data for the log returns than a normal distribution. In this section we do a hypothesis testing to find out if we have sufficient evidence to reject the null hypothesis that the data for the log returns is normally distributed (see the appendix A for the Shapiro-Wilk test for normality).

H_0 : The log returns data for the S&P500 share index is normally distributed.
H_a : The log returns data for the S&P500 share index is not normally distributed.

Table 4.5 shows the Shapiro-Wilk test for normality. Under a 5% significant level we only fail to reject the null hypothesis provided that the probability value (p-value) is sufficiently greater than 5%. The Shapiro-Wilk test in Table 4.5 shows that the p-value (< 0.0001) is significantly lower than 0.05, indicating that there is sufficient evidence to reject the null hypothesis of saying the S&P500 log returns are normally distributed. The hypothesis test gives us the same conclusion as the histogram and q-q plot.

Table 4.5: Hypothesis test for normality of S&P500 log returns data

Test	Statistic		P-value	
Shapiro-Wilk	W	0.952984	Pr $<$ W	< 0.0001

4.3 Fitting the models to the South African market

In this section we apply Brownian motion and the Meixner process to the emerging markets of South Africa. The main aim is to observe the differences that may exist in comparison to the United States market. We will use the data extracted from two Johannesburg stock exchange (JSE) indices, which are FTSE/JSE All Share and FTSE/JSE Top 40 [18]. We use 1 year worth of daily share index data from 09 October 2017 to 08 October 2018. Table 4.6 shows the sample moments for the two indices. The two processes mentioned above are fit to the log returns of the two indices.

Table 4.6: Moments for the South African JSE indices

Sample moments	FTSE/JSE All Share	FTSE/JSE Top 40
Sample mean	-0.0002371	-0.0002643
Sample standard deviation	0.009190	0.0099
Sample skewness	-0.01792	-0.06617
Sample excess kurtosis	1.846	1.833

Table 4.7: Normality test for the JSE indices

Index	Test	Statistics		P-value	
FTSE/JSE All Share	Shapiro-Wilk	W	0.9776	Pr $<$ W	0.0006
FTSE/JSE Top 40	Shapiro-Wilk	W	0.9765	Pr $<$ W	0.0004

From Table 4.6 we observe that the log returns data from both indices are showing negative skewness and a positive excess kurtosis (which indicates heavy tails and higher peaks for the log returns data). A test for normality, under the hypothesis that the log returns data follows a normal distribution, is shown in Table 4.7. Under 5% confidence level we reject the null hypothesis for both indices since the p-values are all less than 0.05. This shows that the log returns for both indices do not follow a normal distribution.

4.3.1 Goodness of fit

In Table 4.8 we show the values of the estimated parameters of the normal and Meixner distribution by making use of the one year historical data of the South African indices, FTSE/JSE All Share and FTSE/JSE Top 40 [18]. As before, we apply the method of moments by matching sample moments to the population moments.

Table 4.8: Estimated parameters for the normal and Meixner distribution for log returns on JSE indices

Model	Estimated parameters	FTSE/JSE All Share	FTSE/JSE Top 40
Normal	$\hat{\mu}$	-0.0002371	-0.002643
	$\hat{\sigma}$	0.009190	0.009946
Meixner	$\hat{a}$	0.01765	0.01901
	$\hat{b}$	-0.01865	-0.06921
	$\hat{d}$	0.5419	0.5468
	$\hat{m}$	-0.0001479	0.00009560

In Figures 4.8 and 4.9 we fit the two distributions to the log returns of JSE indices and we observe that a Meixner distribution is a better fit to the log returns, but both distributions are not able to capture few large log returns on the tails of the distributions indicating that the log returns tails are heavier than the tails of the distributions we are fitting. The negative skewness is mostly visible on the log returns of FTSE/JSE Top 40 log returns and the Meixner distribution manages to capture this as shown in Figure 4.9. The histograms are showing that the Meixner distribution is a better alternative of the normal distribution on fitting log returns for both indices.

Figure 4.8: Histogram of FTSE/JSE All Share log returns overlayed by the normal (dashed) and Meixner (bold) probability density functions

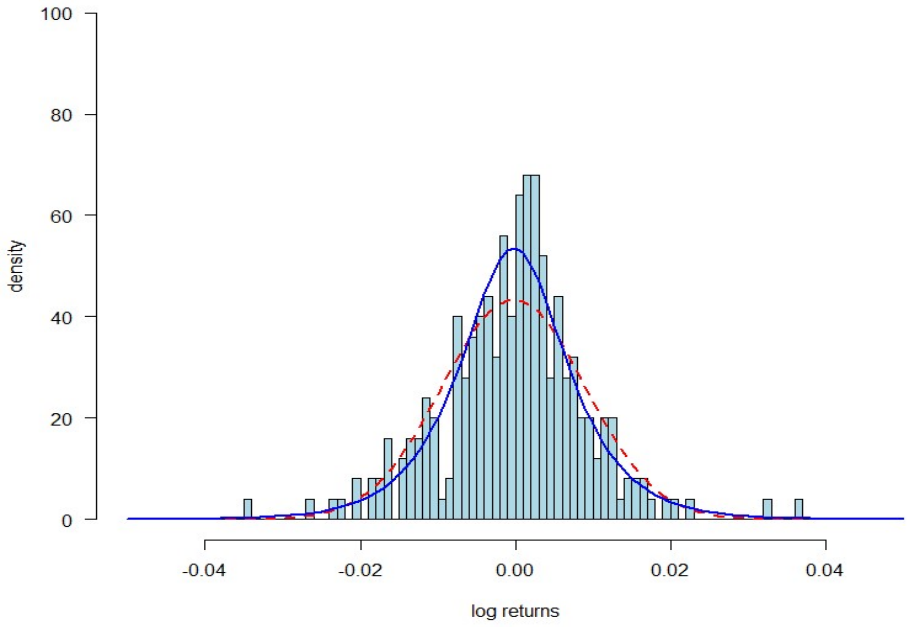

Figure 4.9: Histogram of FTSE/JSE Top 40 log returns overlayed by the normal and Meixner probability density functions

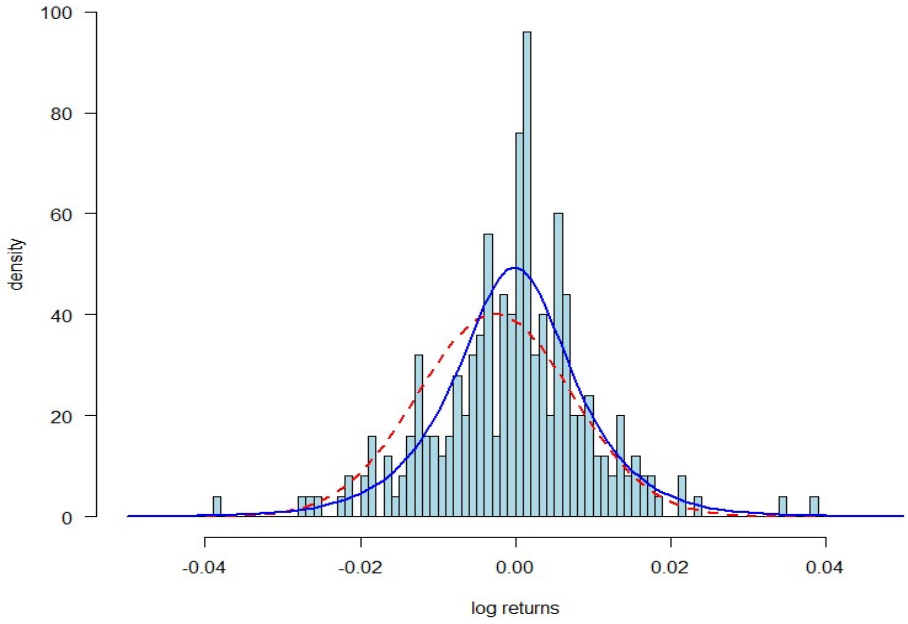

In Figure 4.10 and 4.11 we plot the q-q plots for both distributions to the JSE indices. In Figure 4.10 we see that none of the distributions fits the data well, although the Meixner distribution gives a better fit than normal distribution since many circles are diverting from the line under the normal distribution while under Meixner distribution most circles are close to the line. In Figure 4.11 we observe that the Meixner distribution is a good fit even though its tails are not as heavy as the log returns data, while the normal distribution is not a good fit because its empirical quantiles are different from the theoretical quantiles. It can be argued that another distribution with heavier tails may give a better fit than the Meixner distribution.

Figure 4.10: FTSE/JSE All Shares q-q plots

(a) Normal q-q plots

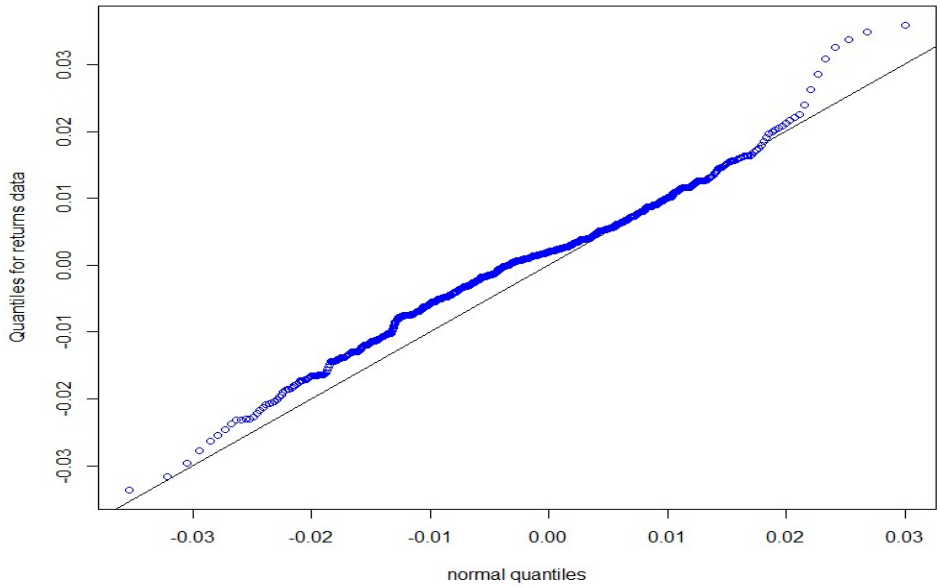

(b) Meixner q-q plots

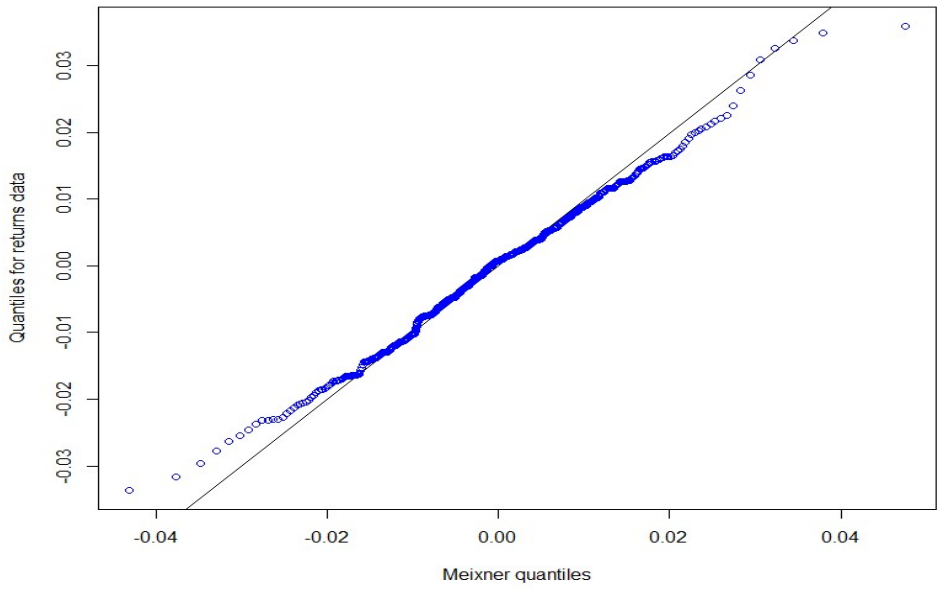

Figure 4.11: FTSE/JSE Top 40 q-q plots

(a) Normal q-q plots

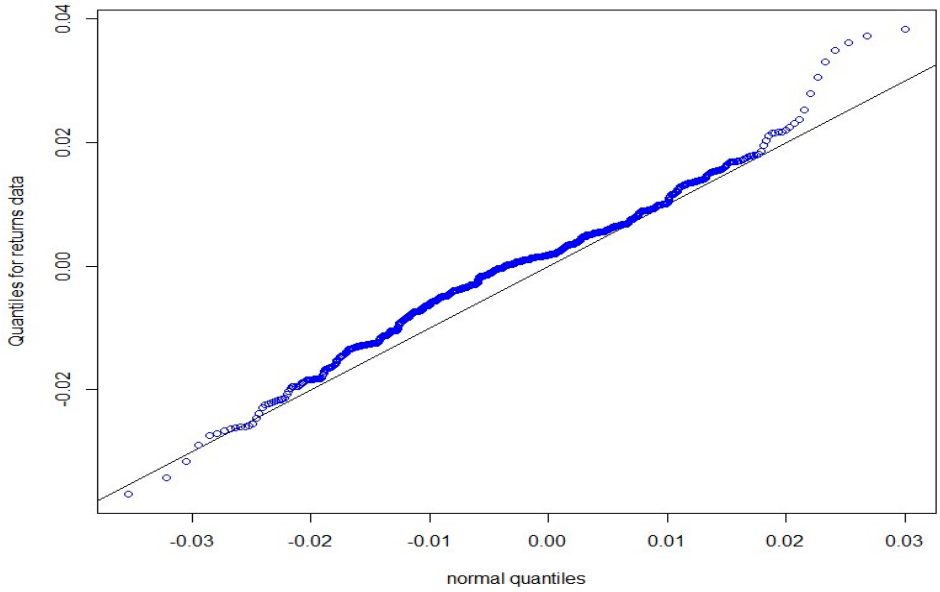

(b) Meixner q-q plots

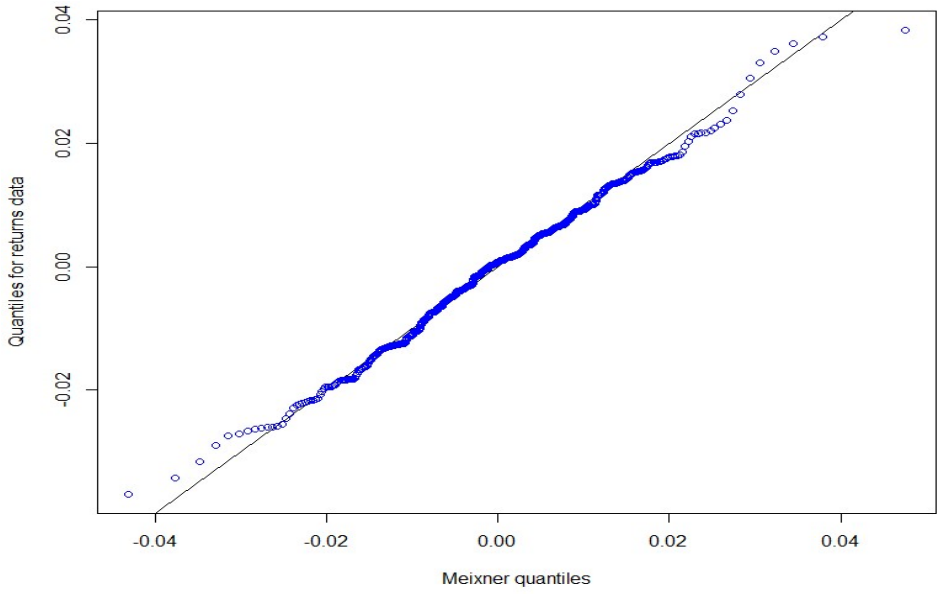

In Tables 4.9 and 4.10 we show the goodness of fit using chi-squared test for JSE indices. We observe that the chi-squared test for the JSE All Share index gives results that contradicts the goodness of fit tests above. In this case we adopt the results from the q-q plots because both the histogram and chi-squared test have a weakness of depending heavily on the choice of the intervals of the data being considered. The chi-squared test for the JSE Top 40 index results are consistent with the histogram and q-q plots that is, we reject the null hypothesis of normality of log returns but we do not reject the null hypothesis that log returns data follows a Meixner distribution.

Table 4.9: Chi-square test for JSE All Share index

Fitted distribution	Test statistic (χ^2)	Critical value	d.f.	p-value	Decision
Normal	16.3150	21.0261	12	0.17723	Do not reject
Meixner	9.2946	18.3070	10	0.50439	Do not reject

Table 4.10: Chi-square test for JSE Top 40 index

Fitted distribution	Test Statistic (χ^2)	d.f.	Critical value	p-value	Decision
Normal	36.3363	12	21.0261	0.0003	Reject
Meixner	13.0614	10	18.3070	0.2203	Do not reject

Chapter 5

Pricing of options

5.1 Option contract

An option contract is an agreement that involves a seller (sometimes called the writer) and a buyer (option holder). Under a call option contract the seller grants the buyer the right, without any obligation, to buy the underlying asset at a specified price (the strike price), within a given time duration (time to maturity) in return for a premium (sometimes referred to as the option price), while under a put option contract the writer gives the holder the right (with no obligation) to sell an underlying asset at an agreed price and duration [16, p. 6]. Underlying assets may be in the form of shares or a share index. Some options are only exercised at maturity of the contract (European options), while others are exercised at any time (American options). When an option contract is exercised, the option holder receives a payoff, which is the cash flow that the holder gains from exercising the right granted by the seller. Vanilla options are those with payoffs given by either $\max\{S_T - K, 0\}$ (for vanilla call options) or $\max\{K - S_T, 0\}$ (for vanilla put options) [29, p. 142]. K represents the strike price and S_T is the value of the underlying asset at time T.

Under a call option, a rational option holder will only exercise it if its payoff is positive, that is if the price of the underlying asset is greater than the strike price. For the put option it is rational to exercise the option if the strike price is greater than the price of the underlying asset. Table 5.1 illustrates this.

Table 5.1: The payoffs for vanilla call and vanilla put options at maturity

Vanilla option	$S_T < K$	$S_T > K$
Call	0	$S_T - K$
Put	$K - S_T$	0

5.2 Pricing of European vanilla call options

As mentioned before, to acquire the right under the option contract, the buyer will have to pay a premium. This premium is always non-negative to compensate for the non-binding nature (no obligation to exercise) of the option contract [3, p. 3]. We need to determine

the price of the option that will ensure that there is no arbitrage opportunity available. An arbitrage opportunity arises if one can start at time $t = 0$ with no capital, but there is a zero probability of losing more and there is a positive probability of making some positive returns. In this section we consider the pricing of European vanilla options. We will use the distributions fitted to the log returns in the previous chapter. As we have noticed in previous chapters, the two processes governing the log returns discussed above belong to the family of Lévy processes, hence we are going to price European vanilla options by using Lévy processes.

We are considering a market that has a riskless asset (for example a bond), with a price given by the process $B_t = e^{rt}$ and a risky asset (for example a stock or a stock index), with a price defined by a process S_t as in (4.1.1) [32]. Here r is the risk-free interest rate and t is the time.

The log returns given by $\ln(\frac{S_{t+s}}{S_t})$ of the price model above follows a distribution of stationary increments of time length s (that is $(t+s)-t$) of a Lévy process. Pricing models for financial assets that adopt Lévy processes like the Meixner process are able to capture large price changes that usually happen since they incorporate jumps. Geman et al [12] put forward a suggestion that pricing models should have a jump component but the diffusion component is not a necessary condition. A diffusion component is responsible for capturing very small movements in prices of financial assets that tend to happen more frequently [33, p. 76]. A Meixner process is an infinite activity Lévy process (that is for a Lévy measure $\nu(dx)$, we have $\int_{\mathbb{R}} \nu(dx) = \infty$ (see [33, p. 76])), hence it can capture the jumps in prices and small price movements that are frequent. Schoutens [33, p. 76] pointed out that adding the diffusion component for returns does not improve the performance of the model.

By ensuring that a no-arbitrage assumption holds, we model the prices of options. We build the pricing models under the risk-neutral framework (for more explanations see [5] and [8]). We consider a risk-neutral probability measure referred to as a martingale measure $\mathbb{Q}$, that is equivalent to the historical (original) probability measure $\mathbb{P}$, such that the discounted price of the underlying asset is a martingale, that is $S_0 = E^{\mathbb{Q}}(e^{-rt}S_t)$ [32]. A σ-field sequence given by $\{\mathcal{F}_t : t \geq 0\}$ is called a filtration if, for all $0 \leq s \leq t$, $\mathcal{F}_s \subseteq \mathcal{F}_t$ [29, p. 108]. A stochastic process $X = \{X_t : 0 \leq t \leq T\}$ is a martingale if X is adapted to the filtration $\mathcal{F}_t$ at time t with $E[|X_t|] < \infty$ for all $t \in [0, T]$ and for all $s > t$ such that $E[X_s|\mathcal{F}_t] = X_t$ [7, p. 41]. We see a martingale as a process that is constant under the conditional expected value [3, p. 32]. It is very important to note that a no-arbitrage assumption will only hold if and only if a martingale measure $\mathbb{Q}$ exists [3, p. 141, Theorem 10.5, First Fundamental Theorem]. For in-depth explanations of the equivalence of $\mathbb{Q}$ and $\mathbb{P}$ as well as martingales, we refer the reader to Björk [3, pp. 32 and 504-512].

The call option price C_t, under the no-arbitrage assumption, is given by the martingale pricing formula [32]

$$C_t = E^{\mathbb{Q}}[\exp(-r(T-t))\max(S_T - K, 0)|\mathcal{F}_t], \text{ for } 0 \leq t \leq T. \tag{5.2.1}$$

5.2.1 Pricing models

On this dissertation we are focusing on two option pricing models which are the Meixner model and the normal (Black-Scholes) model. The Meixner model is the pricing model that assumes that log returns of the underlying asset are modeled by a Meixner distribution while the Black-Scholes model assumes that the log returns of the underlying asset are modeled by a normal distribution. The Meixner model allows jumps (since a Meixner process' paths have left limits and they are right continuous) which allows it to capture large price changes. This differs from the Black-Scholes model that is modelled by Brownian motion with continuous paths.

The following are some of the assumptions we have adopted for both models [32, p. 8]:

- market option prices are determined by demand and supply of options hence one financial agent cannot influence the price. This eliminates the possibility of one or a group of financial agents monopolising the option trading;
- there is no-arbitrage;
- there are no dividends payable on the underlying assets;
- volatility of log returns of the underlying asset is constant throughout the duration of the option contract;
- the market is frictionless, which implies that we ignore all trading costs like taxes and margin payments;
- the market is liquid, which makes the options highly tradable and we eliminate the possibility of delays on transactions;
- short selling is allowed;
- both parties involved in the option agreement are looking for profitable gains, hence more is better;
- trading parties do not default;
- information is available for all traders, which eliminates the possibility of inside trading being of any advantage.

5.2.2 Deriving the price of the put option from a call option

It is possible to find the price of European put options P_t from the price of European call options C_t in (5.2.1) by using the put-call parity [16, p. 174]

$$P_t = C_t + Ke^{-r(T-t)} - S_t, \text{ for } 0 \leq t \leq T. \tag{5.2.2}$$

We show that (5.2.2) holds by constructing two portfolios. The first portfolio will have a long position on a European put option, while the second portfolio will have long position on a European call option, short position on a stock and a bank investment that pays amount

K at time T. Under the assumption that both the call option and the put option have the same maturity and strike price, the two portfolios will yield the same value at maturity regardless of the movement of the stock prices, as shown in Table 5.2. Therefore, under the no-arbitrage assumption the prices of the two portfolios are supposed to be the same which gives us (5.2.2). If this fails to hold, we will have an arbitrage opportunity.

Table 5.2: Pay-off table showing put-call parity

Portfolio	$S_T > K$	$S_T < K$
P_t	0	$K - S_T$
$C_t + Ke^{-r(T-t)} - S_t$	$(S_T - K) + K - S_T = 0$	$0 + K - S_T = K - S_T$

5.2.3 Self-financing strategy

For a given stock price process $\{S(t) : t \geq 0\}$, if we ignore consumption, a portfolio value $V^m(t) = \sum_{k=1}^{N} m_k(t)S_k(t)$ at time t, is said to be self-financing if [3, p. 87, Definition 6.2]

$$dV^m(t) \quad = \quad \sum_{k=1}^{N} m_k(t)dS_k(t),$$

where:

- N denotes different types of stocks,
- $m_k(t)$ denotes number of stocks of type k held at time t,
- m is the portfolio $[m_1(t), m_2(t), ..., m_N(t)]$,
- $S_k(t)$ denotes the price of stock of type k at time t.

5.2.4 Completeness, no-arbitrage and hedging

We will show why an option pricing model based on the Meixner process (Meixner model) is incomplete while the model based on the Brownian motion (Black-Scholes or normal model) is both complete and arbitrage free. It is worth noting that completeness and no-arbitrage behave in an opposite manner (see [3, p. 122]).

Suppose N represents the number of tradable underlying assets (excluding the risk-free asset) and R denotes the sources of the randomness of the pricing model then by the Meta-theorem [3, p. 122, Theorem 8.3.1]:

- there is no-arbitrage if and only if $R \geq N$,
- there is completeness if and only if $R \leq N$,
- both completeness and no-arbitrage exists when $R = N$.

We now check our models for both completeness and no-arbitrage. Under the normal or Black-Scholes model we have one underlying asset (stock or stock index) and we have one random source which is a Brownian motion that drives the price of options. This shows that $R = N = 1$ which implies that the model is complete and there is no-arbitrage. The Meixner model has only one underlying asset (stock or stock index) but it has two processes that bring in the randomness of the model which are the Poisson process, that governs the frequencies of the jumps, and the Meixner process, that governs the price of the underlying assets. In this case $R = 2 > N = 1$. This shows that the model has no-arbitrage but it is not complete. The number of random sources under the Meixner model can be more than two if we relax some of the assumptions on the model. Suppose we allow friction to be available in the market, then there is another random source that models the sources of friction. Several models modeled by Lévy processes are incomplete and the Black-Scholes model is an exception.

The knowledge of completeness of a model will help us to check if it is possible to use the model to hedge a portfolio. A portfolio can be hedged if it can be replicated by another self-financing portfolio and also, if a portfolio can be hedged, then the market is said to be complete [3, p. 115, Definition 8.1]. Now the contrapositive implies that, if the market is not complete, then a portfolio cannot be perfectly hedged. This means that under the Black-Scholes world a portfolio can be hedged, whilst if we adopt the Meixner model pricing which is incomplete, then we cannot achieve a perfect hedge of a portfolio. Since the Meixner model pricing is incomplete, there are multiple martingale measures that give prices that are arbitrage free (see [3, p. 36, Proposition 3.14, Second Fundamental Theorem]), hence we have to adopt only one martingale measure and ensure that the prices from the model are always corresponding to the market prices through a calibration process.

5.2.5 Equivalent martingale measures by mean-correcting of the exponential of a Lévy process

As pointed out already, we need to use the martingale measure $\mathbb{Q}$ instead of the original probability measures $\mathbb{P}$ to arrive at risk-neutral probabilities. There are several ways to find the martingale measure, but we have selected the method which involves the mean-correcting of the exponential of a Lévy process. The underlying idea that governs the mean-correcting martingale measure is the adjustment of the location parameter of a specified probability distribution that governs the underlying asset price process so as to satisfy a required drift condition [44]. The risk-neutral process using this method is given as [32]

$$S_t^{\text{risk-neutral}} = S_0 \exp(X_t) \left[\frac{\exp(rt)}{E(\exp(X_t))} \right], \tag{5.2.3}$$

where $X = \{X_t : t \geq 0\}$ denotes a Lévy process that models log returns of an underlying asset (either Meixner process or Brownian motion) and S_t is the price of an underlying asset (stock or index) at time t.

At time t, X_t denotes a random variable which is a path of a Lévy process X that models log returns. Under the assumption that log returns are modeled by a Brownian motion, X_t follows a normal distribution $Normal(\mu t, \sigma^2 t)$ and we have the mean of the log

returns given by $E(X_t) = \mu t$ while for the Meixner case, X_t follows a Meixner distribution $Meixner(a, b, dt, mt)$ and we have the mean of the log returns given by $E(X_t) = [(ad)\tan\left(\frac{b}{2}\right) + m]t$. If we define the mean at $t = 0$ by m_{old} then $m_{old} = E(X_0) = 0$. The mean under the risk-neutral probability measure is given by the sum of the original mean (m_{old}) and the drift from the mean denoted by ω, (see [33, p. 79]), that is

$$m_{\text{risk-neutral}} = m_{old} + \omega. \tag{5.2.4}$$

The drift term is defined such that $S_0 = E^{\mathbb{Q}}(e^{-rt}S_t)$. Yao [44] showed that the drift from the mean is given by the following formula:

$$\omega = r - \Psi(-i), \tag{5.2.5}$$

where r denotes the risk-free rate and $\Psi(u) = \ln(\Phi(u))$ (which is the log of the characteristic function in (3.0.1)). By considering this, we derive the martingale measures for the two processes under consideration.

5.2.5.1 Under normal distribution

By using (3.1.4) we have

$$\Psi(-i) = \mu + \frac{1}{2}\sigma^2,$$

and by using (5.2.4) and (5.2.5) the mean under the risk-neutral probability for the normal distribution is given by

$$\begin{aligned} \mu_{\text{risk-neutral}} &= \mu + r - \left(\mu + \frac{1}{2}\sigma^2\right) \\ &= r - \frac{1}{2}\sigma^2. \end{aligned} \tag{5.2.6}$$

5.2.5.2 Under the Meixner distribution

By using (3.2.4) we have

$$\Psi(-i) = 2d\,\ln\left(\frac{\cos\frac{b}{2}}{\cos\left(\frac{a+b}{2}\right)}\right) + m,$$

and by using (5.2.4) and (5.2.5), for the Meixner distribution we have

$$\begin{aligned} m_{\text{risk-neutral}} &= m + r - \left(2d\,\ln\left(\frac{\cos\frac{b}{2}}{\cos\left(\frac{a+b}{2}\right)}\right) + m\right) \\ &= r - 2d\,\ln\left(\frac{\cos\frac{b}{2}}{\cos\left(\frac{a+b}{2}\right)}\right). \end{aligned} \tag{5.2.7}$$

Therefore for the Brownian motion, the martingale measure $\mathbb{Q}$ now follows a $Normal(\mu_{\text{risk-neutral}}, \sigma^2)$ and for the Meixner process, $\mathbb{Q}$ now follows a $Meixner(a, b, d, m_{\text{risk-neutral}})$ by making use of the mean-correcting martingale measure. The results in (5.2.6) and (5.2.7) are crucial in option pricing.

5.2.6 Fourier transform and option pricing

As a next step, the Fourier transform method is used to find the formulae for option prices since we know the characteristic functions of both the Meixner and normal distributions analytically. The main advantage of using Fourier methods is that if the characteristic function of a distribution is known then the option prices are easily calculated. The European vanilla options are calculated based on the price of underlying asset denoted by S_t with strike price K and time of expiry T. We define the following notation [6]:

- $k = \ln(K)$,
- $s_T = \ln(S_T)$,
- $f_T(s)$ denotes the risk neutral probability density function of $\ln(S_T)$ and
- $\phi_T(u)$ denotes the characteristic function of $\ln(S_T)$ such that [6, Equation 2]

$$\phi_T(u) \quad = \quad \int_{-\infty}^{\infty} e^{ius} f_T(s) ds. \tag{5.2.8}$$

If we work with a European vanilla call option then the option will have a non-zero value if $S_T > K$ and 0 otherwise. Using the notation above, the call option has an intrinsic value if $e^{s_T} > e^k$, which gives a payoff of $e^{s_T} - e^k$. Now we establish the formula for the price of the call option as follows [6]:

$$C_T(k) \quad = \quad \int_k^{\infty} e^{-rT}(e^s - e^k) f_T(s) ds. \tag{5.2.9}$$

When $k \to -\infty$, $C_T(k) \to S_0$ (this implies that as the strike price K of a call option approaches 0, the value of a call option will move towards the initial value of the underlying asset S_0), therefore the expression in (5.2.9) is not square-integrable [6]. We say that a function $g(x)$ is square-integrable on $(-\infty, \infty)$, provided that

$$\int_{-\infty}^{\infty} |g(x)|^2 dx \quad < \quad \infty. \tag{5.2.10}$$

As k approaches $-\infty$, $C_T(k)$ approaches S_0 and (5.2.10) cannot hold for $C_T(k) = S_0$. But if we force $C_T(k) \to 0$ as $k \to -\infty$ then (5.2.10) will hold.

Therefore to make (5.2.9) square-integrable, we define a modified call option price formula [6, Equation 3]

$$c_T(k) \quad = \quad e^{\alpha k} C_T(k), \tag{5.2.11}$$

where $\alpha > 0$ is a dumping factor which allows the expression in (5.2.11) to be square-integrable in k for all $\mathbb{R}$. We now find the Fourier transform of $c_T(k)$ as follows [6]:

$$c_T^*(v) \quad = \quad \int_{-\infty}^{\infty} e^{ivk} c_T(k) dk, \tag{5.2.12}$$

$$c_T(k) = \frac{1}{2\pi}\int_{-\infty}^{\infty} c_T^*(v)e^{-ivk}dv. \tag{5.2.13}$$

Now we combine expression (5.2.11) and (5.2.13) to get the following [6, Equation 5]:

$$\begin{aligned} C_T(k) &= e^{-\alpha k}c_T(k) \\ &= \frac{e^{-\alpha k}}{2\pi}\int_{-\infty}^{\infty} c_T^*(v)e^{-ivk}dv. \end{aligned} \tag{5.2.14}$$

Expression (5.2.14) is further simplified by noting that call prices fall on the real space, therefore by using $c_T^*(v)$ defined in (5.2.12), the following conditions will hold [27]:

- if $C_T(k)$ is real and even then $c_T^*(v)$ is real and even;
- if $C_T(k)$ is real and odd then $c_T^*(v)$ is imaginary and odd;
- if $C_T(k)$ is real then $c_T^*(-v)$ is the conjugate of $c_T^*(v)$.

Therefore expression (5.2.14) can be simplified by using the above conditions to be [6, Equation 5]

$$C_T(k) = \frac{e^{-\alpha k}}{\pi}\int_{0}^{\infty} c_T^*(v)e^{-ivk}dv. \tag{5.2.15}$$

We simplify further the expression for $c_T^*(v)$ by simplifying the expression in (5.2.12) as follows:

$$\begin{aligned} c_T^*(v) &= \int_{-\infty}^{\infty} e^{ivk}c_T(k)dk \\ &= \int_{-\infty}^{\infty} e^{ivk}e^{\alpha k}C_T(k)dk \text{ (from (5.2.11))} \\ &= \int_{-\infty}^{\infty} e^{ivk}e^{\alpha k}\int_{k}^{\infty} e^{-rT}(e^s - e^k)f_T(s)dsdk \text{ (from (5.2.9))} \\ &= \int_{-\infty}^{\infty} e^{-rT}f_T(s)\int_{-\infty}^{s} e^{ivk}(e^{s+\alpha k} - e^{k+\alpha k})dkds \text{ (by interchanging integrals)} \\ &= \int_{-\infty}^{\infty} e^{-rT}f_T(s)\left[\frac{e^{ivs+\alpha s+s}}{iv+\alpha} - \frac{e^{ivs+\alpha s+s}}{iv+\alpha+1}\right]ds \\ &= \int_{-\infty}^{\infty} e^{-rT}f_T(s)\left[\frac{e^{ivs+\alpha s+s}}{(iv+\alpha)(iv+\alpha+1)}\right]ds \\ &= \frac{e^{-rT}}{(iv+\alpha)(iv+\alpha+1)}\int_{-\infty}^{\infty} f_T(s)e^{ivs+\alpha s+s}ds \\ &= \frac{e^{-rT}}{(iv+\alpha)(iv+\alpha+1)}\int_{-\infty}^{\infty} f_T(s)e^{-i(iv+\alpha+1)is}ds \\ &= \frac{e^{-rT}}{(iv+\alpha)(iv+\alpha+1)}\int_{-\infty}^{\infty} f_T(s)e^{(v-i(\alpha+1))is}ds \\ &= \frac{e^{-rT}}{(iv+\alpha)(iv+\alpha+1)}\phi_T(v-i(\alpha+1)) \text{ (from (5.2.8)).} \end{aligned} \tag{5.2.16}$$

Combining expressions (5.2.15) and (5.2.16) we get the following expression that is used to price an option:

$$C_T(k) = \frac{e^{-\alpha k}}{\pi}\int_0^\infty \left[\frac{e^{-rT}}{(iv+\alpha)(iv+\alpha+1)}\phi_T(v-i(\alpha+1))\right]e^{-ivk}dv. \quad (5.2.17)$$

By replacing $\phi_T(v-(\alpha+1))$ with the characteristic functions of risk-neutral probabilities for normal distribution and Meixner distribution, we find analytical expressions for the call options using expression (5.2.17).

5.2.7 Characteristic functions of the log returns of the underlying assets

By considering that a Meixner process and Brownian motion are Lévy processes and by making use of the mean-correcting of the martingale measure method, we model the risk-neutral underlying asset price under the two processes by (5.2.3) which can be simplified to be [10]

$$S_t = S_0 e^{X_t+(m_{\text{risk-neutral}})t}, \quad (5.2.18)$$

where where $X = \{X_t : t \geq 0\}$ denotes a Lévy process (either Meixner process or Brownian motion).

We use the risk-neutral stock price given above and (5.2.8) to find an expression for the characteristic of $\ln(S_t)$ as follows [10]:

$$\begin{aligned}\phi_T(u) = \phi_{\ln S_T}(u) &= E[e^{iu\ln S_T}]\\ &= E[e^{iu(\ln S_0+X_T+(m_{\text{risk-neutral}})T}]\\ &= E[e^{iu(\ln S_0+(m_{\text{risk-neutral}})T)+iuX_T}]\\ &= e^{iu(\ln S_0+(m_{\text{risk-neutral}})T)}E(e^{iuX_T})\\ &= e^{iu(\ln S_0+(m_{\text{risk-neutral}})T)}\Phi_{X_T}(u). \quad (5.2.19)\end{aligned}$$

We use the expression in (5.2.19) and substitute in (5.2.16) by replacing a u in (5.2.19) with $(v-i(\alpha+1))$ to get an expression for $c_T^*(v)$. It is worth pointing out that under the risk-neutral set-up, we are considering a martingale measure $\mathbb{Q}$, hence the characteristic function $\Phi_{X_T}(u)$ will ignore the drift (restricting the drift parameter to be zero) because under a martingale measure, there is no systematic drift term [3, p. 47]. This is clearly illustrated in the following two subsections.

5.2.7.1 Characteristic function under the normal model

From (3.1.3) we can find the characteristic function under the normal distribution for a time to maturity T of an option as follows:

$$\Phi_{X_T}(u) = e^{\left(iu\mu-\frac{1}{2}u^2\sigma^2\right)T}. \quad (5.2.20)$$

We use (5.2.20) and ensure that the risk-neutral condition holds by eliminating the drift term ($\mu = 0$) to get

$$\Phi_{X_T}(u) = e^{-\frac{1}{2}u^2\sigma^2 T}. \tag{5.2.21}$$

Under the normal model, we use (5.2.19) and we substitute (5.2.6) and (5.2.21) to get the following:

$$\begin{aligned}\phi_T(u) &= e^{iu(\ln S_0 + (r-\frac{1}{2}\sigma^2)T} e^{-\frac{1}{2}u^2\sigma^2 T} \\ &= e^{iu(\ln S_0 + rT) - \frac{1}{2}\sigma^2 T\left(iu+u^2\right)}.\end{aligned} \tag{5.2.22}$$

5.2.7.2 Characteristic function under the Meixner model

Under the Meixner process we use (3.1.3) and incorporate the time to maturity T of an option, where X_T is a Meixner process such that:

$$\begin{aligned}\Phi_{X_T}(u) &= \left(\frac{\cos\frac{b}{2}}{\cosh\left(\frac{au-ib}{2}\right)}\right)^{2dT} \exp(imuT) \\ &= \left(\frac{\cos\frac{b}{2}}{\cos\left(\frac{aiu+b}{2}\right)}\right)^{2dT} \exp(imuT).\end{aligned} \tag{5.2.23}$$

We use (5.2.23) and ensure the risk-neutral condition is satisfied by eliminating the drift term ($m = 0$) to get

$$\Phi_{X_T}(u) = \left(\frac{\cos\frac{b}{2}}{\cos\left(\frac{aiu+b}{2}\right)}\right)^{2dT} \tag{5.2.24}$$

By using (5.2.19), (5.2.7) and (5.2.24) we get the characteristic function for the Meixner distribution as

$$\phi_T(u) = \exp\left\{iu\left[\ln S_0 + \left(r - 2d\ln\left(\frac{\cos\frac{b}{2}}{\cos\left(\frac{a+b}{2}\right)}\right)\right)T\right]\right\}\left(\frac{\cos\frac{b}{2}}{\cos\left(\frac{aiu+b}{2}\right)}\right)^{2dT} \tag{5.2.25}$$

5.2.8 Choosing the value of α

There is a need to determine the value of α to be used. Carr and Madan [6] pointed out that $c_T^*(0)$ must be finite to ensure that the modified call value is both square-integrable and also integrable for a positive log strike direction. From expression (5.2.16) it can be noted that $c_T^*(0)$ is finite if $\phi_T(-i(\alpha+1))$ is finite. From (5.2.8) we deduce that

$$\begin{aligned}\phi_T(-i(\alpha+1)) &= E[e^{i(-i(\alpha+1))s_T}] \\ &= E[e^{(\alpha+1)\ln(S_T)}] \\ &= E[S_T^{(\alpha+1)}].\end{aligned} \tag{5.2.26}$$

We are going to illustrate these bounds for only Meixner process since for a Brownian motion there are no constraints for the α value [41].

From (5.2.23) we obtain

$$\begin{aligned}\Phi_{X_T}(-i(\alpha+1)) &= \left(\frac{\cos\frac{b}{2}}{\cos\left(\frac{ai(-i)(\alpha+1)+b}{2}\right)}\right)^{2dT} \exp(imT(-i)(\alpha+1)) \\ &= \left(\frac{\cos\frac{b}{2}}{\cos\left(\frac{a(\alpha+1)+b}{2}\right)}\right)^{2dT} \exp(m(\alpha+1)T). \qquad (5.2.27)\end{aligned}$$

In order to find the bounds for α, we use (5.2.19) and (5.2.7) and we require $\phi_T(-i(\alpha+1)) = E[S_T^{(\alpha+1)}] < \infty$. Using the fact that $\lim_{x\to\infty}\frac{1}{x} = 0$, and since $-\pi < b < \pi$ and $a > 0$ under a Meixner process, we get the following:

$$\begin{aligned}&\left[\left(\frac{\cos\frac{b}{2}}{\cos\left(\frac{a(\alpha+1)+b}{2}\right)}\right)^{2dT} \exp(m(\alpha+1)T)\right]^{-1} > 0 \\ &\left(\frac{\cos\frac{b}{2}}{\cos\left(\frac{a(\alpha+1)+b}{2}\right)}\right)^{-2dT} > 0 \\ &\left(\frac{\cos\left(\frac{a(\alpha+1)+b}{2}\right)}{\cos\frac{b}{2}}\right)^{2dT} > 0 \\ &\cos\left(\frac{a(\alpha+1)+b}{2}\right) > 0 \text{ (since } -\pi < b < \pi, \text{ therefore} \cos\frac{b}{2} > 0). \qquad (5.2.28)\end{aligned}$$

We solve (5.2.28) further as follows:

$$\begin{aligned}\cos\left(\frac{a(\alpha+1)+b}{2}\right) &= 0 \\ \frac{a(\alpha+1)+b}{2} &= \arccos(0). \qquad (5.2.29)\end{aligned}$$

From (5.2.29) we have

$$\frac{a(\alpha+1)+b}{2} = \frac{\pi}{2}.$$

This can be simplified to get $\alpha = \frac{\pi-a-b}{a}$ for $a > 0$. Hence, from (5.2.28) we have

$$\alpha < \frac{\pi-a-b}{a}$$

But since we restricted α to be positive earlier, the new bounds will be

$$0 \quad < \quad \alpha < \frac{\pi - a - b}{a}. \tag{5.2.30}$$

We can use any value of α that satisfy the interval in (5.2.30) without loss of generality. On this dissertation we use $\alpha = 2$ but it is worthy noting that any different value of α that satisfies (5.2.30) will not contribute to significant differences in the prices of the options.

5.2.9 Fast Fourier Transform (FFT)

We apply the results of the above sections about Fourier transformation to the pricing of options using the FFT algorithm for at-the-money and in-the-money European vanilla call options. We start by defining the sum structure we can apply FFT to, which is as follows [21]:

$$z(k) \quad = \quad \sum_{j=1}^{N} e^{-i\frac{2\pi}{N}(j-1)(k-1)} x(j) \text{ for } k = 1, 2, 3, \ldots, N, \tag{5.2.31}$$

where $x(j)$ are complex numbers and N being a power of 2 and the FFT algorithm simplify order N^2 to order $N \log_2 N$ as pointed out by Ng [27]. We transform the integration given in (5.2.15) to be similar to (5.2.31) so that we can apply the FFT method.

By applying the trapezium rule to the integral in (5.2.15) and by defining $v_j = \triangle v(j-1)$, the discretised expression is as follows [6, Equation 17]:

$$C_T(k) \quad \approx \quad \frac{e^{-\alpha k}}{\pi} \sum_{j=1}^{N} c_T^*(v) e^{-iv_j k} \triangle v. \tag{5.2.32}$$

This discretization process introduces two errors as pointed out by Kwok et al [21], that is, the truncation error which comes from changing the infinite upper limit of (5.2.15) to a finite upper limit and the sampling error which emanates from changing the Fourier variable v, which is continuous to be discrete.

As a next step, we establish a grid in the domain for k and we restrict the grid to be focused around the strikes that are at-the-money which is mostly common in the market by using the following [6, Equation 19]:

$$k_m \quad = \quad -\frac{1}{2} N \triangle k + \triangle k(m-1) \text{ for } m = 1, 2, 3, \ldots, N. \tag{5.2.33}$$

With the expression (5.2.33) we can have log strike prices ranging from $-\frac{1}{2}N\triangle k$ to $\frac{1}{2}N\triangle k$. Now we use expression (5.2.33) and substitute it in expression (5.2.32) to get the following:

$$\begin{aligned} C_T(k) &\approx \frac{e^{-\alpha k}}{\pi}\sum_{j=1}^{N} c_T^*(v)e^{-iv_j[-\frac{1}{2}N\triangle k+\triangle k(m-1)]}\triangle v \\ C_T(k) &\approx \frac{e^{-\alpha k}}{\pi}\sum_{j=1}^{N} c_T^*(v)e^{-i(\triangle v(j-1))[-\frac{1}{2}N\triangle k+\triangle k(m-1)]}\triangle v \\ &= \frac{e^{-\alpha k}}{\pi}\sum_{j=1}^{N} c_T^*(v)e^{\triangle v(j-1)(\frac{1}{2}N\triangle k)i-\triangle v\triangle k(j-1)(m-1)i}\triangle v \\ &= \frac{e^{-\alpha k}}{\pi}\sum_{j=1}^{N} c_T^*(v)e^{\triangle v(j-1)(\frac{1}{2}N\triangle k)i}e^{-\triangle v\triangle k(j-1)(m-1)i}\triangle v. \end{aligned} \tag{5.2.34}$$

By equating summation in (5.2.34) with the summation in (5.2.31), we notice the following:

$$\begin{aligned} c_T^*(v)e^{\triangle v(j-1)(\frac{1}{2}N\triangle k)i}\triangle v &= x(j), \\ \triangle v\triangle k &= \frac{2\pi}{N}. \end{aligned} \tag{5.2.35}$$

This implies that we can apply the FFT method. It can be noted on the expression (5.2.35) that if the value of N can be fixed, choosing a small value of $\triangle v$ to improve the integration accuracy, $\triangle k$ will be forced to be high which may not be in line with the desired grid for the log strike prices. With that in mind there is a need to use a small value of $\triangle k$ with a big value of $\triangle v$ without affecting the accuracy of the integration. This allows us to adopt the Simpson rule as suggested by Carr and Madan [6] to obtain the following [6, Equation 24]:

$$C_T(k) \approx \frac{e^{-\alpha k}}{\pi}\sum_{j=1}^{N}(c_T^*(v)e^{\triangle v(j-1)(\frac{1}{2}N\triangle k)i})e^{-\frac{2\pi}{N}(j-1)(m-1)i}\frac{\Delta v}{3}[3+(-1)^j-\omega_{j-1}], \tag{5.2.36}$$

where $\omega_n = \begin{cases} 1 & \text{for } n=0 \\ 0 & \text{otherwise.} \end{cases}$

To evaluate the expression (5.2.36) which is simply a direct application of FFT method, we need values for both Δv and α. In this dissertation, we calculate the option prices using either the Fourier transform (5.2.17) or Fast Fourier transform (5.2.36) for both normal and Meixner models whichever is the most applicable. One can simply replace the normal model with the Black-Scholes model (see appendix A) and get the same results.

5.3 Greeks

We are going to explain the greeks that measure the sensitiveness of the option prices to changes in the prices of the underlying assets. The greeks we define in this section are going to be used for hedging in the next chapter. The general formulae of the option delta and option gamma are given as follows [3, p. 127]:

$$\Delta_C \text{ (call option delta)} = \frac{\partial C}{\partial S}, \tag{5.3.1}$$

$$\Gamma_C \text{ (call option gamma)} \;=\; \frac{\partial^2 C}{\partial S^2}. \tag{5.3.2}$$

The delta of an option measures the sensitivity of an option price in relation to the changes in the prices of the underlying asset while the gamma of an option measures the sensitivity of the delta of an option to the changes in the prices of the underlying asset (see [16, pp. 310 and 332]). A higher option delta corresponds to a higher sensitivity and also a higher option gamma denotes a higher sensitivity. By using a characteristic function in (5.2.19) and a call pricing function in (5.2.17) we get the following expression:

$$\begin{aligned} C_T(k) \;&=\; \frac{e^{-\alpha k}}{\pi}\int_0^\infty \frac{e^{-rT}e^{-ivk}}{(iv+\alpha)(iv+\alpha+1)} \\ &\quad \left[e^{i(v-i(\alpha+1))(\ln S_0+(m_{\text{risk-neutral}})T}\Phi_{X_T}(v-i(\alpha+1))\right]dv \end{aligned} \tag{5.3.3}$$

We use (5.3.3) to find the analytical general expressions for both option delta and option gamma under the Fourier transform method by using (5.3.1) and (5.3.2), respectively, as follows:

$$\Delta_C \;=\; \frac{e^{-\alpha k}}{\pi S_0}\int_0^\infty \left[\frac{i(v-i(\alpha+1))e^{-rT}}{(iv+\alpha)(iv+\alpha+1)}\phi_T(v-i(\alpha+1))\right]e^{-ivk}dv, \tag{5.3.4}$$

where $\phi_T(v-i(\alpha+1))$ is from (5.2.19) and by differentiating (5.3.4) with respect to S_0 using product rule, we have

$$\begin{aligned} \Gamma_C &= -\frac{e^{-\alpha k}}{\pi S_0^2}\int_0^\infty \left[\frac{i(v-i(\alpha+1))e^{-rT}}{(iv+\alpha)(iv+\alpha+1)}\phi_T(v-i(\alpha+1))\right]e^{-ivk}dv + \\ &\qquad \frac{e^{-\alpha k}}{\pi S_0^2}\int_0^\infty \left[\frac{-(v-i(\alpha+1))^2e^{-rT}}{(iv+\alpha)(iv+\alpha+1)}\phi_T(v-i(\alpha+1))\right]e^{-ivk}dv \\ &= -\frac{e^{-\alpha k}}{\pi S_0^2}\int_0^\infty \left[\frac{(i(v-i(\alpha+1))+(v-i(\alpha+1))^2)\,e^{-rT}}{(iv+\alpha)(iv+\alpha+1)}\phi_T(v-i(\alpha+1))\right]e^{-ivk}dv \end{aligned} \tag{5.3.5}$$

To find the analytical expressions for both the normal model and the Meixner model greeks, we substitute the characteristic functions of $\ln S_T$ in (5.2.22) and (5.2.25) respectively in both (5.3.4) and (5.3.5).

Chapter 6

Hedging and calibration

In this chapter we are going to compare the models we have explained in the previous chapters with the market prices of European options and later introduce hedging of a portfolio of European options and stocks. The performance of the model is judged based on the size of the distance between the price of the model and the market price. A smaller distance is preferred. If we assume that the market prices are the true values then the distance can be referred to as the measurement of the error size. In this chapter the term "options" is referring to "European vanilla options". The results from this chapter make reference to appendix B. We are going to consider the following three error measures:

1. average percentage error (APE);
2. average relative percentage error (ARPE);
3. average absolute error (AAE).

6.1 Definition of error measures

We define the following:

- P^{model} denotes the model option price,
- P^{market} denotes the market option price,
- N denotes the number of option prices under quotation,
- x denotes the parameters of the model,
- $\bar{P}^{market}$ denotes the average of the option prices.

6.1.1 Average percentage error

Under APE the distance of the model prices from the market prices is obtained as follows [19, p. 435]:

$$APE(x) = \sum_{i=1}^{N} \frac{|P_i^{market} - P_i^{model}(x)|}{N\left(\bar{P}^{market}\right)},$$

with

$$\bar{P}^{market} = \sum_{i=1}^{N} \frac{P_i^{market}}{N}.$$

6.1.2 Average relative percentage error

ARPE is closely related to APE, but instead of weighting by the mean of the market prices as on APE, the ARPE is weighting the deviations from the market prices by the observed option market prices. Hence, we have [19, p. 435]

$$ARPE(x) = \sum_{i=1}^{N} \frac{|P_i^{market} - P_i^{model}(x)|}{N\left(P_i^{market}\right)}.$$

6.1.3 Average absolute error

AAE looks similar to the distance measures above, but under the AAE the absolute deviations are not weighted with either the market prices or the mean market prices. That is [19, p. 435]

$$AAE(x) = \sum_{i=1}^{N} \frac{|P_i^{market} - P_i^{model}(x)|}{N}.$$

6.2 Estimation of the model parameters

The most important aspect of option pricing is being able to identify the best parameters that fit the data. Therefore we need to find the parameters that miminises the distance from the true option prices. There are basically two methods we are going to consider.

The first method involves calibrating the market option prices with the model prices. We estimate the model parameters by choosing parameters that gives us a better fit to the market option prices. We treat this as an unconstrained optimization problem by minimising the average absolute error (AAE) as follows:

$$\min_x f(x) = \sum_{k=1}^{N} \frac{|r_k(x)|}{N},$$

where:

- x is a vector of model parameters,

- N is the number of observations of the option prices,
- $r_k(x) = P_k^{model}(x) - P_k^{market}$.

We invoked the *Matlab* function $fminsearch(\,)$ to find the local minimum of the unconstrained optimization problem. For the optimization problem to be solved, we ensure that the number of parameters being estimated are less than or equal to the number of observations. There is also a need to carefully select the initial values for the optimization problem in order to avoid settling for local minimum points that are not the best possible parameters.

The second method estimates the parameters of the models by using historical data for the underlying asset prices. This was explained in depth when we fit the log returns in chapter 4. The only slight difference here is that we can either estimate parameters corresponding to yearly data or we can estimate the parameters from the daily log returns. We prefer estimating parameters with daily data, because there is sufficient data to get better estimates of the parameters. The risk-free rate can be expressed as rate compounded daily

$$\text{daily risk-free rate} \;=\; (1+r)^{\frac{1}{252}} - 1,$$

where r denotes the risk-free rate compounded yearly. The daily estimates can be scaled up to yearly estimates as follows [22]:

- yearly mean value $= 252 *$ daily mean,
- yearly standard deviation = daily standard deviation $* \sqrt{252}$,
- yearly excess kurtosis $= \frac{\text{daily excess kurtosis}}{252}$,
- yearly skewness $= \frac{\text{daily skewness}}{\sqrt{252}}$.

6.3 Properties of European call options

We expect the following conditions to hold for any European call option, otherwise there will be an arbitrage opportunity:

1. the strike price and the price of a European call option are inversely related, that is the European call price approaches zero as strike price turns to infinity [16, p. 168];
2. the price of the call option can not exceed the value of the underlying [16, p. 171];
3. $C_t \geq \max\left\{0, S_t - Ke^{-r(T-t)}\right\} =$ lower bound [16, p. 171] ;
4. if we have call options that only differ on their time to maturity, then we expect a call option with a longer maturity to cost more than the one with shorter maturity.

We show that condition 4 holds. Suppose the lower bound above holds and we have two maturities T_1 and T_2 such that $T_1 < T_2$. For the sake of clarity we use a slightly different notation to define two European call options with the same strike price and underlying, but different maturities, as $C(K, T_1, S_0)$ and $C(K, T_2, S_0)$, satisfying $C(K, T_1, S_0) > C(K, T_2, S_0)$.

At time $t = 0$, we buy the cheaper call option $C(K, T_2, S_0)$ and sell $C(K, T_1, S_0)$. At time $t = T_1$, we have

$$\begin{aligned} & C(K, T_2, S_{T_1}) - \max\{0, S_{T_1} - K\} \\ \geq & \max\left\{0, S_{T_1} - Ke^{-r(T_2 - T_1)}\right\} - \max\{0, S_{T_1} - K\} \\ \geq & 0. \end{aligned}$$

This shows the presence of an arbitrage opportunity. Therefore the condition $C(K, T_1, S_0) > C(K, T_2, S_0)$ cannot hold.

Suppose we have option prices that are being traded below the lower bound in condition 3 above, and provided information is available among the traders, then we expect the demand of the options to increase as the traders are willing to buy the cheaper options with an intention of gaining risk-free profit. The increase in demand will force the price of the call options to increase to meet the supply of the call options hence equilibrium is reached where there is no-arbitrage. Similarly, if we have a scenario where the value of a call option exceeds the value of its underlying asset for example, we have a call option on a stock exceeding the stock price. It simply means it becomes cheaper to buy shares, than buying a call option on that share. Considering that we assume all parties on an option agreement prefer more to less, the traders will buy more shares and sell the call option on those shares hence flooding the market with the call options hence pushing the price of the call option down until equilibrium is reached where there is no arbitrage.

We use these preconceived conditions as a first test on our models to check whether they are accurate and also to ensure that the market prices we use for calibrating are correctly captured. Before the calibration process is started, we need to be confident that the market prices we use do not show any arbitrage opportunities. As part of data cleaning, we have to ensure that we eliminate prices that allow arbitrage and also prices that seem to be outliers. To remove outliers we first group call options with the same maturity. We expect the options to follow a downward trend with the strike price and the prices need to be close to each other. If the call option prices are much larger or smaller than expected, we remove them as they signify outliers.

6.4 Market data cleaning

As discussed in the above section, we need to ensure that the data for the market prices of options does not show arbitrage opportunities. The data cleaning is done under the assumption that the properties of call options stipulated above are satisfied. In this section we go through the procedure of data cleaning using S&P500 call option prices data. We extracted the data for the call options on 29 April 2018 [43] to be exercised on 18 May 2018 (which corresponds to 15 trading days). The value of the S&P500 stock index was 2669.1 on 29 April 2018 [42]. The risk-free rate used is quoted from the 3 months treasury bill rate from the United States department of treasury [40] which was 1.81%.

In Table 6.1 we show the data cleaning procedure for detecting the option prices that oppose the fact that the call option prices fall as the strike price increases. We use the indicator that returns 0 if the condition is violated. As part of the cleaning process, we eliminate all those option prices with indicator 0. It is worth noting that those conditions may not create arbitrage scenarios if some of the assumptions outlined in the above sections are relaxed. This is because if we relax some of the assumptions, we increase the sources of randomness on the option price modeling which removes arbitrage (see [3, p. 122, Theorem 8.3.1]). But in order to take our assumptions into consideration, we work with the data that does not violate our assumptions. The process is repeated until the indicator is returning only the value 1.

Table 6.2 shows the data cleaning process that test the lower and upper bound conditions. By applying these tests we transform the data in Table 6.2 by eliminating the call option prices that are not satisfying both the lower and upper bound conditions.

Table 6.1: Data cleaning process for the market prices of options (indicator=1 if C falls as K increases)

Strike price (K)	Price (C)	Indicator
1600	1074.40	1
1650	1067.20	1
1675	1105.53	0
1700	1012.60	1
1750	907.95	1
1800	998.00	0
1840	880.45	1
1850	794.19	1
1875	913.50	0

Table 6.2: Lower bound and upper bound condition

Strike price	Price (C)	Lower bound (LB)	Indicator (LB < C)	Indicator (UB > C)
1600	1074.40	1072.346	1	1
1650	1067.20	1022.422	1	1
1700	1012.60	972.499	1	1
1750	907.95	922.575	0	1
1840	880.45	832.712	1	1
1850	794.19	822.727	0	1

The other question that also arises is whether to use closing prices of market prices, ask or bid prices. An ask price is the price the seller of an option is willing to sell an option, while a bid price is the price the buyer of an option is willing to pay [17, p. 221]. Since both parties are motivated in getting gains from the trade, we end up having a scenario of having a gap between an ask price and a bid price. This gap is referred to as the bid-ask spread. For an option to be traded, there is a need for both parties to agree on the price, hence there is

normally another party involved called the market maker who buys an option from the seller at a bid price and then sells the option to the buyer at an ask price. The market maker's profit will be the bid-ask spread [17, p. 221]. Highly liquid options have a very small bid-ask spread. Under the assumption of a highly liquid market, we are trying to eliminate the bid-ask spread, but this assumption tends to be unrealistic if we can consider those markets where the option trading is illiquid. Therefore we are going to consider calibration of model prices to the market prices by also considering the ask and bid prices.

6.5 Behaviour of the model prices

We also need to find out if the prices from the two models are consistent to the properties of the options before we can use them. For the call options under the S&P500 stock index, we consider strike prices from 2400 to 2700 with duration of 15, 58 and 164 trading days and the initial price of the underlying S&P500 stock index is 2669.1. The call option prices are then given as in Tables 6.3 and 6.4 and in Figures 6.1 and 6.2. Taking a closer look at this, we discovered that properties stipulated above are being satisfied by both models, except for the lower bound property. We found out that for small option maturities like $T = 15$ days and for the strike prices that are further from the underlying prices, both our models are giving us prices that are lower than the lower bound. As we increase the maturities or increase the strike price towards the price of the underlying asset, both our models start to give prices that are above the lower bounds. This phenomena emanate from the fact that as the call option price moves towards its non-analytic intrinsic value, the integral in (5.2.17) will be difficult to integrate numerically if maturities are very short [6, p. 7]. It is worth noting that the parameters of the pricing models in this section are estimated using historical data for log returns of S&P500 stock index.

Table 6.3: S&P500 Call option prices under the Meixner pricing model

	T=15 days		T=58 days		T=164 days	
Strike price	Model price	LB	Model price	LB	Model price	LB
2400	271.6843	272.4943	281.2587	279.8873	312.6075	298.0146
2450	221.8487	222.5482	234.1481	230.0952	270.8697	248.6001
2500	172.4220	172.6020	189.3098	180.3030	231.7132	199.1856
2550	124.4497	122.6558	147.8739	130.5109	195.5374	149.7712
2600	80.4530	72.7097	111.0200	80.7187	162.6676	100.3567
2650	44.4939	22.7635	79.7293	30.9266	133.3264	50.9422
2700	20.0976	0	54.5430	0	107.6166	1.5277

Table 6.4: S&P500 Call option prices under the Normal model (BS model)

	T=15 days		T=58 days		T=164 days	
Strike price	Model price	LB	Model price	LB	Model price	LB
2400	271.6656	272.4943	280.9653	279.8873	312.2174	298.0146
2450	221.7673	222.5482	233.7581	230.0952	270.4952	248.6001
2500	172.1814	172.6020	188.8818	180.3030	231.3947	199.1856
2550	124.0128	122.6558	147.5083	130.5109	195.3137	149.7712
2600	80.0658	72.7097	110.8266	80.7187	162.5701	100.3567
2650	44.5582	22.7635	79.7805	30.9266	133.3742	50.9422
2700	20.6069	0	54.8414	0	107.8135	1.5277

Figure 6.1: S&P500 Call option prices under the normal model (Black Scholes model)

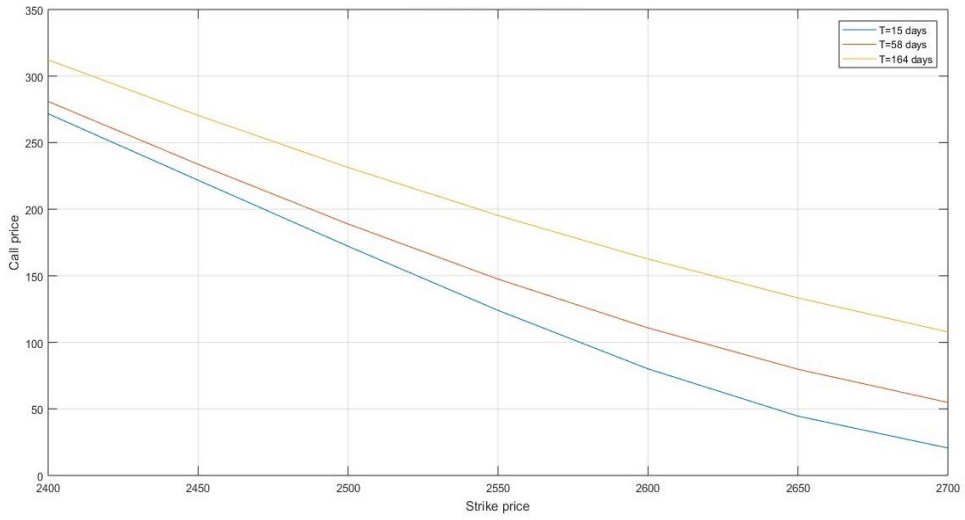

Figure 6.2: S&P500 Call option prices under the Meixner model

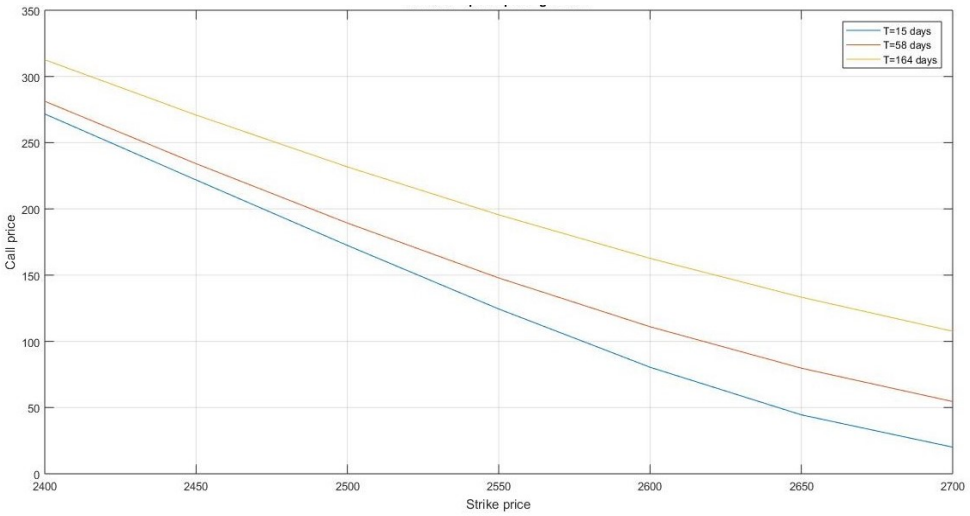

6.6 Fitting the models to the market

6.6.1 Fitting using parameters estimated from historical prices

We compare how our two models are fitting to the market call option prices by using the three error measures explained earlier in this chapter. The parameters of the models are estimated from the historical prices of the log returns of the S&P500 share index.

In Table 6.5 we compare the error measure for the Meixner and normal models (the model parameters are estimated from historical data of log returns of S&P500 share index). The error measures quantifies how the call option prices from the models differs from the market call option prices. We see that the Meixner model is having lower values on all the error measures as compared to the normal model. This shows that the Meixner model is a better pricing model as compared to the normal model (Black-Scholes model). Another discovery is that error measures are smaller on smaller maturities than bigger maturities. This seem to indicate that the volatility is not constant over time. Both models can be significantly improved if we are to incorporate the stochastic nature of the volatility by relaxing the assumption of constant volatility of the log returns of the underlying asset. Shanahan et al [35] pointed out that there is a need to consider stochastic volatility for the underlying asset for longer maturities. In Figures 6.3 and 6.4 we compare the model prices to the market prices, and we observe that both models are giving call prices that are close enough to the market call prices when the strike prices are close to the value of the underlying asset (spot price) but the call prices are slightly deviating from the market call prices as the strike prices move further from the spot prices. An explanation that can address this is that the models are not able to address the issue of volatility smile.

Table 6.5: Error measures (using closing price of call options as market prices) for S&P500 options

Error measure	Model	T= 15 days	T=58 days	T=164 days
AAE	Normal	9.7007	11.1907	23.1998
	Meixner	9.6954	11.1285	22.9892
ARPE	Normal	0.0522	0.0448	0.0784
	Meixner	0.0498	0.0443	0.0778
APE	Normal	0.0418	0.0442	0.0757
	Meixner	0.0418	0.0439	0.0750

Table 6.6: S&P500: Error measures (using average of the bid and ask price of call options as market prices)

Error measure	Model	T= 15 days	T=58 days	T=164 days
AAE	Normal	2.0222	6.3568	17.9917
	Meixner	1.8755	6.2045	17.7810
ARPE	Normal	0.0277	0.0355	0.0653
	Meixner	0.0244	0.0352	0.0647
APE	Normal	0.0088	0.0251	0.0597
	Meixner	0.0081	0.0245	0.0590

Figure 6.3: S&P500 call option prices under the normal (Black-Scholes) model

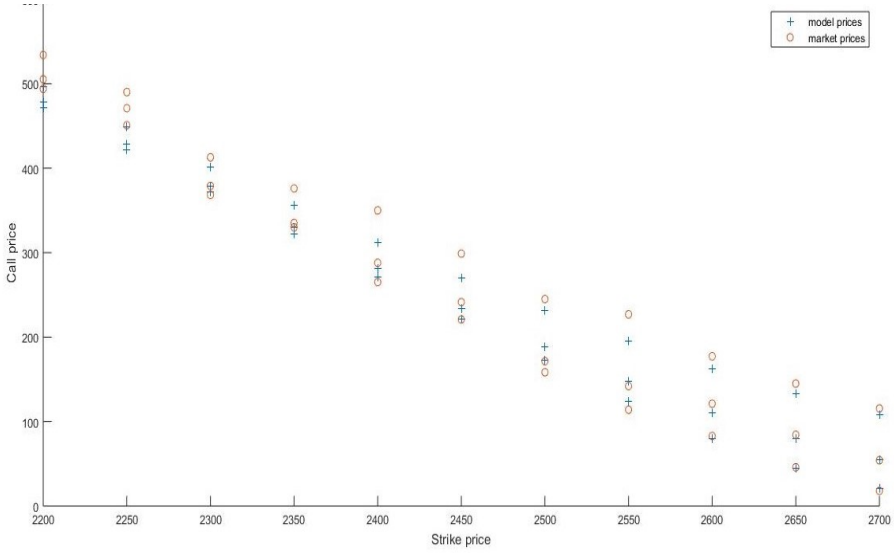

Figure 6.4: S&P500 call option prices under the Meixner model

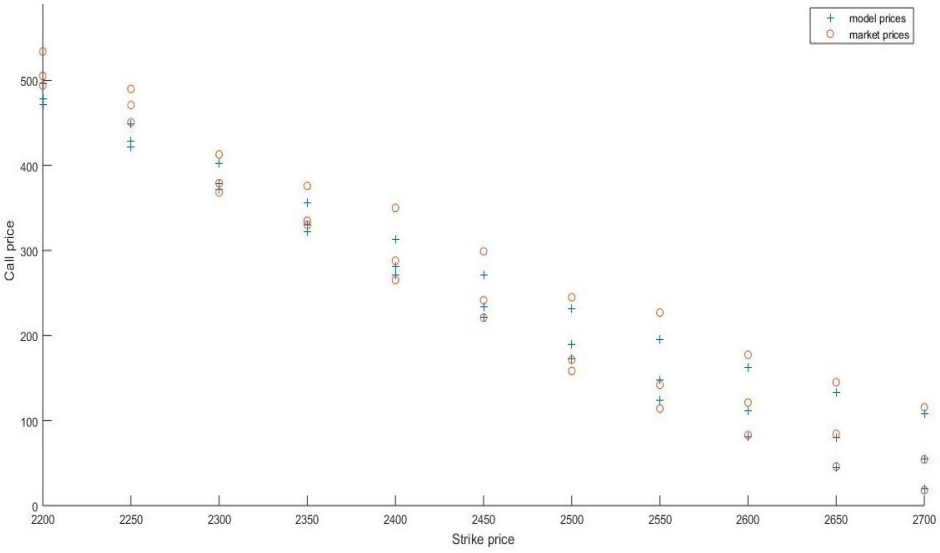

Table 6.6 shows the error measures for both models when model prices are compared to the average of the bid and ask prices. The error measures from Table 6.6 are much smaller as compared to error measures from Table 6.5. This shows that the last traded prices (closing prices) may not be the best prices to use. This is justified by comparing Figures 6.3, 6.4 and 6.5. Therefore, we adopt the average of the ask and bid prices as the market prices when checking how the models are performing in relation to the market.

Figure 6.5: Call option prices by using average of bid and ask prices of S&P500 options

(a) Normal model

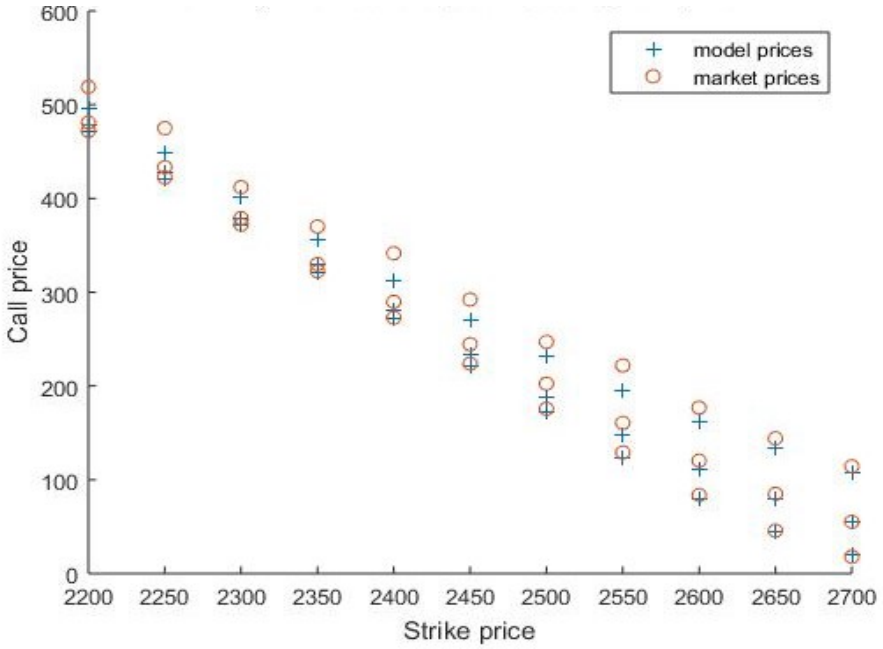

(b) Meixner model

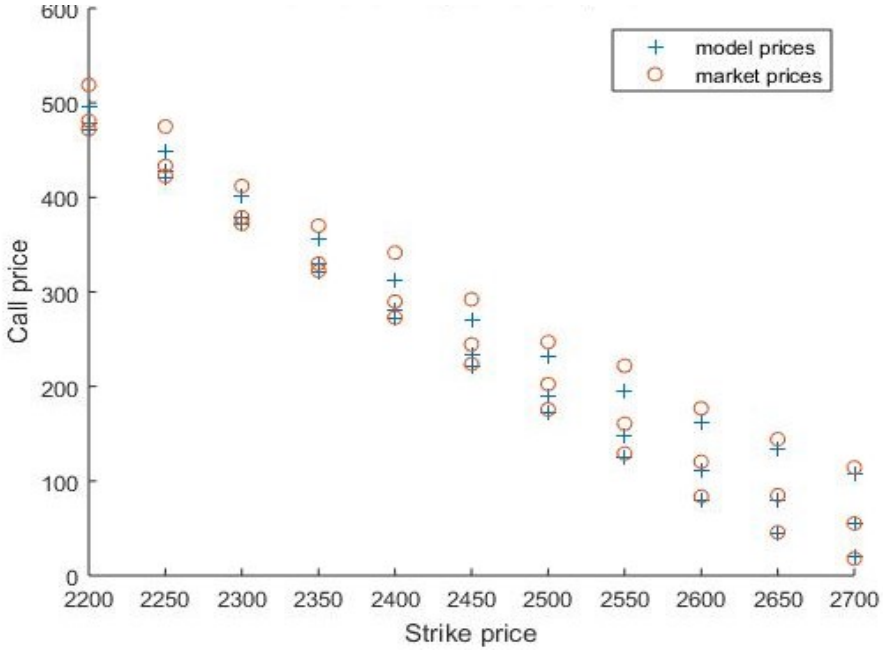

6.6.2 Fitting using calibrated parameters

The parameters of the models are obtained from a calibration procedure explained earlier in this chapter using S&P500 call option prices (the average of the bid and ask price). We calculate the error measures as before and determine if the calibrated parameters are better than the parameters obtained from historical prices of the log returns of the S&P500 share index. Under the normal model we calibrated only one parameter and three parameters under the Meixner model since the location parameter is adjusted by mean-correcting of the exponential of a Lévy process.

By using the parameters that are in Table 6.7, the error measures in Table 6.8 are obtained. We observe significant improvements in fitting both models to the market call options in comparison with parameters obtained from historical log returns by comparing Table 6.6 and Table 6.8 especially on longer maturities. The Meixner model gives a very good fit as compared to the normal model. Taking a closer look at the graphical representation of the model call option prices and the market call option prices in Figure 6.6, we conclude that the Meixner model gives a better fit than the normal distribution. Comparing Figures 6.5 and 6.6, we deduce that calibrated parameters are more accurate in modeling call option prices as compared to the parameters estimated using the historical log returns.

Table 6.7: Calibrated parameters under the S&P500 index

Model	Estimated parameters	Values
Normal	$\hat{\sigma}$	0.0094
Meixner	$\hat{a}$	0.0528
	$\hat{b}$	-2.2758
	$\hat{d}$	0.0103

Table 6.8: The error measures using parameters calibrated to the average of bid and ask prices of S&P500 call options

Error measure	Model	T=15 days	T=58 days	T=164 days
AAE	Normal	2.3030	4.7089	10.3126
	Meixner	1.6540	1.5290	6.098
ARPE	Normal	0.0597	0.0391	0.0402
	Meixner	0.0386	0.0055	0.0191
APE	Normal	0.0100	0.0186	0.0342
	Meixner	0.0072	0.0060	0.0202

Figure 6.6: Fitting calibrated model call option prices to S&P500 option prices (average of bid and ask price)

(a) Normal model

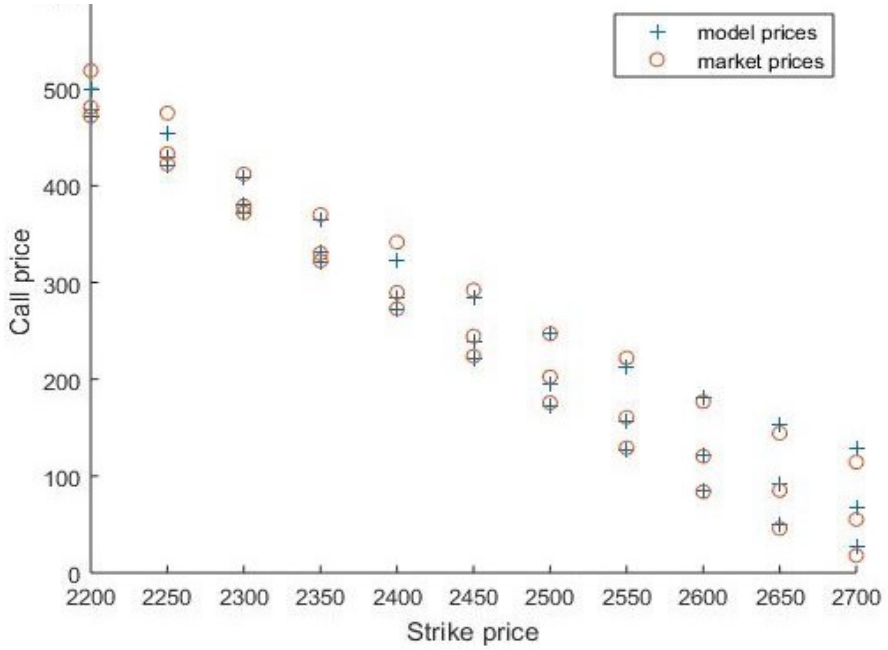

(b) Meixner model

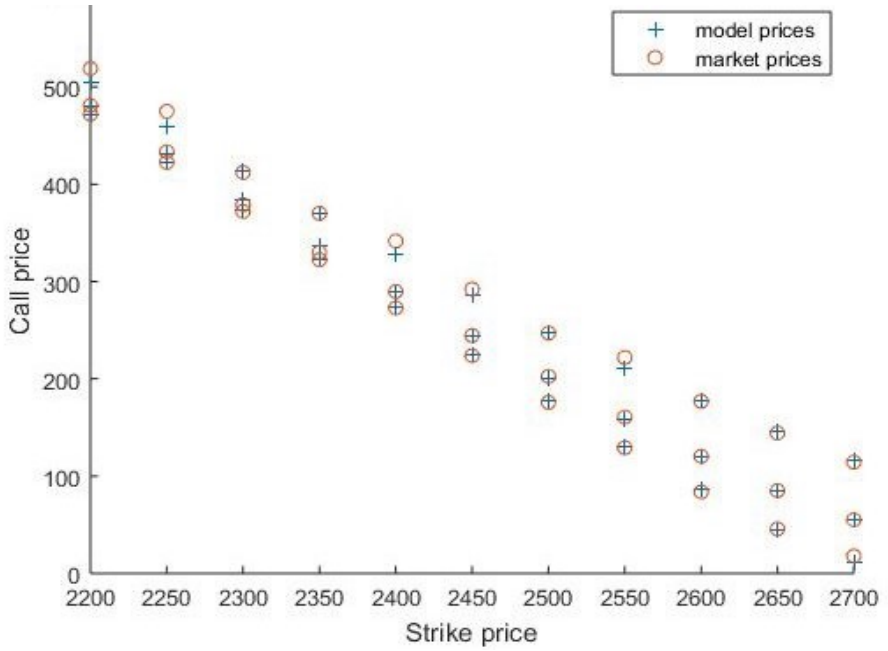

6.7 Fitting the pricing models to South African market

In this section we apply the models to the South African market which is an emerging market and the options market is not as liquid as the United States market. We use the data for the warrants for the Sasol Ltd and BHP Billiton PLC companies. In South Africa warrants

and options have no differences. We apply put-call parity to get the European call option prices. We also use the data for log returns of the stock for both companies to estimate the starting parameters of the model for calibration purposes. The initial and optimal parameters are shown in Table 6.9. The error measures for the Black-Scholes (normal model) and the Meixner model for both Sasol and Billiton are given in Table 6.10.

Table 6.9: Estimated parameters

Model	Estimated parameter	Sasol		Billiton	
		Initial	Optimal	Initial	Optimal
Normal	$\hat{\sigma}$	0.01631	0.0285	0.01611	0.0303
Meixner	$\hat{a}$	0.02362	0.0250	0.005557	0.2089
	$\hat{b}$	0.0003671	-3.012	-0.6399	-0.5434
	$\hat{d}$	0.9532	0.0137	15.14	0.0407

From Table 6.10 it is evident that both models are inaccurate, even though the Meixner model is slightly better than the Black-Scholes model. One of the reasons why the models are not behaving well is that we are calibrating the model using only five European call warrants for Billiton and six European call warrants for Sasol which is a smaller data set than the one we used under the S&P500 call options. Small data sets are easy to approximate the parameters from, but we lose accuracy. These limitations are also emanating from the fact that the South African option market is illiquid.

Table 6.10: Error measures for Black-Scholes (normal) model and the Meixner model for South African data

Error measure	Sasol		Billiton	
	Normal	Meixner	Normal	Meixner
AAE	389.4540	271.6918	98.0997	80.5710
ARPE	0.0321	0.0206	0.0133	0.0109
APE	0.0332	0.0232	0.0146	0.0120

6.8 Greeks and hedging

In this section we analyse the sensitivity of the call option prices for both models in relation to the changes in the prices of the S&P500 share index. We also show that the delta and gamma of an option change as the underlying asset prices and strike prices change.

6.8.1 Call option delta

Tables 6.11 and 6.12 show the call option deltas for the normal and Meixner model respectively for the S&P500 share index and we observe from both tables that if a call option is deeply in-the-money, we have a higher delta and it reduces as the strike price moves towards the at-the-money region. This phenomena is also detected in Figure 6.7 which shows that short-dated call option prices are highly sensitive to changes in the prices of the underlying

asset than the longer-dated call option prices when the call options are in-the-money and the reverse is true when the options are out-of-the money. The question of whether there are significant differences in delta values between the normal and Meixner models cannot be answered, since there is no sufficient evidence from these results.

Figures 6.8 illustrates how the call option delta changes as the underlying price changes by fixing the strike price at 2600. From Figure 6.8 we observe that shorter-dated call options under the Meixner model gives delta values that are initially lower than the normal model when the option is out-of-the-money but they rise sharply when the call option approaches at-the-money point.

Table 6.11: Call option delta under the normal model for S&P500 share index using calibrated parameters

Strike price	T=15 days	T=58 days	T=164 days
2200	1	0.99739	0.96103
2300	0.9998	0.98509	0.91827
2400	0.99849	0.94271	0.85083
2500	0.96751	0.84321	0.75831
2600	0.77876	0.67719	0.64619
2700	0.39411	0.47316	0.52454

Table 6.12: Call option delta under the Meixner model for S&P500 share index using calibrated parameters

Strike price	T=15 days	T=58 days	T=164 days
2200	0.99697	0.98513	0.95394
2300	0.99249	0.96872	0.92150
2400	0.98151	0.93658	0.87236
2500	0.95385	0.87596	0.80196
2600	0.87702	0.76606	0.70710
2700	0.50721	0.57637	0.58780

Figure 6.7: Call option delta as a function of strike prices for S&P500 share index

(a) Normal model

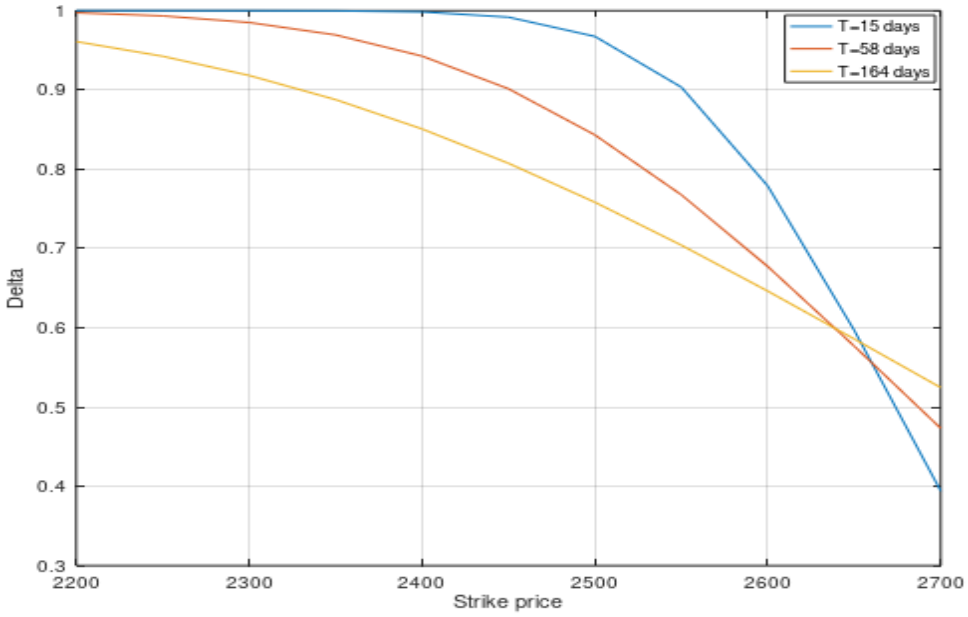

(b) Meixner model

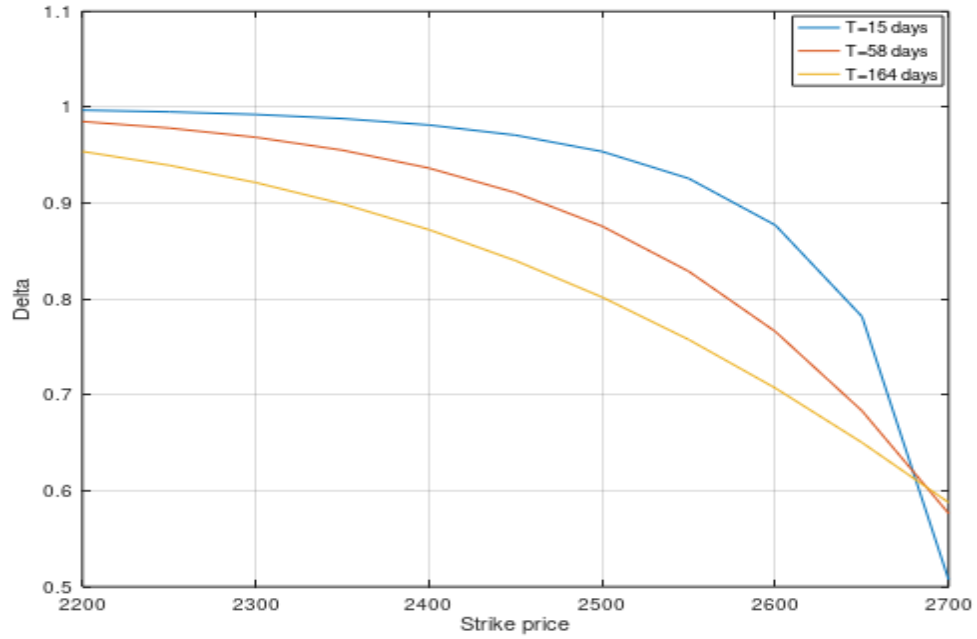

Figure 6.8: Call option delta as a function of the prices of the S&P500 share index

(a) Normal model

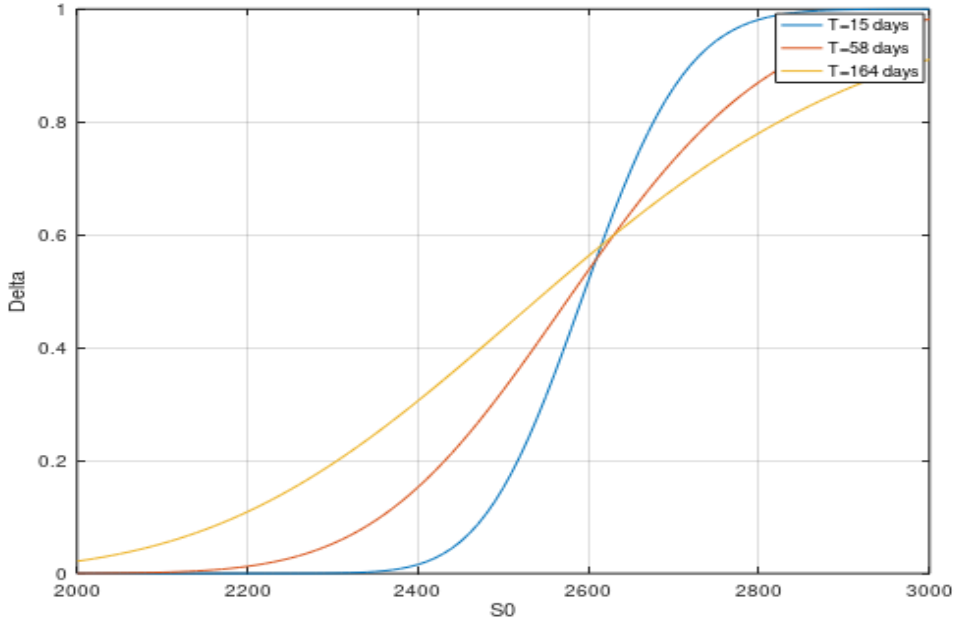

(b) Meixner model

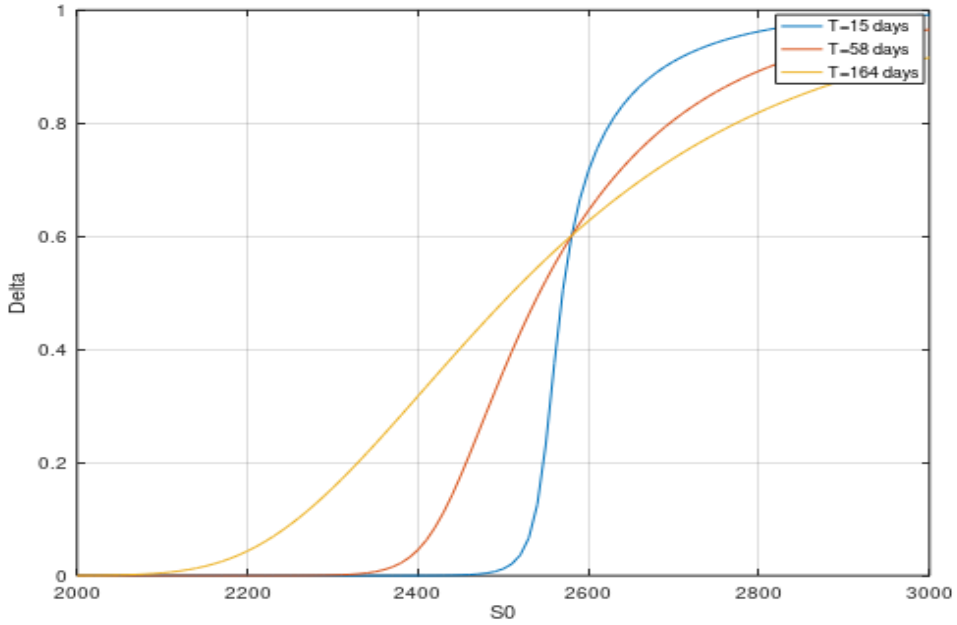

6.8.2 Call option gamma

Figure 6.9 illustrates the call option gamma as a function of the strike prices and we observe that the Meixner model has gammas that are higher than the normal model for different strike prices. Figure 6.10 illustrates the call option gamma as a function of the underlying asset prices by fixing a strike price at 2600. From Figure 6.10 we see that for both models, short-dated call options have higher gammas when the option is at-the-money, but a lower

gamma when the option is out-of-the-money and in-the-money as compared to long-dated call options. We also observe that a Meixner model has higher gammas as compared to the normal model which signifies that the delta under Meixner model is more sensitive to underlying price changes than the normal model. This is very important to consider under delta hedging.

Figure 6.9: Call option gamma as a function of strike prices for S&P500 stock index

(a) Normal model

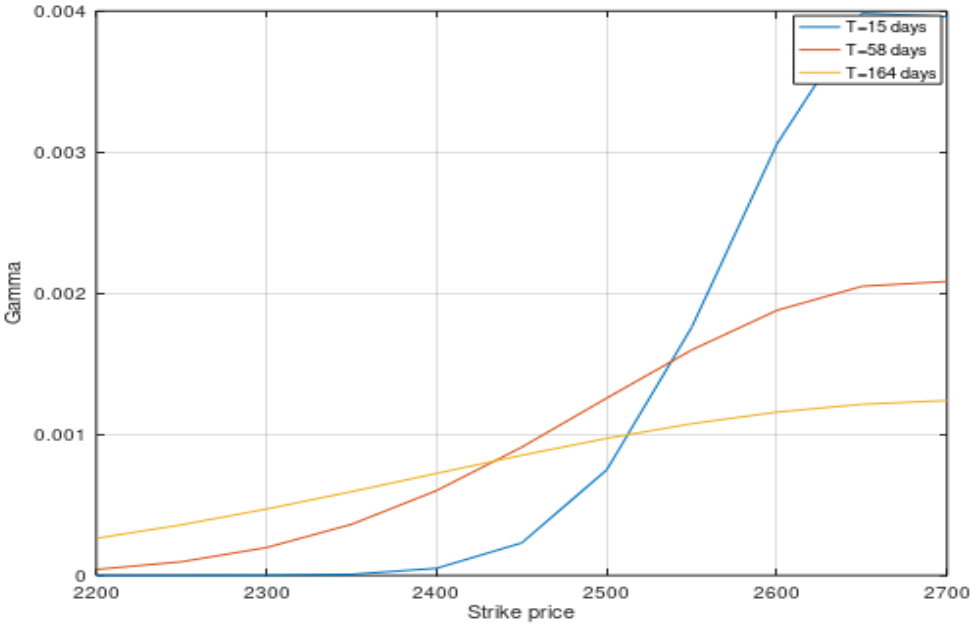

(b) Meixner model

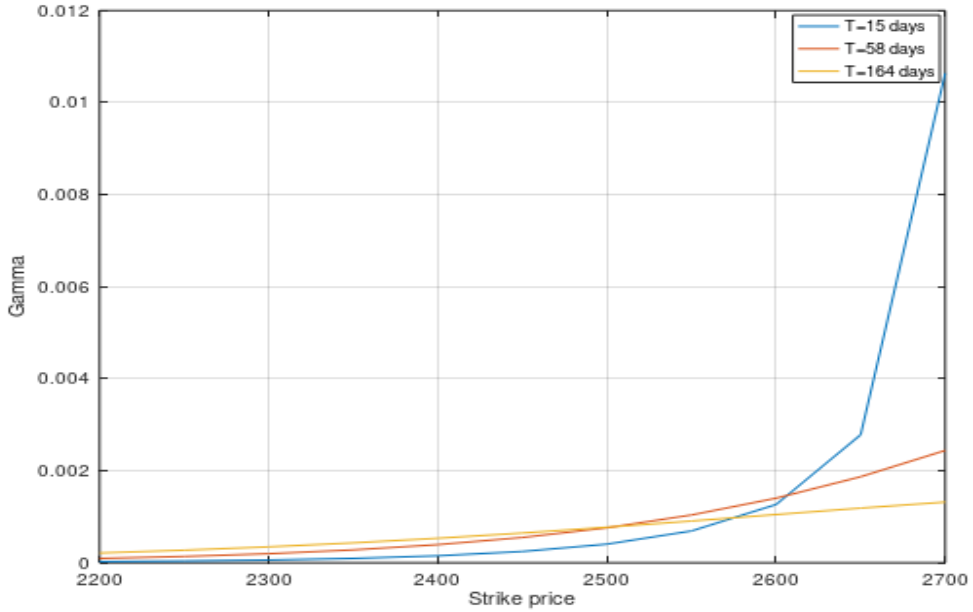

Figure 6.10: Call option gamma as a function of the S&P500 share index prices

(a) Normal model

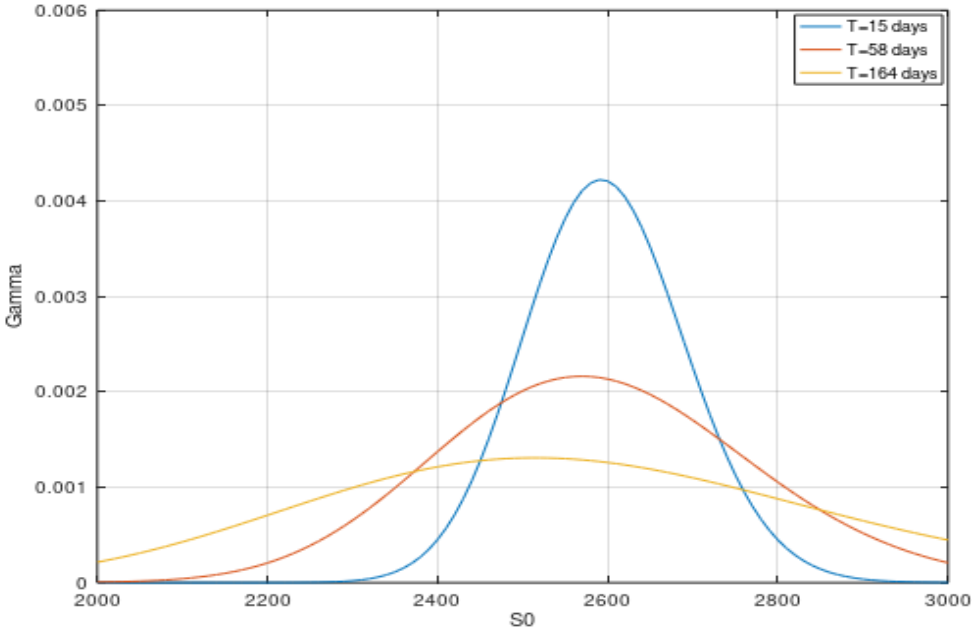

(b) Meixner model

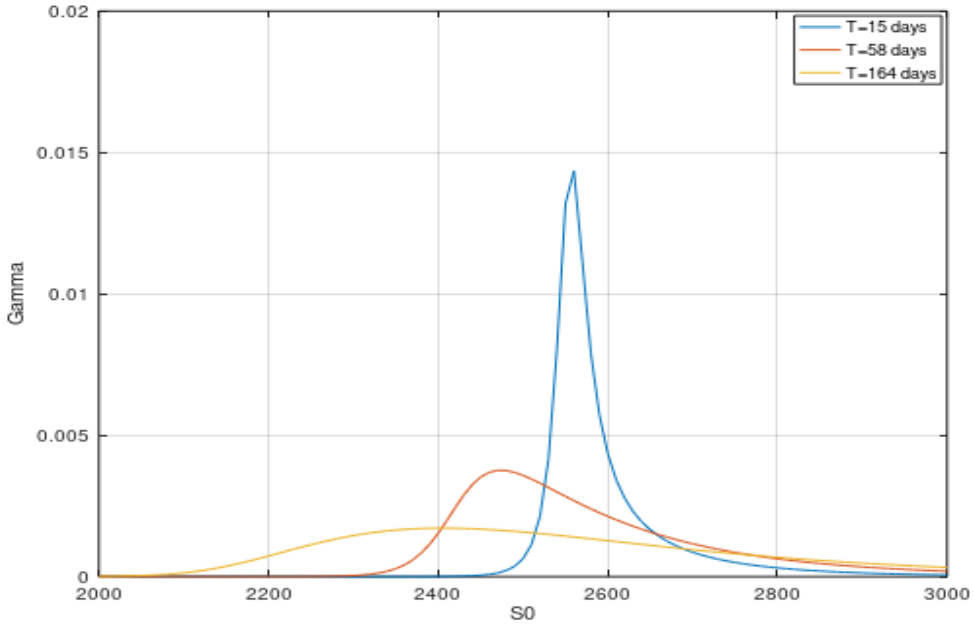

6.8.3 Delta hedging

As pointed out in the last chapter, we cannot have a perfect hedge on the Meixner model because it is incomplete, but we can hedge the portfolio under the normal model. An option trader can use delta hedging under the Meixner model by ensuring that the martingale pricing used is consistent. Under the delta hedging, we want to find a way to protect an option trader from small changes in the prices of the underlying asset. Under this criteria,

we want to ensure that the delta of a portfolio is zero (delta neutral), so that whatever the direction the underlying asset takes, no losses or gains will be realised by the trader. We create a portfolio at time t that has a call option (C_t) and underlying asset (S_t). Under this notion, the value of the portfolio V_t at time t is given by

$$V_t = C_t + xS_t, \tag{6.8.1}$$

where x denotes the number of units of the underlying assets to be added on a portfolio. We choose the value of x such that the portfolio in (6.8.1) will be delta neutral [3, p. 130] as follows:

$$\frac{\partial}{\partial S}V_t = \frac{\partial}{\partial S}C_t + x\frac{\partial}{\partial S}S_t = 0. \tag{6.8.2}$$

We solve for x in (6.8.2) and by using (5.3.1) we get

$$x = -\ \Delta_C.$$

Therefore, if we buy an option then we have to sell Δ_C units of an underlying asset. From the two subsections above we noticed that the call option gamma under the Meixner model is higher than the normal model which shows that the delta is changing frequently under the Meixner model, therefore the portfolio manager need to frequently ensure that delta-neutral is achieved.

Chapter 7

Conclusion

This dissertation focused on option pricing models based on the Meixner process and Brownian motion. These two processes were proved to be Lévy processes that are linked to orthogonal polynomials. The Meixner process and Brownian motion are modeled by the Meixner and normal distribution, respectively. Log returns of stock indices used in the dissertation had heavy tails and highly peaked distributions as well as negative skewness. This motivated the fitting of the Meixner distribution to the log returns in order to capture these features depicted by the log returns data. We also used the normal distribution to fit the log returns data because of its association with the Black-Scholes model. Lévy processes are useful on determining the price of financial assets because they incorporate jumps. Both the Meixner and normal distribution have analytically tractable characteristic functions which made it easier to apply the Fourier transform methods on option pricing. We compared the efficiency of the normal (Black-Scholes) and Meixner model by calibrating the prices from the models to the market prices of options. Efficiency was measured by determining the model with the lowest error measures.

The goodness of fit procedure taken showed that a Meixner distribution gives a better fit to the log returns of the stock indices than a normal distribution which is as a result of the fact that the Meixner distribution adds two more parameters that caters for the skewness and kurtosis. Black-Scholes model is shown to be complete while the Meixner model is incomplete. The Black-Scholes model is superior to the Meixner model on this because under a complete model there exist another self-financing portfolio that can replicate our portfolio of options. Overally, the Meixner model had very small error measures as compared to the Black-Scholes model and this convinced us to conclude that a Meixner model is more efficient on pricing European call options than the Black-Scholes model. After applying the two models to both the South African (SA) market and the United States (US) market, we discovered that the models are more efficient on the US market than the SA market. This is because US markets are more liquid than the SA markets.

The parameters of the two models are estimated from the historical data and calibration. From this, we observed that a model with calibrated parameters was performing better than a model with parameters estimated from historical data. This is because we assumed constant volatility of log returns of the underlying asset when we estimated parameters using historical data but the calibration procedure incorporated the volatility implied by the market prices

of options. Both the Meixner and Black-Scholes models were more accurate for smaller maturities than longer maturities and this is also partially because volatility tend to change with time. The efficiencies of the two models reduced when the strike prices were moving away from the spot prices (in-the-money and out-of-the-money) which suggests that both models were ignoring the volatility smile. This suggests that we cannot rely on the assumption of constant volatility of log returns of an underlying asset.

One major shortfall was on obtaining the options data for the illiquid South African market. We used small data sets available for warrants which compromised the accuracy of the parameters estimated. From the observations we noticed that our models can be greatly improved if we can incorporate stochastic volatility of the log returns of the underlying asset (see [32]). This will improve the accuracy of our models for longer maturities. We also noticed that if we relax some assumptions outlined on the model building, we are able to improve our models. For example if we relax the assumption of frictionless market, we can incorporate trading costs to our models which will improve how our models match the market prices. Our research was focused on only pricing of European options but this can be further extended to exotic options (see [23]). The models developed on this research can be extended to other fields like insurance where we can apply other Lévy processes like Poisson and Gamma processes (see [35]) to calculate the premiums to be charged on insurance products.

Appendix A

Additional information

A.1 Probability space and random variables

A.1.1 Probability space

Suppose we define Ω to be a set of possible outcomes of a phenomenon (that is a sample space) and $\mathcal{F}$ to be a class of all the considered events (that is an event space), then $\mathcal{F}$ is a σ-field if the following holds [4, p. 14]:

- $\Omega \in \mathcal{F}$,
- for a set $A \in \mathcal{F}$ we have $-A \in F$,
- for a sequence of events $A_1,\ A_2,\ A_3, ... \in \mathcal{F}$ we have $\bigcup_{i=1}^{\infty} A_i \in \mathcal{F}$.

If $\mathcal{F}$ is a σ-field, the function $P : \mathcal{F} \to \mathbb{R}$ is called a probability measure if the following holds [4, p. 17]:

- $0 \leq P(A) \leq 1$ for all $A \in \mathcal{F}$,
- $P(\Omega) = 1$,
- for a sequence of mutually exclusive events (disjoint events) $A_1,\ A_2,\ A_3, ... \in \mathcal{F}$ we have $P(\bigcup_{i=1}^{\infty} A_i) = \sum_{i=1}^{\infty} P(A_i)$.

Since we have a sample space Ω, a σ-field $\mathcal{F}$ and a probability measure P, a probability space is defined by $(\Omega, \mathcal{F}, P)$ [1, p. 9-13].

A.1.2 Random variable and probability functions

A random variable X is explicitly defined $X : \Omega \to \mathbb{R}$, which is a mapping from a sample space to the real space so that X is $\mathcal{F}$-measurable on probability space $(\Omega, \mathcal{F}, P)$ [3, p. 484, definition B.1].

We say continuous random variables X_1, X_2, ..., X_n with joint probability density function $f(x_1, x_2, ..., x_n)$ are mutually independent if [9, p. 239]:

$$f(x_1, x_2, ..., x_n) = f(x_1)f(x_2)...f(x_n)$$

for any x_1, x_2, ..., $x_n \in \mathbb{R}$.

A.2 Shapiro-Wilk test for normality

We are going to apply the Shapiro-Wilk test on the data for the log returns to determine whether the data is normally distributed.

H_0 : The log returns data is normally distributed.
H_a : The log returns data is not normally distributed.

The hypothesis is tested using the following test statistic [36]:

$$W = \frac{\left(\sum_{k=1}^{n} a_k x_{(k)}\right)^2}{\sum_{k=1}^{n}(x_k - \bar{x})^2},$$

where:

- $\{x_1, x_2, \ldots, x_n\}$ is a sample of size n,
- $\bar{x} = \frac{1}{n}\sum_{k=1}^{n} x_k$,
- $x_{(k)}$ denotes the k^{th} order statistic which means the k^{th} smallest observation in the sample,
- $(a_1, a_2, \ldots, a_n)$ is a 1 by n matrix, m is an n by 1 matrix of mean values of order statistics and Σ is an n by n covariance matrix of order statistics such that

$$(a_1, a_2, \ldots, a_n) = \frac{m^T \Sigma^{-1}}{\sqrt{m^T \Sigma^{-1} \Sigma^{-1} m}}.$$

The null hypothesis is rejected when very small values of W are obtained or alternatively under a 5% confidence level, we reject the hypothesis of normality if the p-values from the test are less than 0.05.

A.3 Black-Scholes model

Under the assumption of normality of the underlying asset, we can use the Black-Scholes model developed by Fischer Black and Myron Scholes. This model is built under the following assumptions [16, p. 245]:

- transaction costs and tax are ignored;
- there are no dividends payable on the underlying asset;
- returns from an underlying asset are modeled by a normal distribution;
- short-selling of securities is allowed;
- there are no-arbitrage opportunities;
- the market has a risk-free asset (bank account) and a risky asset (stock).

The risk-free asset is given as [31]

$$B_t = \exp(rt) \text{ for } 0 \leq t \leq T.$$

The risky asset is given as follows [34]:

$$S_t = S_0 \exp\{(\mu - \frac{\sigma^2}{2})t + \sigma W_t\},$$

where W_t denotes a Brownian motion. Under the risk-neutral setting we use the mean-correcting martingale measure and get

$$\mu_{\text{risk-neutral}} = r - \frac{1}{2}\sigma^2.$$

The risk-neutral stock is then given as follows:

$$S_t = S_0 \exp\{(r - \frac{\sigma^2}{2})t + \sigma W_t\}.$$

Since under the pricing of the European vanilla options, the value of the stock depends on the value of stock at maturity, the value of the options under the Black-Scholes model with payoff $H(\{S_u, 0 \leq u \leq T\})$ is [31, p. 30]

$$\begin{aligned} V_t &= E^{\mathbb{Q}}[\exp(-r(T-t))H(S_T)] \\ &= \exp(-r(T-t))E^{\mathbb{Q}}[\exp(H(S_T)] \\ &= \exp(-r(T-t))E^{\mathbb{Q}}[H(S_t \exp\{(r - \frac{\sigma^2}{2})(T-t) + \sigma(W_T - W_t)\})] \\ &= \exp(-r(T-t)) \int_{-\infty}^{\infty} H(S_t \exp\{(r - \frac{\sigma^2}{2})(T-t) + \sigma y\}) f(y) dy \text{ where } y \sim N(0, T-t). \end{aligned} \tag{A.3.1}$$

The above expression can be further simplified by specifying the payoffs on a call or put option to give the following expressions [31, p. 31]:

$$C = S_t N(d_1) - K e^{-r(T-t)} N(d_2) \tag{A.3.2}$$

$$P = K e^{-r(T-t)} N(-d_2) - S_t N(-d_1), \tag{A.3.3}$$

$$\text{where } d_1 = \frac{\ln\left(\frac{S_t}{K}\right) + (r + \frac{\sigma^2}{2})(T-t)}{\sigma\sqrt{(T-t)}}$$

$$d_2 = d_1 - \sigma\sqrt{(T-t)}.$$

Given the stock price at time t of the option agreement, maturity time T and strike price K, we calculate the price of options under the Black-Scholes model. We also take note of the following from expressions (A.3.2) and (A.3.3) [28]:

- $N(d_2)$ denotes the probability of the option being exercised at time of maturity.
- $S_t N(d_1) e^{r(T-t)}$ denotes the expected value that if the option is in-the-money, a stock (S_T) is received at maturity.
- If the stock price is very high at maturity, there is a higher chance that a rational investor will exercise the call option. Both $N(d_1)$ and $N(d_2)$ will tend to 1 as stock price turns to infinity and the call option value will be expected to be $S_t - Ke^{-r(T-t)}$.
- If the stock price is turning to infinity, the European vanilla put option will turn to zero since both $N(-d_1)$ and $N(-d_2)$ will turn to zero.
- When the call option is in-the-money, as $\sigma \to 0$, both $d_1, d_2 \to +\infty$ which forces $N(d_1), N(d_2) \to 1$ giving the European vanilla call price of $S_t - Ke^{-r(T-t)}$.
- When the call option is out-of-the-money, as $\sigma \to 0$, both $d_1, d_2 \to -\infty$ which implies that $N(d_1), N(d_2) \to 0$ giving the European vanilla call price of 0.
- Summarising the above two observations, we note that the price of the European vanilla call option is given as $(S_t - Ke^{-r(T-t)})^+$ as $\sigma \to 0$ and the vice versa under the put option to give a European vanilla put of $(Ke^{-r(T-t)} - S_t)^+$as $\sigma \to 0$. In other words the risky asset is now the same as the risk-free asset.
- σ and the price of European vanilla call option are positively related.

Appendix B

Codes

B.1 SAS codes

The SAS codes in this section are used for normality test and explanatory data analysis.

```
proc univariate data=sasuser.jse_all normal;
var returns;
run;
proc univariate data=sasuser.jse_top40 normal;
var returns;
run;
proc univariate data=sasuser.sasol;
var Returns;
run;
proc univariate data=sasuser.billiton;
var Returns;
run;
```

B.2 R codes

The R codes in this section covers the goodness of fit and change of parameters for the normal and Meixner distribution.

B.2.1 Effects of change of parameters

B.2.1.1 Change of Meixner distribution parameters

```
#changing parameters for a Meixner distribution
library(pracma)
Meixner1=function (x)
{
  a=1
  b=0
  d=1
  m=-0.5
A=(2*cos(b/2))^(2*d)
B=2*a*pi*gamma(2*d)
C=(b*(x-m))/a
D=d+(complex(1,0,1)*(x-m))/a
E=abs(gammaz(D))^2
f=(A/B)*exp(C)*E
}
Meixner2=function (x)
```

```
{
  a=1
  b=0
  d=1
  m=0
  A=(2*cos(b/2))^(2*d)
  B=2*a*pi*gamma(2*d)
  C=(b*(x-m))/a
  D=d+(complex(1,0,1)*(x-m))/a
  E=abs(gammaz(D))^2
  f=(A/B)*exp(C)*E
}
Meixner3=function (x)
{
  a=1
  b=0
  d=1
  m=0.5
  A=(2*cos(b/2))^(2*d)
  B=2*a*pi*gamma(2*d)
  C=(b*(x-m))/a
  D=d+(complex(1,0,1)*(x-m))/a
  E=abs(gammaz(D))^2
  f=(A/B)*exp(C)*E
}
plot(Meixner1,-5,5,type="l",col="blue",lwd=2,
main="Meixner(1,0,1,m) pdf (solid blue (m=-0.5),dashed red (m=0) and dotdash black (d=0.5)",
    xlab="x",ylab="f(x)")
plot(Meixner2,-5,5,add=TRUE,type="l",col="red",lwd=2,lty=2)
plot(Meixner3,-5,5,add=TRUE,type="l",col="black",lwd=2,lty=4)
```

B.2.1.2 Change of normal distribution parameters

```
#changing parameters for a normal distribution
library(pracma)
Normal1=function(x)
{mu=0
sigma=sqrt(1)
g=(1/(sigma*sqrt(2*pi)))*exp((-1/2)*((x-mu)/sigma)^2)
}
Normal2=function(x)
{mu=0
sigma=sqrt(2)
g=(1/(sigma*sqrt(2*pi)))*exp((-1/2)*((x-mu)/sigma)^2)
}
Normal3=function(x)
{mu=0
sigma=sqrt(3)
g=(1/(sigma*sqrt(2*pi)))*exp((-1/2)*((x-mu)/sigma)^2)
}

plot(Normal1,-5,5,type="l",col="blue",lwd=2,
     main="Normal(0,sig2) (solid blue(sig2=1),
     dashed red (sig2=2) and dotdashed black (sig2=3))",
     xlab="x",ylab="f(x)")
plot(Normal2,-5,5,type="l",col="red",lwd=2,lty=2, add=TRUE)
plot(Normal3,-5,5,type="l",col="black",lwd=2,lty=4,add=TRUE)
```

B.2.2 Goodness of fit

B.2.2.1 Histograms and other plots

```
library(readxl)
SPdata <- read_excel("C:/Users/User/Desktop/Masters/Dissertation/SPdata.xlsx")

#attaching the data
attach(SPdata)

#plotting the data
```

```
plot(SPdata$Date,SPdata$Shares, xlab="Date", ylab="Share price",
 type="l",col="blue",lwd=2)
plot(SPdata$Date,SPdata$Returns, xlab="Date", ylab="log returns",
 type="l",col="blue",lwd=2)

#Explanatory data analysis

summary(SPdata$Returns)
quantile(Returns,na.rm=TRUE,probs=c(0,0.25,0.5,0.75,1))

#plotting a boxplot and a histogram

boxplot(Returns,main="Boxplot for the Returns data",
 ylab="Returns %")
hist(Returns,prob=T,ylim=c(0,100),
 breaks=seq(from=-0.05, to=0.05, by=0.005),
main="Histogram for Returns data",xlab="log returns",
 ylab="density",col="lightblue",las=1)

#OVERLAYING A HISTOGRAM TO NORMAL AND MEIXNER CURVES

# Defining a Meixner function

library(pracma)
Meixner=function(x)
{a=0.01860433981
b=-0.4767049877
d=0.3400430035
m=0.001946986097
A=(2*cos(b/2))^(2*d)
B=2*a*pi*gamma(2*d)
C=(b*(x-m))/a
D=d+(complex(1,0,1)*(x-m))/a
E=abs(gammaz(D))^2
f=(A/B)*exp(C)*E
}

# Defining a normal function

Normal=function(x)
{mu=0.0004098831
sigma=sqrt(0.00006232218867)
g=(1/(sigma*sqrt(2*pi)))*exp((-1/2)*((x-mu)/sigma)^2)
}

#comparing normal vs meixner

plot(Meixner,-0.04,0.04,type="l",col="blue",lwd=2,
    main="Meixner distribution (solid) and
       normal distribution (dashed) curves",
    xlab="log returns",ylab="density")
plot(Normal,-0.04,0.04,type="l",col="black",lwd=2,lty=2,add=TRUE)
plot(Meixner,0.02,0.05,type="l",col="blue",lwd=2,
    main="Comparing curves of Meixner distribution (solid)
      and normal distribution (dashed) on the right tail",
    xlab="log returns",ylab="density")
plot(Normal,0.02,0.05,type="l",col="black",lty=2,add=TRUE)

# Overlaying both meixner and normal to the histogram

hist(Returns,prob=TRUE,ylim=c(0,100),
   breaks=seq(from=-0.05, to=0.05, by=0.001),
   main="Histogram overlayed with Meixner distribution (blue solid)
      and normal distribution (red dashed) curves",
   xlab="log returns", ylab="density",col="lightblue",las=1)
curve(Normal,add=TRUE,col="red",type="l",lty=2,lwd=2)
curve(Meixner,add=TRUE,col="blue",type="l",lwd=2)
```

B.2.2.2 Quantile-quantile plots

#Q–Q PLOTS

```
#find the q–q plots from a Meixner distribution

MeixnerCDF=function(x){
  a=0.01860433981
  b=−0.4767049877
  d=0.3400430035
  m=0.001946986097
  A=(2*cos(b/2))^(2*d)
  B=2*a*pi*gamma(2*d)
  C=(b*(x–m))/a
  D=d+(complex(1,0,1)*(x–m))/a
  E=abs(gammaz(D))^2
  f=(A/B)*exp(C)*E
  integrate(f=dist,lower=−0.05,upper=x)
}

n=1000
i=1:n
x=seq(from=−0.05,to=0.05,by=(1/n))
q=(i−0.5)/n
Mcdf=function(x){
  integrate(Meixner,−0.05,x)$value
}
INVcdf=function(q){
  uniroot(function(x){Mcdf(x)−q},range(x))$root
}

#using a do loop

TheoreticalQ=0
for(i in 1:n){TheoreticalQ[i]=INVcdf(q[i])}
ImpericalQ=quantile(SPdata$Returns,na.rm=TRUE,
 seq(((1−0.5)/n),((n−0.5)/n),(1/n)))
plot(TheoreticalQ,ImpericalQ,
 main="Q–Q plots under Meixner distribution",
 xlab="Meixner quantiles",
 ylab="Quantiles for returns data",col="blue", abline(0,1))


#find the q–q plots from a Normal distribution

NormalCDF=function(x)
{mu=0.0004098831
sigma=sqrt(0.00006232218867)
g=(1/(sigma*sqrt(2*pi)))*exp((−1/2)*((x–mu)/sigma)^2)
integrate(g=dist,lower=−0.05,upper=x)$value
}
n=1000
j=1:n
x=seq(from=−0.05,to=0.05,by=(1/n))
p=(j−0.5)/n
Ncdf=function(x){integrate(Normal,−0.05,x)$value
  }
N_INVcdf=function(p){
  uniroot(function(x){Ncdf(x)−p},range(x))$root
}
NormalQ=0
for(j in 1:n){NormalQ[j]=N_INVcdf(p[j])}
ImpQ=quantile(SPdata$Returns,na.rm=TRUE,
 seq(((1−0.5)/n),((n−0.5)/n),(1/n)))
plot(NormalQ,ImpQ, main="Q–Q plots under normal distribution",
 xlab="normal quantiles",
 ylab="Quantiles for returns data",col="blue", abline(0,1))
```

B.3 MATLAB codes

The Matlab codes in this section are for the pricing of European call options, calibration and hedging.

B.3.1 Calibration codes

B.3.1.1 Normal model

```
%CALIBRATION

function residual=Normalmodel1(x)
vol=x(1);
% dumping factor
alpha = 2;
% value of the underlying
S0 = 2669.1;
%volatility
%sig=sqrt(0.00006232);
%daily risk free rate
r=(1+0.0181).^(1/252)-1;
% Time vector
T=[15;58;164];
%Market prices
%closing prices
%PM=[494 505.15 534; 450.80 471 490; 368.30 379 412.85; 335.05 330 376;...
    %265.15 287.9 350; 220.86 241.38 298.83; 158.35 171.5 245;114 142.03 227;...
    %82.91 121.2 177.25; 46 84.31 145; 18 54.2 115.55];
%average of bid and ask price
PM=[472.05 480.95 518.95; 422.5 433.35 474.95;372 379 412.025;322.35 330 370.05;...
    272.75 289.75 341.55;223.75 244.55 292.215; 175.75 202.5 247; 129.15 160.65 221.95;...
    83.8 120.5 176.875;45.75 85.1 144.25;17.85 55.15 114.375];
PMvector=reshape(PM,[],1);
%strike price vector
K=2200:50:2700;
Kmat=repmat(K,1,3);
K1=reshape(Kmat,[],1);
%
N = length(T);
M = length(K);
PMaverage=(1/M)*sum(PM);
%pricing function
for j = 1:N
    for i = 1:M
        F=@(x)CharNormal(x,alpha,S0,T(j),K(i),vol,r);
        CV(i,j)=(exp(-alpha*log(K(i)))/pi)*integral(F,0,Inf,'RelTol',1e-8,'AbsTol',1e-13);
        R(i,j)=abs(PM(i,j)-CV(i,j));
    end
end
CV;
Rcomb=reshape(R,[],1);
residual=(1/M)*sum(Rcomb);
end

%characteristic function of the normal distribution
function cfn1=CharNormal(u,alpha,S0,T,K,sig,r)
v=u-(alpha+1)*1i;
phiT=exp(1i*v*log(S0)+1i*v*r*T-0.5*sig.^2*T*(1i*v+v.^2));
cfn= phiT*exp(-r.*T)./(alpha^2+alpha-u.^2+1i*(2*alpha+1)*u);
cfn1=real(exp(-1i*u*log(K)).*cfn);
end

%%IN THE COMMAND WINDOW, PUT INITIAL VALUE AND INVOKE THE fminsearch() FUNCTION
>x=0;
>f=fminsearch(@Normalmodel1,x)
```

B.3.1.2 Meixner model

```
%CALIBRATION

function residual=Meixnermodel1(x)
a=x(1);
b=x(2);
d=x(3);
% Dumping factor
alpha = 2;
% value of the underlying
S0 = 2669.1;
% Daily risk free rate
r=((1+0.0181).^(1/252))-1;
% Meixner parameters for daily log returns data
%param=[0.01860433981;-0.4767049877;0.3400430035];
%Time vector
T= [15;58;164];
% Market data
% closing price
%PM=[494 505.15 534; 450.80 471 490; 368.30 379 412.85; 335.05 330 376;...
   % 265.15 287.9 350; 220.86 241.38 298.83; 158.35 171.5 245;114 142.03 227;...
    %82.91 121.2 177.25; 46 84.31 145; 18 54.2 115.55];
%average of bid and ask
PM=[472.05 480.95 518.95; 422.5 433.35 474.95;372 379 412.025;322.35 330 370.05;...
    272.75 289.75 341.55;223.75 244.55 292.215; 175.75 202.5 247; 129.15 160.65 221.95;...
    83.8 120.5 176.875;45.75 85.1 144.25;17.85 55.15 114.375];
PMvector=reshape(PM,[],1);
%Strike price vector
K=2200:50:2700;
Kmat=repmat(K,1,3);
K1=reshape(Kmat,[],1);

N = length(T);
M = length(K);
PMaverage=(1/M)*sum(PM);

%function for the call option pricing
for j = 1:N
    for i = 1:M
        F=@(x)CharMeixner(x,alpha,S0,T(j),K(i),a,b,d,r);
        CV(i,j)=(exp(-alpha*log(K(i)))/pi)*integral(F,0,Inf,'RelTol',1e-8,'AbsTol',1e-13);
        %R(i,j)=(PM(i,j)-CV(i,j)).^2;
        R(i,j)=abs(PM(i,j)-CV(i,j));
    end
end
CV;
CV1=reshape(CV,[],1);
Rcomb=reshape(R,[],1);
residual=(1/M)*sum(Rcomb);
end
%function for the characteristic function of a meixner distribution
function cf1=CharMeixner(u,alpha,S0,T,K,a,b,d,r)
v=u-(alpha+1)*1i;
m=r-2*d.*log(cos(b/2)/cos((a+b)/2));
phiX=((cos(b/2)./cos((a*v*1i+b)/2)).^(2*d.*T));
phiT=phiX.*exp(1i*v*(log(S0)+m.*T));
cf= phiT*exp(-r.*T)./(alpha^2+alpha-u.^2+1i*(2*alpha+1)*u);
cf1=real(exp(-1i*u*log(K)).*cf);
end
%% IN THE COMMAND WINDOW INITIALISE AND INVOKE THE FUNCTION fminsearch()
>x=[0.0186,-0.4767,0.34];
>f=fminsearch(@Meixnermodel1,x)
```

B.3.2 Pricing using Fourier transform and distance measures

B.3.2.1 Normal model

```
% Fourier Transform for the Normal model
```

```
function DirectFourierTransformNormal

% dumping factor
alpha = 2;

% value of the underlying
S0 = 2669.1;

%volatility
sig=sqrt(0.00006232);

%daily risk free rate
r=(1+0.0181).^(1/252)-1;

% Time vector
T=[15;58;164];

%Market prices

%closing prices
%PM=[494 505.15 534; 450.80 471 490; 368.30 379 412.85; 335.05 330 376;...
    %265.15 287.9 350; 220.86 241.38 298.83; 158.35 171.5 245;114 142.03 227;...
    %82.91 121.2 177.25; 46 84.31 145; 18 54.2 115.55];

%average of bid and ask price
PM=[472.05 480.95 518.95; 422.5 433.35 474.95;372 379 412.025;322.35 330 370.05;...
    272.75 289.75 341.55;223.75 244.55 292.215; 175.75 202.5 247; 129.15 160.65 221.95;...
    83.8 120.5 176.875;45.75 85.1 144.25;17.85 55.15 114.375];
PMvector=reshape(PM,[],1);

%strike price vector
K=2200:50:2700;
Kmat=repmat(K,1,3);
K1=reshape(Kmat,[],1);
%
N = length(T);
M = length(K);
PMaverage=(1/M)*sum(PM);

%pricing function
for j = 1:N
    for i = 1:M
        F=@(x)CharNormal(x,alpha,S0,T(j),K(i),sig,r);
        CV(i,j)=(exp(-alpha*log(K(i)))/pi)*integral(F,0,Inf,'RelTol',1e-8,'AbsTol',1e-13);
        R(i,j)=abs(PM(i,j)-CV(i,j));
        R2(i,j)=abs(PM(i,j)-CV(i,j))/PM(i,j);
        R3(i,j)=abs(PM(i,j)-CV(i,j))/PMaverage(1,j);
    end
end
CV
CV1=reshape(CV,[],1)
AAE=(1/M)*sum(R)
ARPE=(1/M)*sum(R2)
APE=(1/M)*sum(R3)
%plot(K,CV),xlabel('Strike price'),ylabel('Call price'),...
   %title('Normal option pricing model'),...
   %legend('T=15 days','T=58 days','T=164 days','market prices'), grid on
scatter(K1,CV1,'+'),
hold on
scatter(K1,PMvector),legend('model prices','market prices'),xlabel('Strike price'),...
 ylabel('Call price'),title('Normal (Black-Scholes) call option pricing model')
hold off
end

%characteristic function of the normal distribution
function cfn1=CharNormal(u,alpha,S0,T,K,sig,r)
v=u-(alpha+1)*1i;
phiT=exp(1i*v*log(S0)+1i*v*r*T-0.5*sig.^2*T*(1i*v+v.^2));
cfn= phiT*exp(-r.*T)./(alpha^2+alpha-u.^2+1i*(2*alpha+1)*u);
cfn1=real(exp(-1i*u*log(K)).*cfn);
```

```
end
```

B.3.2.2 Meixner model

```
% Fourier Tranform for the Meixner model

function DirectFourierTransformMeixner

% Dumping factor
alpha = 2;

% value of the underlying
S0 = 2669.1;

% Daily risk free rate
r=((1+0.0181).^(1/252))-1;

% Meixner parameters for daily log returns data (from the calibration)
param=[0.01860433981;-0.4767049877;0.3400430035];

%Time vector
T= [15;58;164];

% Market data

% closing price
%PM=[494 505.15 534; 450.80 471 490; 368.30 379 412.85; 335.05 330 376;...
   % 265.15 287.9 350; 220.86 241.38 298.83; 158.35 171.5 245;114 142.03 227;...
    %82.91 121.2 177.25; 46 84.31 145; 18 54.2 115.55];

%average of bid and ask
PM=[472.05 480.95 518.95; 422.5 433.35 474.95;372 379 412.025;322.35 330 370.05;...
    272.75 289.75 341.55;223.75 244.55 292.215; 175.75 202.5 247; 129.15 160.65 221.95;...
    83.8 120.5 176.875;45.75 85.1 144.25;17.85 55.15 114.375];
PMvector=reshape(PM,[],1);

%Strike price vector
K=2200:50:2700;
Kmat=repmat(K,1,3);
K1=reshape(Kmat,[],1);

N = length(T);
M = length(K);
PMaverage=(1/M)*sum(PM);

%function for the call option pricing
for j = 1:N
    for i = 1:M
        F=@(x)CharMeixner(x,alpha,S0,T(j),K(i),param(1,1),param(2,1),param(3,1),r);
        CV(i,j)=(exp(-alpha*log(K(i)))/pi)*integral(F,0,Inf,'RelTol',1e-8,'AbsTol',1e-13);
        R(i,j)=abs(PM(i,j)-CV(i,j));
        R2(i,j)=abs(PM(i,j)-CV(i,j))/PM(i,j);
        R3(i,j)=abs(PM(i,j)-CV(i,j))/PMaverage(1,j);
    end
end
CV
CV1=reshape(CV,[],1);
AAE=(1/M)*sum(R)
ARPE=(1/M)*sum(R2)
APE=(1/M)*sum(R3)
%plot(K,CV),xlabel('Strike price'),ylabel('Call price'),...
    %title('Meixner option pricing model'),...
    %legend('T=15 days','T=58 days','T=164 days','market prices'), grid on
scatter(K1,CV1,'+'),
hold on
scatter(K1,PMvector),legend('model prices','market prices'),xlabel('Strike price'),...
 ylabel('Call price'),title('Meixner call option pricing model')
hold off
end
```

```
%function for the characteristic function of a meixner distribution

function cf1=CharMeixner(u,alpha,S0,T,K,a,b,d,r)
v=u-(alpha+1)*1i;
m=r-2*d.*log(cos(b/2)/cos((a+b)/2));
phiX=((cos(b/2)./cos((a*v*1i+b)/2)).^(2*d.*T));
phiT=phiX.*exp(1i*v*(log(S0)+m.*T));
cf= phiT*exp(-r.*T)./(alpha^2+alpha-u.^2+1i*(2*alpha+1)*u);
cf1=real(exp(-1i*u*log(K)).*cf);
end
```

B.3.3 Fast Fourier Transform

B.3.3.1 Normal model

```
function CV=NormalPricing(S0,T,K,sig,r)
alpha=1;
N=4096;
c=600;
deltav=c/N;
b_new=pi/deltav;
deltak=(2*b_new)/N;
u=[0:N-1]*deltav;
position=((log(K)+b_new)/deltak)+1;
v=u-(alpha+1)*i;
m=r-0.5*sig^2;
phiT=exp(i*v*(log(S0)+m*T)-0.5*sig^2*T*v.^2);
Cstar= phiT*exp(-r*T)./(alpha^2+alpha-u.^2+i*(2*alpha+1)*u);
Simp=(1/3)*(3+(-1).^[1:N]-[1,zeros(1,N-1)]);
A=exp(i*b_new*u).*Cstar*deltav.*Simp;
payoff=real(fft(A));
CV_k=(exp(-log(K)*alpha))'*payoff/pi;
format short
CV=CV_k(round(position));
end
```

B.3.3.2 Meixner model

```
function CV=MeixnerPricing(S0,T,K,a,b,d,r)
alpha=5;
N=4096;
c=600;
deltav=c/N;
b_new=pi/deltav;
deltak=(2*b_new)/N;
u=[0:N-1]*deltav;
position=((log(K)+b_new)/deltak)+1;
v=u-(alpha+1)*i;
m=r-2*d*log(cos(b/2)/cos((a+b)/2));
phiX=((cos(b/2)./cos((a*v*i+b)/2)).^(2*d.*T));
phiT=phiX.*exp(i*v*(log(S0)+m.*T));
Cstar= phiT*exp(-r.*T)./(alpha^2+alpha-u.^2+i*(2*alpha+1)*u);
Simp=(1/3)*(3+(-1).^[1:N]-[1,zeros(1,N-1)]);
A=exp(i*b_new*u).*Cstar*deltav.*Simp;
payoff=real(fft(A));
CV_k=(exp(-log(K)*alpha))'*payoff/pi;
format short
CV=CV_k(round(position));
end
```

B.3.4 Greeks: Delta

B.3.4.1 Normal model

```
%Normal delta as a function of S0
function NormDeltaChangeS
% dumping factor
```

```
alpha = 2;
% value of the underlying
S0 = 2000:100:3000;
%volatility
%sig=sqrt(0.00006232);
sig=0.0094;
%daily risk free rate
r=(1+0.0181).^(1/252)-1;
% Time vector
T=[15;58;164];
K=2600;
Kmat=repmat(K,1,3);
K1=reshape(Kmat,[],1);
%
N = length(T);
M = length(K);
H=length(S0);

%pricing function
for j = 1:N
    for i = 1:H
        F=@(x)CharNormalDel(x,alpha,S0(i),T(j),K,sig,r);
        Delta(i,j)=(exp(-alpha*log(K))./(pi.*S0(i)))*integral(F,0,Inf,'RelTol',1e-8,'AbsTol
            ',1e-13);

    end
end
Delta
plot(S0,Delta),legend('T=15 days','T=58 days','T=164 days'),xlabel('S0'),ylabel('Delta')
end
%characteristic function of the normal distribution
function cfn1=CharNormalDel(u,alpha,S0,T,K,sig,r)
v=u-(alpha+1)*1i;
phiT=exp(1i*v*log(S0)+1i*v*r*T-0.5*sig.^2*T*(1i*v+v.^2));
cfn= phiT*exp(-r.*T).*(1i*v)./(alpha^2+alpha-u.^2+1i*(2*alpha+1)*u);
cfn1=real(exp(-1i*u*log(K)).*cfn);
end
```

B.3.4.2 Meixner model

```
%Delta as a function of S0
function MeixnerDeltaChangeS
% Dumping factor
alpha = 2;
% value of the underlying
S0=2000:10:3000;
% Daily risk free rate
r=((1+0.0181).^(1/252))-1;
% Meixner parameters for daily log returns data
param=[0.0528;-2.2758;0.0103];
%Time vector
T= [15;58;164];

%Strike price vector
K=2600;
Kmat=repmat(K,1,3);
K1=reshape(Kmat,[],1);

N = length(T);
M = length(K);
H=length(S0);

%function for the call option pricing
for j = 1:N
      for k=1:H
        F=@(x)CharMeixnerDel(x,alpha,S0(k),T(j),K,param(1,1),param(2,1),param(3,1),r);
        Delta(k,j)=(exp(-alpha*log(K))/(pi*S0(k)))*integral(F,0,Inf,'RelTol',1e-8,'AbsTol',1
            e-13);
      end
end
```

```
Delta
plot(S0,Delta),legend('T=15 days','T=58 days','T=164 days'),xlabel('S0'),ylabel('Delta')
end
%function for the characteristic function of a meixner distribution
function cf1=CharMeixnerDel(u,alpha,S0,T,K,a,b,d,r)
v=u-(alpha+1)*1i;
m=r-2*d.*log(cos(b/2)/cos((a+b)/2));
phiX=((cos(b/2)./cos((a*v*1i+b)/2)).^(2*d.*T));
phiT=phiX.*exp(1i*v*(log(S0)+m.*T));
cf= phiT*exp(-r.*T).*(1i*v)./(alpha^2+alpha-u.^2+1i*(2*alpha+1)*u);
cf1=real(exp(-1i*u*log(K)).*cf);
end
```

B.3.5 Greeks: Gamma

B.3.5.1 Normal model

```
%normal gamma as a function of S0
function NormGammaChangeS
% dumping factor
alpha = 2;
% value of the underlying
S0 = 2000:10:3000;
%volatility
%sig=sqrt(0.00006232);
sig=0.0094;
%daily risk free rate
r=(1+0.0181).^(1/252)-1;
% Time vector
T=[15;58;164];
K=2600;
Kmat=repmat(K,1,3);
K1=reshape(Kmat,[],1);
%
N = length(T);
M = length(K);
H=length(S0);

%pricing function
for j = 1:N
    for i = 1:H
        F=@(x)CharNormalGamma(x,alpha,S0(i),T(j),K,sig,r);
        Gamma(i,j)=(-exp(-alpha*log(K))./(pi.*S0(i).^2))*integral(F,0,Inf,'RelTol',1e-8,'
            AbsTol',1e-13);

    end
end
Gamma;
plot(S0,Gamma),legend('T=15 days','T=58 days','T=164 days'),xlabel('S0'),ylabel('Gamma')
end
%characteristic function of the normal distribution
function cfn1=CharNormalGamma(u,alpha,S0,T,K,sig,r)
v=u-(alpha+1)*1i;
phiT=exp(1i*v*log(S0)+1i*v*r*T-0.5*sig.^2*T*(1i*v+v.^2));
cfn= phiT*exp(-r.*T).*(1i*v+v.^2)./(alpha^2+alpha-u.^2+1i*(2*alpha+1)*u);
cfn1=real(exp(-1i*u*log(K)).*cfn);
end
```

B.3.5.2 Meixner model

```
%Meixner gamma as a function of S0
function MeixnerGammaChangeS
% Dumping factor
alpha = 2;
% value of the underlying
S0 = 2000:10:3000;
% Daily risk free rate
r=((1+0.0181).^(1/252))-1;
% Meixner parameters for daily log returns data
```

```
param=[0.0528;-2.2758;0.0103];
%Time vector
T= [15;58;164];

%Strike price vector
K=2600;
Kmat=repmat(K,1,3);
K1=reshape(Kmat,[],1);

N = length(T);
M = length(K);
H=length(S0)

%function for the call option pricing
for j = 1:N
    for i = 1:H
        F=@(x)CharMeixnerGamma(x,alpha,S0(i),T(j),K,param(1,1),param(2,1),param(3,1),r);
        Gamma(i,j)=(-exp(-alpha*log(K))/(pi.*S0(i).^2))*integral(F,0,Inf,'RelTol',1e-8,'
            AbsTol',1e-13);
    end
end
Gamma;
plot(S0,Gamma),legend('T=15 days','T=58 days','T=164 days'),xlabel('S0'),ylabel('Gamma')
end
%function for the characteristic function of a meixner distribution
function cf1=CharMeixnerGamma(u,alpha,S0,T,K,a,b,d,r)
v=u-(alpha+1)*1i;
m=r-2*d.*log(cos(b/2)/cos((a+b)/2));
phiX=((cos(b/2)./cos((a*v*1i+b)/2)).^(2*d.*T));
phiT=phiX.*exp(1i*v*(log(S0)+m.*T));
cf= phiT*exp(-r.*T).*((1i*v)+v.^2)./(alpha^2+alpha-u.^2+1i*(2*alpha+1)*u);
cf1=real(exp(-1i*u*log(K)).*cf);
end
```

Bibliography

[1] Bain, L. J. and Engelhardt, M. (1992). *Introduction to Probability and Mathematical Statistics*. Brooks/Cole.

[2] Bandorff-Nielsen, O. E., Mikosch, T., and Resnick, S. I. (2001). *Lévy Processes: Theory and Applications*. Springer.

[3] Björk, T. (2009). *Arbitrage Theory in Continuous Time*. Oxford University Press, third edition.

[4] Borovkov, K. (2014). *Elements of Stochastic Modelling*. Word Scientific Publishing.

[5] Bu, Y. (2007). Option Pricing Using Lévy Processes. Master's thesis, Chalmers University of Technology.

[6] Carr, P. and Madan, D. B. (1999). Option Valuation Using the Fast Fourier Transform. *Journal of Computational Finance*, 2(4):61–73.

[7] Cont, R. and Tankov, P. (2004). *Financial Modelling with Jump Processes*. Chapman and Hall.

[8] Dennis, P. and Mayhew, S. (2002). Risk-Neutral Skewness: Evidence from Stock Options. *Journal of Financial and Quantitative Analysis*, 37(3):471–493.

[9] Devore, J. L. and Berk, K. N. (2012). *Modern Mathematical Statistics with Applications*. Springer.

[10] Ferreiro-Castilla, A. and Schoutens, W. (2012). The Beta-Meixner Model. *Journal of Computational and Applied Mathematics*, 236(9):2466–2476.

[11] Gautschi, W. (2004). *Orthogonal Polynomials Computation and Approximation*. Oxford Science publications.

[12] Geman, H., Madan, D., and Yor, M. (2001). Time Changes for Lévy Processes. *Mathematical Finance*, 11(1):79–96.

[13] Grigelionis, B. (1999). Processes of Meixner Type. *Lithuanian Mathematical Journal*, 39(1):33–41.

[14] Grigoletto, M. and Provasi, C. (2008). Simulation and Estimation of the Meixner Distribution. *Communications in Statistics*, 38(1):58–77.

[15] Hess, M. (2018). Cliquet option pricing with Meixner process. *Moden Stochastics: Theory and Applications*, 5(1):81–97.

[16] Hull, J. C. (2000). *Options, Futures and Other Derivatives*. Prentice-Hall International, fourth edition.

[17] Hull, J. C. (2014). *Fundamentals of Futures and Options Market*. Pearson, eighth edition.

[18] Investing.com (2018). JSE indices. `https://za.investing.com`. [Online; Accessed on 8 October 2018].

[19] Kienitz, J. and Wetterau, D. (2012). *Financial Modeling : Theory, Implementation and Practice (with Matlab source)*. John Wiley and Sons Ltd.

[20] Koekoek, R., Lesky, P. A., and Swarttouw, R. F. (2010). *Hypergeometric Orthogonal Polynomials and their q-Analogues*. Springer.

[21] Kwok, Y. K., Leung, K. S., and Wong, H. Y. (2011). Efficient Options Pricing Using the Fast Fourier Transform. In Duan, J., Härdle, W. K., and Gentle, J. E., editors, *Handbook of Computational Finance*, pages 579–604. Springer.

[22] Lau, H. and Wingender, J. R. (1989). The Analytics of the Intervaling Effect on Skewness and Kurtosis of Stock Returns. *The Financial Review*, 24(2):215–233.

[23] Lozza, S. O. and Staino, A. (2007). Exotic Options with Lévy Processes: the Markovian Approach. *University of Bergamo*.

[24] Mandelbrot, B. (1963). The Variation of Certain Speculative Prices. *The Journal of Business*, 36(4):394–419.

[25] Mazzola, E. and Muliere, P. (2010). Reviewing Alternative Characterizations of Meixner Process. *Probability Survey*, 8(2011):127–154.

[26] Nannavecchia, A. (2015). The Meixner Process for Financial Data. *Megatrend Review*, 12(2):33–44.

[27] Ng, M. (2005). Option Pricing via the FFT and its Application to Calibration. Master's thesis, Delft University of Technology.

[28] Nielsen, L. T. (1992). Understanding N(d1) and N(d2): Risk-Adjusted Probabilities in the Black-Scholes Model. *Finance*, 14(1993):95–106.

[29] Rachev, S. T., Kim, Y. S., Bianchi, M. L., and Fabozzi, F. J. (2010). *Financial Models with Lévy Processes and Volatility Clustering*. John Wiley and Sons.

[30] Rolski, T., Schmidli, H., Schmidt, V., and Teugels, J. (1998). *Stochastic Processes for Insurance and Finance*. John Wiley and Sons.

[31] Schoutens, W. (2000). *Stochastic Processes and Orthogonal Polynomials*. Springer.

[32] Schoutens, W. (2002). The Meixner Process: Theory and Applications in Finance. Technical report, EURANDOM.

[33] Schoutens, W. (2003). *Lévy Processes in Finance*. John Wiley.

[34] Schoutens, W. and Teugels, J. L. (1998). Lévy Processes, Polynomials and Martingales. *Communications in Statistics*, 14(1-2):335–349.

[35] Shanahan, B., Fard, F. A., and van der Hoek, J. (2017). Pricing Participating Policies under the Meixner Process and Stochastic Volatility. *Scandinavian Actuarial Journal*, 2017(7):559 – 583.

[36] Shapiro, S. S. and Wilk, M. B. (1965). An Analysis of Variance Test for Normality (Complete Samples). *Biometrika*, 52(3/4):591–611.

[37] Steutel, F. W. and Van Harn, K. (1979). Discrete Analogues of Self-decomposabilility and Stability. *The Annals of Probability*, 7(5):893 – 899.

[38] Stewart, J. (2008). *Calculus Early Transcendentals*. Thomson Brooks, sixth edition.

[39] Trabs, M. (2014). Calibration of Self-decomposable Lévy Models. *Bernoulli*, 20(1):109–140.

[40] United States Department of the Treasury (2018). Daily Treasury Bill Rates Data. `https://www.treasury.gov/resource-center/data-chart-center/interest-rates/Pages/TextView.aspx?data=billRatesYear&year=2018`. [Online; accessed on 29 April 2018].

[41] White, R. (2013). Option Pricing with Fourier Methods. *OpenGamma Quantitative Research*.

[42] Yahoo Finance (2018a). S&P500 Historical Data. `https://finance.yahoo.com/`. [Online; Accessed on 29 April 2018].

[43] Yahoo Finance (2018b). S&P500 Options. `https://finance.yahoo.com/`. [Online; Accessed on 29 April 2018].

[44] Yao, L., Yang, G., and Yang, X. (2010). A Note on the Mean Correcting Martingale Measure for Geometric Lévy Processes. *Applied Mathematics Letters*, 24(5):593–597.

[45] Zhang, S. and Wang, L. (2012). A Fast Fourier Transform Technique for Pricing European Options with Stochastic Volatility and Jump Risk. *Mathematical Problems in Engineering*, 2012:1–17.